ACTA PROTOZOOLOGICA

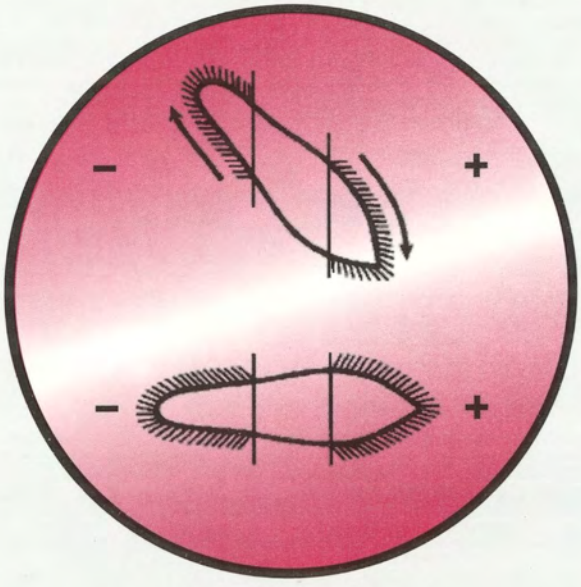

NENCKI INSTITUTE OF EXPERIMENTAL BIOLOGY
WARSAW, POLAND
1993
VOLUME 32 NUMBER 4
ISSN 0065-1583

Polish Academy of Sciences
Nencki Institute of Experimental Biology

ACTA PROTOZOOLOGICA

International Journal on Protistology

ACTA PROTOZOOLOGICA appears quarterly.

Printed at the MARBIS, 60 Kombatantów Str., 05-070 Sulejówek, Poland

Front cover: The ciliary reversal on cathodal side of *Paramecium.* S. Dryl 1963, Acta Protozool. 1,193-199

Acta Protozoologica (1993) 32: 199 - 200

GEORGE I. POLIANSKY
(1904-1993)

Professor Dr George Ivanovich Poliansky passed away on June 26, 1993, in St. Petersburg. Four days before his sudden and unexpected death he experienced serious heart problems, which did not want to admit even to himself, and he also contrived to keep his feelings a secret from his family and friends. His death was a serious blow to his family, to all his numerous friends, colleagues and students in Russia and all over the world.

Prof. Poliansky was one of the most outstanding Russian biologists and well known protozoologist over the world. He began his higher education at St. Petersburg University in 1921, where he majored in zoology having been greatly influenced by V.A. Dogiel. In 1924 he graduated from the University and started to work at the Pedagogical Institute, as an assistant. In 1932 he earned directly his D.Sc. degree for his original and comprehensive investigation of the sexual process in the ciliate *Bursaria truncatella*, and soon became Professor and obtained the Chair of Zoology at the Pedagogical Institute.

His scientific career was interrupted in 1941, when the 2nd World War broke out and Prof. Poliansky volunteered to serve at the front. In 1945, after the war ended he returned to Leningrad to resume his research at the Pedagogical Institute and the University. For two years (1946-1947) he was Prorector of Leningrad University. However, in 1948, during the dismal time for the Soviet biological sciences, he was dismissed from both Leningrad institutions and had to leave for the Karelian region of the USSR. For 4 years he was a senior scientist of the Murmansk

Biological Station, and in 1952 he was elected Director of the Institute of Biology, Karelian Branch of the Soviet Academy of Sciences.

In the early fifties, when the situation in biology changed, Prof. Poliansky was able to return to Leningrad. After the sudden death of his adviser and great friend, Prof. Dogiel in 1955, Prof. Poliansky obtained the Chair of Invertebrate Zoology at Leningrad University, and remained at this post until 1982. Simultaneously, he was actively engaged in organizing, the Institute of Cytology, Academy of Sciences of the USSR. Prof. Poliansky became head of the Laboratory of Cytology of Unicellular Organisms, and simultaneously held the post of Vice-Director of this Institute. He headed the Laboratory for 30 years, and in 1987 handed over the administrative post to his former student and successor, Prof. I.B. Raikov.

In 1976, he became Editor-in-Chief of a series of annual proceedings dedicated to some actual problems of modern protozoology, 14 volumes on free-living and parasitic protozoa having appeared by 1993.

Speaking three European languages, he attended several International and regional meetings on protozoology and parasitology (e.g., in Czechoslovakia 1961, England 1965, France 1973, Poland 1981), invariably making bridges between scientists and science on either side of the artificially created "curtain" that existed at that time. Despite tremendous political difficulties in his country at the end of the sixties, he succeeded in organizing 3rd International Congress of Protozoology in Leningrad in 1969.

Shortly before his death, Prof. Poliansky was actively engaged in the foundation of the Association of National Protozoological Science, established recently in the former republics of the USSR. He knew that their successful work might be possible only in cooperation with the Russian protozoologist and other colleagues abroad. This realization resulted from his own successful experience of working abroad, primarily in France (e.g. Sorbonne University). His French colleagues greatly appreciated his contribution, elected him an honorary member of two scientific societies: The Zoological Society and The Protozoological Society, and awarded him with a bronze medal of the Zoological Society. Simultaneously, the German Parasitological Society also awarded him with the Rudolph Leuckart Medal (1974). The Polish Academy of Sciences awarded him with the Mikołaj Kopernik Medal, and the Czechoslovak Zoological Society and the American Society of Protozoology elected him to honorary membership in Their societies. He was also decorated by the Soviet government with six orders and 9 medals. In 1968 he was awarded the title "The Honored Scientist of Russian Federation", and in 1979 was elected Corresponding Member of the Soviet Academy of Sciences. In 1981, he was given the Mechnikov Prize for his comprehensive research on variation and evolution of Protozoa. Less than a month before his death, Prof. Poliansky was given the Kirpichnikov Prize for his outstanding contribution in the field of protozoan genetics.

He had over 60 graduate students, and was the author and co-author of many scientific papers (over 300). His monograph of 1955 was dedicated to the parasitic fauna of fishes inhabiting the northern seas of Russia. In collaboration with his colleagues and students he published and edited a number of text-books and manuals: a two-volume monograph on the theory of evolution, a two-volume manual on "The Extended Practicum in Invertebrate Zoology", and a text-book for the middle school. He is probably best known for his involvement in the comprehensive collective books "General Protozoology" and "General Parasitology".

Prof. Poliansky was himself the editor and a member of the Editorial Boards of a number of scientific journals both within the country and abroad: "Tsitologia", "Parasitoloiya", "Zoologicheskyi Zhurnal", "Vestnik of Leningrad University", "Angewandte Parasitologie", "Cahierrs de Biologie Marine" as well as "Acta Protozoologica".

The death of Prof. Poliansky is a severe loss for biological science. He himself often stated that he had lived not only a long life, but also a happy life. Indeed, he had seen and done a lot. He attracted people's attention by his broad knowledge in many spheres of life - in literature, history, music. He was invariably friendly and gallant. For the last 2-3 years he was engaged in writing a book of his memoirs which he designated as "My Life Experience", in which he described his life from childhood. The book is expected to be published in several months. For all of us this will be another new acquaintance with this magnificent human being who will remain in our hearts forever.

Anna Wasik

ACTA
PROTOZOOLOGICA

Acta Protozoologica (1993) 32: 201 - 210

Composition, Organization, and Function of the Motor Systems of Free-living *Dictyostelium* Amoeba

Yoshio FUKUI

Cell, Molecular, and Structural Biology, Northwestern University Medical School, Chicago, Illinois, USA

Summary. In the last several years, a quite few numbers of cytoskeletal components have been identified in *Dictyostelium* and their mutants isolated and characterized. The most provocative idea evolved from these studies is the concept that the cell is equipped with multiple mechanisms responsible for the force generation and those mechanisms are potentially able to compensate each other. Demonstration of commitment of each individual component to specific function await future studies. Occurrence of mechanisms unique to different motile activities also must be materialized. Regulation of the cytoskeletal organization through signal transduction pathway seems to be one of the major aspects to be focussed in the next decade.

Key words. Slime mold, *Dictyostelium*, cytoskeleton, actin, myosin, actin-binding protein.

1. INTRODUCTION

A cellular slime mold *Dictyostelium discoideum* serves as an excellent model system for studying various aspects of cell motility at molecular, cellular, and developmental levels (Spudich 1989). The major mechanochemical components actin and myosin as well as various actin-binding proteins (ABPs) of this organism have been characterized. High-fidelity polarization video-microscopy, assisted by digital image enhancement, has revealed the cytoskeletal dynamics at resolution close to the theoretical limit (Fukui and Inoué 1991, 1992). In the last several years, spectacular number of genes comprising of novel myosin and ABP gene families have been identified (Hammer 1991, Schleicher and Noegel 1992). At the same time, quite a few numbers of cytoskeletal mutants were created by gene targeting techniques. The disclosure of a spectrum of "unconventional" myosin gene families in a wide variety of non-muscle cells represents the outcome of the molecular genetics in the last four years (Cheney et al. 1993). Surprisingly, many of these mutants exhibited only subtle defects, if any. The superficial masking of the genetic defect in physiological activities seems to be derived from compensation with alternative cytoskeletal components (Witke et al. 1992). To support this idea is the biological forces generated by the motor systems as measured *in vitro*. The theoretical evaluation of the motile mechanism also suggested the occurrence of quite fascinating new mechanisms for cell motility

Paper presented at the Symposium Motility, Behaviour and Orientation at the IXth International Congress of Protozoology, July 25th - August 1st, 1993, Berlin, Germany.

Address for correspondence: Y. Fukui, CMSB, Northwestern Medical School, 303 East Chicago Avenue, Chicago, IL 60611, USA.

(Fukui 1993). In this paper, I will review the major advances in the research of *Dictyostelium* motor systems made primarily in the last several years.

2. CYTOSKELETAL COMPONENTS

2.1. Myosin superfamily

2.1.1. Conventional myosin (myosin-II)

This myosin refers to a muscle type, two-headed myosin. The native protein consists of two heavy chains of 210,000-daltons, and each of which is attached with a 16,000-dalton regulatory light chain (RMLC) and a 18,000-dalton essential light chain (EMLC). It assembles into bipolar thick filaments *in vitro* and *in vivo* (Clarke and Spudich 1977, Yumura and Fukui 1985). The carboxyl terminus of the heavy chain has two threonine residues subject to phosphorylation (Pagh et al. 1984), and the domain located next to this region is essential for the filament assembly mapped at the 200 Å long tail, extending from 900 to 1100 Å from the head-tail junction (Pasternak et al. 1989). So far, a single gene encoding myosin-II (*mhcA*) has been identified, characterized, and the mutants have been created by the gene targeting studies (De Lozanne et al. 1985, Knecht and Loomis 1987, De Lozanne and Spudich 1987, Manstein et al. 1989, Egelhoff et al. 1991) (Table 1).

2.1.2. Small myosin's (myosin-I)

A low-molecular-weight, single-headed myosin, similar to *Acanthamoeba* myosin-I, was isolated from *Dictyostelium* by Côté and Bukiejko (1987). This myosin has a native molecular weight of 150,000-daltons and consists of a single heavy chain of 117,000-daltons that is probably associated with light chains (Côté and Bukiejko 1987). This class of myosin is the product of a gene family comprising multiple genes. The most conspicuous feature of this class of myosin is the lack of tail domain necessary for assembly into filaments (Korn 1991, Pollard et al. 1991). *Dictyostelium* appears to have at least five, probably nearly ten, myosin-I genes (Hammer 1991). Four of the genes (*abmA*, DMIB, DMID, and DMIE) have been cloned and sequenced (Jung et al. 1989, 1993; Titus et al. 1989, 1993; Urrutia et al. 1993) (Table 1). Their head domain is highly homologous to myosin-II and among these myosin's-I, ~65% of it being the exact copy of muscle myosin subfragment-1 (S1). The deduced sequence of the tail domain of at least two (DMIB, DMID) of those myosin-I isoforms has three similar domains, namely, (1) "membrane-binding", (2) "ATP-insensitive actin-binding", and (3) "SH-3" domains (the "tail homology", TH-1, 2, 3 domains, respectively). *AbmA* and DMIE have sequences similar to DMIB and DMID except the tail domain that lacks the ATP-insensitive actin-binding region (Titus 1989, 1993; Urrutia et al. 1990, 1993). *AbmA*, DMIB, *AbmC*, DMID, and DMIE genes are also called as *myo*A, *myo*B, *myo*C, *myo*D, and *myo*E, respectively, according to the nomenclature proposed by Kuspa et al. (1993).

Table 1

Dictyostelium myosin's

Class	Type		Reference
Conventional myosin	myosin-II	(P)	Clarke & Spudich (1974)
	*mhc*A	(G)	De Lozanne et al. (1985)
		[M]	De Lozanne & Spudich (1987)
		[M]	Knecht & Loomis (1987)
	EMLC	(G) [M]	Pollenz & Chisholm (1991)
Unconventional myosin	myosin-I	(P)	Côté & Bukiejko (1987)
	*myo*A (*abm*A)	(G)	Titus et al. (1989)
		[M]	Titus et al. (1993)
	*myo*B	(G)	
	=*myosin-I*		Jung et al. (1989)
	=*abmB*		Titus et al. (1989)
	=DMIHC	[M]	Jung & Hammer (1990)
	=DMIB	[M]	Wessels et al. (1991)
	*myo*C (*abmC*)	(G)	Titus et al. (1989)
	*myo*D (DMID)	(G)	Urrutia et al. (1990)
		[M]	Jung et al. (1993)
	*myo*E (DMIE)	(G)	Urrutia et al. (1993)

(P) Protein, (G) Gene, [M] Mutant

Dictyostelium myosin-I has been localized at the leading edges of lamella in migrating as well as dividing amoebae (Fukui et al. 1989). This antibody recognizes both myoB and myoD (John Hammer personal communication). This localization, supported by the postulated membrane-binding domain at the tail and the second ATP-insensitive actin-binding domain near the head, led the authors to suggest a role of myosin-I in the membrane protrusion at the lamella. It is also possible that some of the myosin-I family might be localized at certain population of the membrane vesicles and involved in their movement in the cytoplasm. The feasibility for the myosin-I function remains to be verified. It must be reminded that, at the time of writing this paper, seven different myosin subfamilies have been identified in a variety of systems and myosin-I and II are only two of them (Cheney et al. 1993). Therefore, another class of myosin may be identified from *Dictyostelium*, in the near future.

2.2. New actin-binding proteins

2.2.1. Profilins

Profilin is a monomer-binding type actin-binding protein that is believed to play a role in regulating the actin polymerization *in vivo*. This protein has been suggested to be involved in the signal transduction in linking the membrane events to the cytoskeletal reorganization through binding to phosphatidylinositol 4,5-bisphosphate (PIP_2) (Lassing and Lindberg 1985). A ligand-stimulated activation of phospholipase C (PLC) results in splitting PIP_2 into diacylglycerol (DAG) and 1,4,5-inositoltriphosphate (IP_3). In *Dictyostelium*, it has been indicated that IP_3 brings in secretion of calcium from the reservoir (Newell 1986, Europe-Finner and Newell 1986). Shariff and Luna (1993) recently showed that DAG interacts with actin in such a way that accelerate the polymerization, probably assisted with not yet determined factor(s). Two profilin isomers (I, II) have been isolated from *Dictyostelium* (Haugwitz et al. 1991). In this study, they produced a monoclonal antibody against profilin-I and used to clone a gene and cDNA for profilin-I and II, respectively. They verified that these isoforms have similar properties to profilins from other organisms (Table 2). The interaction of *Dictyostelium* profilins with PIP_2, however, has not been demonstrated. The current concept for the possible link between the signal transduction and the actin cytoskeleton is illustrated in Fig. 1.

2.2.2. Aginactin

Aginactin ("agonist-regulated-inhibitor of actin polymerization" is a new barbed-end-capping protein isolated as an inhibitor of actin polymerization in *Dictyostelium* lysate (Sauterer et al. 1991). It is a 70,000-dalton globular protein, is a Ca^{2+}-insensitive actin-binding protein, and its activity decreases to about 50% of the original inhibition after five seconds of a cyclic-AMP stimulation. A possible role of this protein for the chemotactic migration *via* stimulating the actin polymerization, by increasing free barbed ends, has been proposed (Condeelis 1992). Neither the nucleation nor severing activity has been observed *in vitro* (Sauterer et al. 1991).

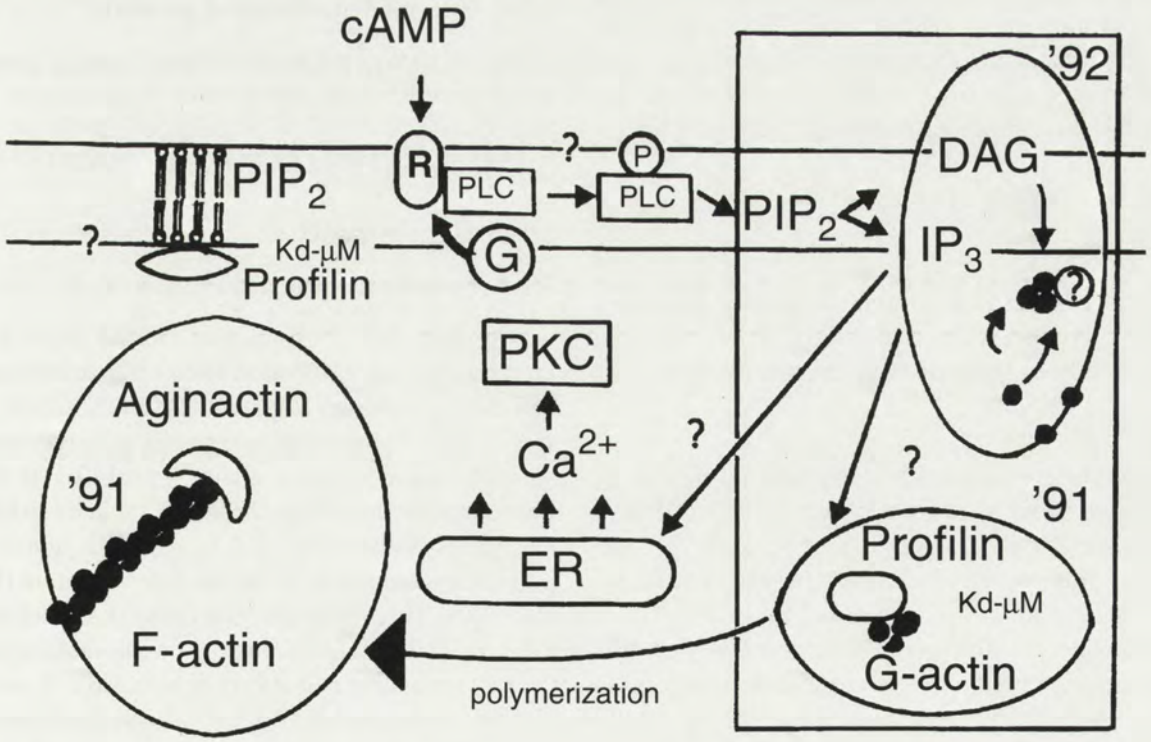

Fig. 1. Possible linkage between the signal transduction and the actin polymerization in *Dictyostelium discoideum* as of June, 1993. Aginactin is a newly identified "agonist-regulated-inhibitor of actin polymerization" (Sauterer et al.1991). Two profilin isoforms (profilin-I and II) have been isolated and characterized (Haugwitz et al. 1991). A possible role of diacylglycerol (DAG) for regulating actin assembly has been suggested (Shariff and Luna 1992)

Table 2

Property of *Dictyostelium* Profilin Isoforms.

Isoform	Size	pI	Kd vs. G-actin
I	0.7 kb (13,064 Da)	5.2	5.1×10^{-6} M
II	0.6 kb (12,729 Da)	6.81.	8×10^{-6} M

(Source) Haugwitz M., Noegel A. A., Rieger D., Lottspeich F., Schleicher M. (1991) *J. Cell Sci.* 100, 481-489.

2.2.3. Coronin

Coronin is a 55,000-dalton protein isolated from the actomyosin complex of *Dictyostelium* that exhibits a crosslinking activity of filamentous (F-) actin *in vitro* (Hostos et al. 1991). The co-sedimentation with F-actin was Ca^{2+}-insensitive. They also suggested that coronin, as predicted from cDNA, has an isoelectric point of 7.4, and molecular weight of 49,000 daltons. Interestingly, the primary sequence showed a high similarity to the β subunit of human transducin, a type of G protein. They named this protein *"coronin"* because it was localized at the crown-like surface projections. The null mutants (*cor*$^-$) have been created by the gene replacement (Hostos et al. 1993). They grew and migrated more slowly than the wild type and were particularly defective in cell division, forming multinucleated cells. This indicated a role of this protein in cytokinesis. However, the *cor*$^-$ cells still formed the crown-shaped projections and the actin organization appeared normal in these structures.

2.3. Other cytoskeletal components

2.3.1. Tubulins

α and β-tubulins were immunologically identified from *Dictyostelium* (White et al. 1983). So far, however, they have not been isolated from *Dictyostelium*.

2.3.2. Kinesin

A kinesin-like protein has been partially purified from *Dictyostelium* (McCaffrey and Vale 1989). It had a molecular weight of 105,000-daltons in SDS gel, and sedimented at about 9S in sucrose gradient centrifugation.

The *in vitro* motility assay demonstrated that this protein induced microtubule translocation along glass surface at the velocity four times greater than that by squid kinesin (2.0 μm/sec versus 0.5 μm/sec). Uniquely, the *Dictyostelium* kinesin was immunologically distinctive from both squid and bovine neuronal kinesins. Another distinctive feature of the *Dictyostelium* kinesin was that the binding to microtubules was decreased by a nonhydrolyzable ATP analog, adenylyl imidodiphosphate (AMP-PNP), that is usually promoted in other kinesins.

2.3.3. Dynein

Dictyostelium dynein has been isolated as a high molecular weight microtubule binding protein (Koonce and McIntosh 1990). It had a sedimentation velocity of 20S and showed an ATP-sensitive binding to microtubules as well as the UV-vanadate mediated fragmentation and a prominent CTPase activity that is unique to cytoplasmic dyneins. It also exhibited a property to support the microtubule movement *in vitro*. The immunofluorescence staining localized the dynein at the region of microtubule organizing center as well as vesicular structures in the cytoplasm. The same group cloned a dynein heavy chain gene (Koonce et al. 1992). The predicted molecular weight was 538,482-daltons, and it had a high homology to β-dynein heavy chain from sea urchin flagellar. The primary sequence suggested that the amino terminus might be responsible for the differences between the cytoplasmic or flagellar type dyneins.

2.3.4. Intermediate filament proteins

As of today, no intermediate filament proteins or genes have been identified from *Dictyostelium*.

3. PHENOTYPES OF THE MUTANTS

3.1. Myosin mutants

3.1.1. Conventional myosin mutants

The first myosin-II mutant (*hmm*) created by the homologous recombination showed a severe defect in cell division and development (De Lozanne and Spudic 1987). This mutant only expresses a heavy meromyosin-like truncated heavy chain (hmm140). It has been demonstrated that while these mutant cells exhibit normal phagocytosis, they fail to establish authentic cell polarity and is unable to cap surface receptors (Fukui et al. 1990). This study also revealed the mechanism of irregular cell division occurring on the substratum when the cell maintains cell-substrate adhesion. It was found that the contractile ring formation was abolished but the actin organization appeared to be normal. They named this mechanism "traction-mediated cytofission". They also showed that the Triton X-100 permeabilized=cytoskeleton of *hmm* cell does not contract in response to Mg^{2+}-ATP. Wessels et al. (1988) showed that this cell

moves slowly (2.3 μm/min) compared with wild type (5.9 μm/min) by using a computer-assisted motion analysis.

The mutant that lacks a complete myosin-II heavy chain (*mhcA*$^-$) has been generated by the gene replacement (Manstein et al. 1989). This null mutant manifested basically the same phenotypes as *hmm* cells. Egelhoff et al. (1991) demonstrated that a tail domain responsible for the phosphorylation of threonine residues (C34) is necessary for the myosin filament disassembly. In this study, the mutant (pSB-3) that expressed a truncated heavy chain lacking the 34,000-dalton carboxyl terminus exhibited a temporal defect in filament dissociation from beneath the capped surface receptors. More recently, a mutant that expresses only less than 0.5% of normal essential light chain (EMLC) was created (Pollenz et al. 1992). This mutant also showed a similar phenotypic defect as the heavy chain mutants. The summary of the phenotypes of conventional myosin mutants is shown in Table 3.

3.1.2. Small myosin mutants

Jung et al. (1990) isolated a mutant defective in DMIHC gene by the gene replacement (DMIHC$^-$). This mutant was capable of cytokinesis and showed normal growth in suspension. However, it showed a delay in aggregating movement and in initial uptake of bacteria. Since then, Titus' and Hammer's groups have identified at least five myosin-I genes in *Dictyostelium* (Titus et al. 1989, Hammer 1990) and, therefore, the original DMIHC$^-$ mutant was later named DMIB$^-$. Its motility has been characterized in detail using a motion analysis system (Wessels et al. 1991). They showed that DMIB$^-$ cell does form lateral pseudopods three times more than the wild type, turn more often, and moves slowly. Titus et al. (1993) recently isolated *myo*A$^-$ mutant to reveal that the phenotype of this mutant closely resembles that of DMIB$^-$. Novak and Titus (1993) reported that the double mutants, *myo*A/B and *myo*B/C, manifest slower growth and development. The summary of the phenotypes of myosin-I mutant's is shown in Table 4.

3.2. Actin-binding protein (ABP) mutants

3.2.1. α-Actinin mutants

Wallraff et al. (1986) isolated a mutant that expressed only a trace amount of α-actinin by the colony blotting technique. The mutant (HG1130) grew and developed normally. It also exhibited normal patching as well as capping of surface glycoproteins. Schleicher et al. (1988) further characterized this mutant to reveal that it expressed 1.1% of the normal level of α-actinin as revealed by a radio-immuno competition assay. The immunoblotting using several monoclonal antibodies recognizing different epitopes verified that almost the entire molecule of α-actinin was lacking from this mutant. A careful measurement of the growth indicated that there appeared to be a slight disadvantage as compared to the wild type (Table 5).

3.2.2. Severin mutant

Severin is a 40,000-dalton actin-binding protein that severs F-actin in a Ca^{2+}-dependent manner (Brown et al. 1982). It has been revealed that *Dictyostelium* has a single copy of severin gene and its actin severing domain shares a homology with gelsolin and villin (André et al. 1988). However, a mutant (HG1132), selected by the colony blotting method, grew, aggregated, and formed apparently normal fruiting bodies bearing viable spores (André et al. 1989) (Table 5).

Table 3

Phenotypes of Myosin-II Mutants of *Dictyostelium*

Mutant	Motility	Cell Division	Development	Capping	Phagocytosis	Reference
hmm	Abnormal	Do not divide in suspension	Arrested at ripple stage		Normal	DeLozzane & Spudich (1987)
*mhcA**	Abnormal	Do not divide in suspension	Arrested at ripple stage		Normal	Knecht & Loomis (1987)
hmm	Loss of Polarity (Actin normal)	"Traction- mediated cytofission"		Arrested	Normal	Fukui et al. (1990)
7-11 (EMLC)*	?	Do not divide in suspension	Arrested at ripple stage	Arrested	?	Pollenz et al. (1992)

*Anti-sense mRNA mutation. A low level of normal protein is co-expressed.

Table 4

Phenotypes of Myosin-I Mutants of *Dictyostelium*

Mutant	Motility	Cell Division	Development	Phagocytosis	Reference
*myo*A$^-$	Turn more often	Looks normal	Slight delay	?	Titus et al. (1993)
*myo*B$^-$ (DMIHC$^-$)	Turn more often	Looks normal	Slight delay	Slow	Jung & Hammer (1990) Wessels et al. (1991)
*myo*A/B$^-$ *myo*B/C$^-$	?	Slow	Slow	?	Novak & Titus (1993)
*myo*D$^-$ (DMID$^-$)	?	Looks normal	?	?	Jung et al. (1993)

Table 5

Phenotypes of ABP Mutants of *Dictyostelium*

Component	Motility	Cell Division	Development	Capping	Phagocytosis	Reference
α-actinin * (1.1% of normal level)	Looks normal	Slight dis-advantage	Looks normal	Normal	Looks normal	Wallraff et al. (1986) Schleicher et al. (1988)
severin *	Very normal	Looks normal	Looks normal	?	Looks normal	André et al. (1989)
ABP=120*	Looks normal	Looks normal	Looks normal	Looks normal	?	Brink et al .(1990)
ABP=120	Slow movement Defects in pseudopod	?	?	?	?	Cox et al. (1992)
α-actinin* and ABP=120 or α-actinin and ABP=120*	Looks normal	Looks normal	Arrested at ripple stage	?	Looks normal	Witke et al. (1992)
coronin	Slow movement, Large size	Multi-nucleation in liquid culture	Capable to develop	?	Defictive ? (slow growth on bacteria)	Hostos et al. (1993)

*: Low level of the protein expressed.

3.2.3. Gelation factor (ABP-120) mutant

Brink et al. (1990) isolated the mutant (HG1264) by the colony blotting method after mutagenesis with nitrosoguanidine. This mutant expressed no detectable level of the gelation factor ABP-120. The deletion appeared to occur on the entire molecule. The cell fraction did not induce gelation of F-actin, further demonstrating the lack of ABP-120 from this mutant. Surprisingly, this mutant did not manifest visible abnormality in growth, morphology, motility, aggregation, and development. Witke et al. (1992) created the double mutants (AG3, AG11) that lack both gelation factor ABP-120 and α-actinin genes by disrupting the ABP-120 gene in the HG1130 mutant. The mutant did not exhibit apparent defects in growth, aggregation, or phagocytosis. However, the development was arrested at the ripple stage and the mutant did not develop into the slug.

More recently, Condeelis and colleagues created the ABP-120 mutants by the gene targeting (Cox et al. 1992). They characterized nine independent transformants demonstrating that the mutants were defective in pseudopod formation. This conclusion was made based on a collaborative study with Soll's group using a high-sensitive motion analysis system. They showed that the mutants move more slowly than the wild type and are defective in both the rate and extent of pseudopod formation. It seems that the lack of ABP-120 causes only a subtle change in motility to the extent that they are not visible using standard techniques (Table 5).

3.2.4. Coronin mutant

The null mutant (*cor*$^-$) was generated by the gene replacement (Hostos et al. 1990). Among ten isolates, they characterized four clones (HG1568, HG1569, HG1570, and HG1571). All of them showed a clear defect in cell division and became multinucleated in both liquid and dish cultures. This defect seem to be responsible for slow growth. The slow growth was observed in both axenic and bacterial cultures. The cells looked irregular in shape (probably because of multinucleation) and had numerous vacuoles. These defects were superficially similar to the myosin-II mutants. However, different from the latter, *cor*$^-$ was able to develop on substratum and formed fruiting bodies. Since coronin had been localized at the crown-shaped surface projections, they carefully investigated the mutant's phenotype with this respect. They observed that the *cor*$^-$ cells still formed apparently normal-looking crowns and the actin organization in this structure was also normal (Table 5).

3.2.5. Summary of the ABP mutants

α-Actinin is one of the most conservative actin-binding proteins, and it has a distinctive F-actin crosslinking activity *in vitro*, usually in a Ca^{2+}-sensitive manner. Severin is also a type of actin-binding protein existing in a wide variety of systems. Therefore, it is mysterious why the mutants of these major ABPs reportedly do not exhibit clear defects. The defect of ABP-120 seems very specific and very subtle in a sense that it is not visualized without using the state-of-the-art motion analysis system. It is probably fair to say that we may not have adequate method to measure the cell's behavioral defects. The coronin mutants showed clear defects in cell division in both suspension and Petri dishes. The biochemical property of this protein must be fully understood. A possible significance of the G-protein-like domain of coronin must be also elucidated.

Table 6

Models of the nonmuscle cell motility for the actomyosin system.

Category	Components	Models	Reference
Flow	Actin	Tread milling	Wang (1985)
	Lipid	Membrane flow	Bretcher (1988)
	F-Actin	Cortical flow	Bray and White (1988)
	F-Actin	Retrograde flow	Forscher and Smith (1988)
	Membrane-cytoskeleton	Centripetal flow	Grębecki (1990)
	Lipid	Tank track	Lee et al. (1990)
Polymerization	Actin	Polymerization force	Tilney and Inoué (1985)
	Actin	Brownian ratchet	Oster and Perelson (1993)
Osmosis	Actin gel	Gel osmosis	Oster (1988)
	Actin gel	Cortical expansion	Condeelis (1992)
	Actin gel	Solation-expansion	Oster and Perelson (1993)
	Acrosomal process	Osmotic-hydrostatic pressure	Oster and Perelson (1993)
Motor	Myosin-II	Sliding filament	Clarke and Spudich (1977) Fukui and Yumura (1986)
	Myosin-I	Projectile force	Fukui et al. (1989)
	Myosin-I	Motor-induced	Sheetz et al. (1992)
	Myosin-II oligomers	Biased friction	Fukui (1993)
Others	Myosin-II	Continuous cortical contraction	Grębecki (1990)
	F-Actin	Nucleation-release	Theriot & Mitchison (1991)
	Network complex	Stick and string tensegrity	Ingber (1993)

4. MECHANISMS

A wide spectrum of mechanisms for the force generation in nonmuscle cell motility has been proposed in the last decade. This includes the "lipid flow", "cortical flow", "centripetal flow", "tread milling", "actin polymerization", "gel osmosis", and "motor-induced projection" and "retraction" to mention a few (Table 6).

The "lipid flow" model by Bretcher (1988) has been questioned by Jacobson's group and the latter proposed a "tank track" model as an alternative mechanism (Lee et al., 1990). The "centripetal flow" of the membrane-cytoskeleton has been proposed for free-living amoebas, including *Amoeba proteus* and *Chaos* (Grębecki 1990). For a comprehensive review about the membrane flow models, refer to Grębecki (1993). A rearward flow of

actin (Wang 1985, Forsher and Smith 1988) and the rearrangement of actin filaments ("cortical flow": Bray and White 1988) could be classified into the same category. The "polymerization" force derived by the subunit addition on actin filament (Tilney and Inoué 1985) has been reevaluated by Oster and Perelson (1993). The latter proposes a "Brownian ratchet" model instead. The "nucleation-release" model by Mitchison and colleagues (Theriot and Michison 1991) suggests that the locomotion of goldfish epithelial keratocytes are driven by assembly of new actin filament at the leading edge. In this system, they observed no net rearward flux of the actin subunits. Without doubts, there is a dynamic change of actin organization coupled with cell movement. There also seems to be a variation in its mechanism depending on the system.

The "gel swelling" provides an attractive mechanism for cell movement (Oster 1988). Condeelis (1992) suggested a similar mechanism named the "cortical expansion" model. In this model, he suggests that the cAMP-induced pseudopod formation derives from action of an agonist-regulated actin capping protein. Oster and Perelson (1993) recently suggested that the elongation of the acrosomal process occurs by virtue of actin polymerization driven by the hydrostatic pressure difference ("osmotic-hydrostatic pressure" model), rather than the direct polymerization force. The expansion, and possibly the retraction, of pseudopods and lamellipods appear to be driven by a stoichiometric change in the gel structure that is independent from both actin polymerization and myosin-dependent mechanochemical transduction mechanisms. The ability of formation of cortical structure in myosin null mutants fortifies the feasibility of the gel osmosis model.

The myosin-based motors, without reservation, participate in contractile as well as projectile force generation in cell motility. The mechanisms include the "sliding-filament" (Clarke and Spudich 1977, Fukui and Yumura 1986) and the "projectile force" mechanisms (Fukui et al. 1989, Sheetz et al. 1992). Grębecki suggests that the myosin-II-based sliding brings in a "continuous contraction" to the cortical cytoskeleton (for review, refer to Grębecki 1993). Fukui recently suggested a frictional force ("biased friction") that is brought about with the vectorial translocation of myosin-II subunits of oligomers toward the posterior cortex (Fukui 1993).

There have been substantial evidence accumulated for the building of integrated architecture consisting different cytoskeletal components. Ingber's "tensegrity" model suggests a torsional force produced at receptor-extracellular matrix complex in response to the mechanical stress (Ingber 1993). He proposes a stick-and-string toy model that may transduce the mechanical stress applied to the complex to the cytoplasm. This is an attractive model that may be applicable to a broad spectrum of mechano-transduction systems.

The biomechanical forces responsible for the cell motility have been measured *in vivo* and *in vitro*. Some of the forces have been also theoretically estimated. All those forces are several thousands fold greater than the force necessary to bring in shape change and locomotion. Another necessary consideration is that there are multiple isoforms that appear sharing similar functions. Provided that two isoforms in a single subfamily that consists ten different components were involved in manifesting one phenotype, the total number of the random combination of two is forty-five. In other words, the chances that one could find a clear functional defect caused by a double knocking out experiment were 2.2%. If three components were involved, this probability goes down to one in one-hundred twenty; that is 0.8%. Taking these possibilities into consideration, the idea now evolves why many of the cytoskeletal mutants do not exhibit clear phenotypic defects. One should be also aware that some of the defects only manifest themselves as behavioral abnormality, and currently we do not have simple techniques to measure the cell's misbehavior. This subject has been discussed in a recent review (Fukui 1993).

Acknowledgments. This study was supported by NIH GM39548.

REFERENCES

André E., Brink M., Gerisch G. (1989) A *Dictyostelium* mutant deficient in severin, an F-actin fragmenting protein, shows normal motility and chemotaxis. J. Cell Biol. 108: 985-995.

André E., Lottspeich F., Schleicher M., Noegel A. (1988) Severin, gelsolin, and villin share a homologous sequence in regions presumed to contain F-actin severing domains. J. Biol. Chem. 263: 722-727.

Bray D., White J. G. (1988) Cortical flow in animal cells. Science 239: 883-888.

Bretcher M. S. (1988) Fibroblasts on the move. J. Cell Biol. 106, 235-237.

Brink M., Gerisch G., Isenberg G., Noegel A. A., Segall J. E., Wallraff E., Schleicher M. (1990) A *Dictyostelium* mutant lacking an F-actin cross-linking protein, the 120-kD gelation factor. J. Cell Biol. 111: 1477-1489.

Brown S. S., Yamamoto K., Spudich J. A. (1982) A 40,000-dalton protein from *Dictyostelium discoideum* affects assembly properties of actin in a Ca^{2+}-dependent manner. J. Cell Biol. 93: 205-210.

Cheney R. E., Rile M. A., Mooseker M. S. (1993) Phylogenetic analysis of the myosin superfamily. Cell Motil. Cytoskel. 24: 215-223.

Clarke M., Spudich J. A. (1974) Biochemical and structural studies of actomyosin-like proteins from non-muscle cells. J. Mol. Biol. 86: 209-222.

Clarke M., Spudich J. A. (1977) Nonmuscle contractile proteins: The role of actin and myosin in cell motility and shape determination. A. Rev. Biochem. 46: 797-822.

Condeelis J. (1992) Are all pseudopods created equal. Cell Motil. Cytoskel. 22: 1-6.

Côté G. P., Bukiejko U. (1987) Purification and characterization of a myosin heavy chain kinase from *Dictyostelium discoideum*. J. Biol. Chem. 262: 1065-1072.

Cox D., Condeelis J., Wessels D., Soll D., Kern H., Knecht D. A. (1992) Targeted disruption of the ABP-120 gene leads to cells with altered motility. J. Cell Biol. 116: 943-955.

De Lozanne A., Spudich J. A. (1987) Disruption of the *Dictyostelium* myosin heavy chain gene by homologous recombination. Science 236: 1086-1091.

De Lozanne A., Lewis M., Spudich J. A., Leinwand L. A. (1985) Cloning and characterization of a nonmuscle myosin heavy chain cDNA. Proc. natl. Acad. Sci. U.S.A. 82: 6807-6810.

Egelhoff T. T., Brown S. S., Spudich J. A. (1991) Spatial and temporal control of nonmuscle myosin localization: identification of a domain that is necessary for myosin filament disassembly *in vivo*. J. Cell Biol. 112: 677-688.

Europe-Finner G. N., Newell P. C. (1986) Inositol 1,4,5-triphosphate induces calcium release from a non-mitochondrial pool in amoebae of *Dictyostelium*. Biochem. Biophys. Acta 887: 335-340.

Forscher P., Smith S. J. (1988) Actions of cytochalasins on the organization of actin filaments and microtubules in a neuronal growth cone. J. Cell Biol. 107: 1505-1516.

Fukui Y. (1993) Toward a new concept of cell motility: Cytoskeletal dynamics in amoeboid movement and cell division. Int. Rev. Cyt. 144: 85-127.

Fukui Y., Inoué S. (1991) Cell division in *Dictyostelium* with special emphasis on actomyosin organization in cytokinesis. Cell Motil. Cytoskel. 18: 41-54.

Fukui Y., Inoué S. (1992) Cytokinesis in *Dictyostelium discoideum*. Cell Motil. Cytoskel. Video Suppl. vol. 3, (Eds. J. M. Sanger, J. W. Sanger), Wilet-Liss and Sons, Inc., New York.

Fukui Y., Yumura S. (1986) Actomyosin dynamics in chemotactic amoeboid movement of *Dictyostelium*. Cell Motil. Cytoskel. 6: 662-673.

Fukui Y., De Lozanne A., Spudich J. A. (1990) Structure and function of the cytoskeleton of a *Dictyostelium* myosin-defective mutant. J. Cell Biol. 110: 367-78.

Fukui Y., Lynch T. J., Brzeska H., Korn E. D. (1989) Myosin I is located at the leading edges of locomoting *Dictyostelium* amoebae. Nature 341: 328-331.

Grębecki A. (1990) Dynamics of the contractile system in the pseudopodial tips of normally locomoting amoebae, demonstrated in vivo by video-enhancement. Protoplasma 154: 98-111.

Grębecki A. (1993) Membrane and cytoskeleton flow in motile cells with emphasis on the contribution of free-living amoebae. Int. Rev. Cyt. (in press).

Hammer J. A. III (1991) Novel myosins. Trends in Cell Biology, 1: 50-56.

Haugwitz M., Noegel A. A., Rieger D., Lottspeich F., Schleicher M. (1991). *Dictyostelium discoideum* contains two profilin isoforms that differ in structure and function. J. Cell Sci. 100: 481-489.

Hostos E. L. de, Bradtke B., Lottespeich F., Guggenheim R., Gerisch G. (1991) Coronin, an actin binding protein of *Dictyostelium discoideum* localized to cell surface projections, has sequence similarities to G protein β subunits. EMBO J. 10: 4097-4104.

Hostos E. L. de, Rehfueß C., Bradtke B., Waddell D. R., Albrecht R., Murphy J., Gerisch G. (1993) *Dictyostelium* mutants lacking the cytoskeletal protein coronin are defective in cytokinesis and cell motility. Cell Biol. 120: 163-173.

Ingber D. E. (1993) Cellular tensegrity: defining new rules of biological design that govern the cytoskeleton. J. Cell Sci. 104: 613-627.

Jung G., Hammer J. A. III (1990) Generation and characterization of *Dictyostelium* cells deficient in a myosin I heavy chain isoforms. J. Cell Biol. 110: 1955-1964.

Jung G., Fukui Y., Martin B., Hammer J. A. III (1993) Sequence, expression pattern, intracellular localization and targeted disruption of the *Dictyostelium* myosin ID heavy chain isoform. J. Biol Chem. 268: 14981-14990.

Jung G., Saxe C. L., Kimmel A. R., Hammer J. A. III (1989) *Dictyostelium discoideum* contains a gene encoding a myosin I heavy chain. Proc. natl. Acad. Sci. U.S.A. 86: 6186-6190.

Knecht D. A., Loomis W. F. (1987) Antisense RNA inactivation of myosin heavy chain gene expression in *Dictyostelium discoideum*. Science 236: 1081-1086.

Koonce M. P., McIntosh J. R. (1990) Identification and immunolocalization of cytoplasmic dynein in *Dictyostelium*. Cell Motil. Cytoskel. 15: 51-62.

Koonce M. P., Grissom P. M., McIntosh J. R. (1992) Dynein from *Dictyostelium*: Primary comparison between a cytoplasmic motor enzyme and flagellar dynein. J. Cell Biol. 119, 1597-1604.

Korn E. D. (1991) *Acanthamoeba* myosin I: Past, present, and future. In: Ordering the Membrane-Cytoskeleton Trilayer. Current Topics in Membranes. (Eds. M. S. Mooseker and J. S. Morrow). Academic Press, San Diego, 30: 13-30.

Kuspa A., Maghakian D., Bergesch P., Loomis W. F. (1993) Physical mapping of genes to specific chromosomes in *Dictyostelium discoideum*. Genomics 13: 49-61.

Lassing I., Lindberg U. (1985) Specific interaction between phosphatidylinositol 4,5-bisphosphate and profilactin. Nature 314: 472-474.

Lee J., Gustafsson M., Magnusson K.-E., Jacobson K. (1990) The direction of membrane lipid flow in locomoting polymorphonuclear leukocytes. Science 247: 1229-1233.

Manstein D. J., Titus M. A., De Lozanne A., Spudich J. A. (1989) Gene replacement in *Dictyostelium*: Generation of myosin null mutants. EMBO J. 8: 923-932.

McCaffrey G., Vale R. D. (1989) Identification of a kinesin-like microtubule-based motor protein in *Dictyostelium discoideum*. EMBO J. 8: 3229-3234.

Newell P. C. (1986) The role of actin polymerization in amoebal chemotaxis. BioEssays 5: 208-211.

Novak K. D., Titus M. A. (1993) *Dictyostelium* cells devoid of two unconventional myosins show defects in growth. Mol. Biol. Cell 3: 3a.

Oster G. (1988) Biophysics of the leading lamella. Cell Motil. Cytoskel. 10: 164-171.

Oster G., Perelson A. S. (1993) Cell protrusions. In: Frontiers in Mathematical Biology. Lecture Notes in Biomathematics. (Ed. S. Levin), Springer-Verlag, Berlin, 100: (in press).

Pagh K., Maruta H., Claviez M., Gerisch G. (1984) Localization of two phosphorylation sites adjacent to a region important for polymerization on the tail of *Dictyostelium* myosin. EMBO J. 3: 3271-3278.

Pasternak C., Flicker P. F., Ravid S., Spudich J. A. (1989) Intermolecular versus intramolecular interactions of *Dictyostelium* myosin: Possible regulation by heavy chain phosphorylation. J. Cell Biol. 109: 203-210.

Pollard T. D., Doberstein S. K., Zot H. G. (1991) Myosin-I. A. Rev. Physiol. 53: 653-681.

Pollenz R. S., Tung-Ling L. C., Trivinos-Lagos L., Chisholm R. L. (1992) The *Dictyostelium* essential light chain is required for myosin function. Cell 69: 951-962.

Sauterer R. A., Eddy R. J., Hall A. L., Condeelis J. S. (1991) Purification and characterization of aginactin, a newly-identified agonist-regulated actin capping protein from *Dictyostelium* amoebae. J. Biol. Chem. 266: 24533-24539.

Schleicher M., Noegel A. A. (1992) Dynamics of the *Dictyostelium* cytoskeleton during chemotaxis. The New Biologist 4: 461-472.

Schleicher M., Noegel A., Schwarz T., Wallraff E., Brink M., Faix J., Gerisch G., Isenberg G. (1988) A *Dictyostelium* mutant with severe defects in -actinin: its characterization using cDNA probes and monoclonal antibodies. J. Cell Sci. 90: 59-71.

Shariff A., Luna E. J. (1992) Diacylglycerol-stimulated formation of actin nucleation sites at plasma membranes. Science 256: 245-247.

Sheetz M. P., Wayne D. B., Pearlman A. L. (1992) Extension of filopodia by motor-dependent actin assembly. Cell Motil. Cytoskel. 22: 160-169.

Spudich J. A. (1989) In pursuit of myosin function. Cell Regul. 1: 1-11.

Theriot J. A., Mitchison T. J. (1991) Actin microfilament dynamics in locomoting cells. Nature 352: 126-131.

Tilney L. G., Inoué S. (1985) Acrosomal reaction of *Thyone* sperm. III. The relationship between actin assembly and water influx during the extension of the acrosomal process. J. Cell Biol. 100: 1273-1283.

Titus M. A., Warrick H., Spudich J. A. (1989) Multiple actin-based motor genes in *Dictyostelium*. Cell Regul. 1: 55-63.

Titus M. A., Wessels D., Spudich J. A., Soll D. (1993) The unconventional myosin encoded by the *myo*A gene plays a role in *Dictyostelium* motility. Mol. Biol. Cell 4: 233-246.

Urrutia R. A., Jung G., Hammer J. A. III (1990) Cloning of the *Dictyostelium* myosin IE gene. J. Cell Biol. 111: 168a.

Urrutia R. A., Jung G., Hammer J.A. III (1993) The *Dictyostelium* myosin IE heavy chain gene encodes a truncated isoform that lacks sequences corresponding to the actin binding site in the tail. Biochem. Biophys. Acta 1173: 225-229.

Wallraff E., Schleicher M., Modersitzki M., Rieger D., Isenberg G., Gerisch G. (1986) Selection of *Dictyostelium* mutants defective in cytoskeletal proteins: use of an antibody that binds to the ends of alpha-actinin rods. EMBO J. 5: 61-67.

Wang. Y.-L. (1985) Exchange of actin subunits at the leading edge of living fibroblasts: Possible role of treadmilling. J. Cell Biol. 101: 597-602.

Wessels D., Murray J., Jung G., Hammer J. A. III, Sol D. R. (1991) Myosin IB null mutants of *Dictyostelium* exhibit abnormalities in motility. Cell Motil. Cytoskel. 20: 301-315.

Wessels D., Soll D. R., Knecht D., Loomis W. F., De Lozanne A., Spudich J. A. (1988) Cell motility and chemotaxis in *Dictyostelium* amoebae lacking myosin heavy chain. Dev. Biol. 128: 164-177.

White E., Tolbert E. M., Katz E. R. (1983) Identification of tubulin in *Dictyostelium discoideum:* Characterization of some unique properties. J. Cell Biol. 97: 1011-1019.

Witke W., Schleicher M., Noegel A. A. (1992) Redundancy in the microfilament system. *Dictyostelium* cells that lack two F-actin crosslinking proteins show abnormal multicellular development. Cell 68: 53-62.

Yumura S., Fukui Y. (1985) Reversible cyclic AMP-dependent change in distribution of myosin thick filaments in *Dictyostelium*. Nature 314: 194-196.

Received on 3rd August, 1993

ACTA
PROTOZOOLOGICA

Acta Protozoologica (1993) 32: 211 - 227

Structural and Physiological Basis of Axopodial Dynamics

Colette FEBVRE-CHEVALIER and Jean FEBVRE

Laboratoire de Biologie Cellulaire Marine URA 671 C.N.R.S., Observatoire Océanologique de Villefranche-sur-Mer, Villefranche-sur-Mer, France

1. INTRODUCTION

Axopodia, one of the major categories of cytoplasmic projections in single cell eukaryotes (Protozoa), extend radially in all directions from the cell surface in the Phylum Actinopoda (Classes: Acantharia, Heliozoa, Radiolaria=Polycystina and Phaeodaria). Only 5-15 µm in diameter at their bases, the axopodia are stiff, slender and unbranched processes that project 40-800 µm into the surrounding water. As noted by early protozoologists, axopodia are sustained by an axial core consisting of parallel fibers (stereoplasm) surrounded by a thin sheet of cytoplasm (rheoplasm) (Haeckel 1862, Schewiakoff 1926).

During the last 30 years, ultrastructural data have provided evidence that the axial fibers consist of patterned arrays of microtubules (Mts) or axonemes (Cachon and Cachon 1974, Cachon et al. 1990, Dustin 1978, Febvre 1990, Febvre-Chevalier 1990). A closely related system is the cytoplasmic stalk found in some benthic heliozoans. Since it is larger than conventional axopodia, it has allowed us to study the role of the Mts during contraction and subsequent regrowth (Febvre-Chevalier 1980, Febvre-Chevalier and Febvre 1992). The axonemes arise from discrete or conspicuous cytoplasmic foci called microtubule organizing centers (MTOCs) (Pickett-Heaps 1969). These are known to organize the Mt-arrays and to play an active part in Mt-based movements (Tucker 1984, Brinkley 1985, Rose et al. 1993).

Axopodia are involved in a wide number of physiological activities such as food capture (Suzaki et al. 1980, Patterson and Hausmann 1981, Hausmann and Patterson 1982), reproduction (Ockleford 1974, Suzaki et al. 1978), morphogenesis (Bardele 1972) and locomotion (Watters 1968, Cachon et al. 1977). These activities depend upon two distinct but interactive types of cellular functions: membrane sensitivity and cell motility. Axopodia are highly sensitive processes which respond to external triggers by two categories of movements, cytoplasmic transport (Hyams and Stebbings 1979, Edds 1981, Schliwa 1984) and a remarkably rapid and obvious length change of their axopodia accompanied by a complete remodeling of their microtubules (Ando and Shigenaka 1989, Febvre-Chevalier 1981, Febvre-Chevalier and Febvre 1992). Therefore, both axopodia and cytoplasmic stalks of Actinopoda are amenable model systems for studying the cellular and molecular bases of membrane sensitivity and Mt-based dynamics.

This paper reviews the structure of the axopodia in the 4 classes of Actinopoda with attention to patterns

Paper presented at the Symposium Motility, Behaviour and Orientation of the IXth International Congress of Protozoology, July 25th - August 1st, 1993, Berlin, Germany.

Address for correspondence: C.Febvre-Chevalier, Laboratoire de Biologie Cellulaire Marine, URA 671 C.N.R.S., Observatoire Océanologique de Villefranche-sur-Mer, 06230, Villefranche-sur-Mer, France.

and pattern formation. Then, after a brief review of some physiological activities, membrane sensitivity and axopodial motility are examined with special reference to the possible mechanisms of catastrophic Mt-dissociation and axopodial shortening in some species of Heliozoans.

2. STRUCTURE OF THE AXOPODIA

2.1. Microtubules

As in all other eukaryotic cells, the axopodial Mts of Actinopoda are long, hollow cylinders made of the alignment of 13 protofilaments (Tilney et al. 1973), each consisting of alternating heterodimers of α and ß tubulin joined head to tail (Dustin 1984). This molecular organization, makes microtubules polar filaments with "minus" and "plus" ends. This polarity can be revealed by a labelling method in which exogenous tubulin (Heidemann and McIntosh 1980) is added in conditions that promote the formation of asymmetric decorations on the wall of cytoplasmic microtubules during their assembly. It has been shown that all the microtubules in the axonemes of the heliozoan *Actinosphaerium* are oriented with their "plus" ends distal to the cell center and their "minus" ends attached to the MTOC (Euteneur and McIntosh 1981). Microtubules are unstable structures which assemble and disassemble faster from their "plus" than their "minus" ends. In *in vitro* conditions and in living cells, Mts oscillate between phases of growth and rapid shrinkage. This phenomenon, called dynamic instability and suggested 10 years ago, is one of the most stimulating and relevant models of microtubule assembly and disassembly (Mitchison and Kirschner 1984, Mandelkow and Mandelkow 1989). The dynamic instability model may be consistent with the slow contraction or elongation of axopodia. However, it cannot account alone for the catastrophic disassembly kinetics observed in some species during the fast contraction (Febvre-Chevalier and Febvre 1992). Identification and characterization of axopodial tubulins in *Echinosphaerium (Actinosphaerium) nucleofilum* reveals an unusually fast electrophoretic mobility of ß-tubulin. Furthermore, when compared with tubulins from other cells, several differences were found in the two-dimensional peptide maps of tubulin subunits. This distinctiveness of tubulins may reflect the different functional requirements of axopodial microtubules in Heliozoa (Hoffman et al. 1983, Little et al. 1983).

Another general property of Mts is their ability to link with specific structural proteins, mechanoenzymes and other specific microtubule associated proteins (MAPs), nucleotides and ligands. They pack and link to one another to form tightly cohesive and geometric architectures. Although rapid progress has been made in the last few years in the domain of non-motor MAPs, (especially brain MAPs), no data indicating the exact nature of the linkers is presently available for the Actinopoda. In addition, Mt-associated motor molecules that generate forces through the use of energy *via* hydrolysis of nucleotides (Vale 1990) provide direct intra-axopodial traffic, as they do in Amoebae and Foraminifera (Allen et al. 1982; Koonce and Schliwa 1985, 1986; Koonce et al. 1986; Koonce and McIntosh 1990; Travis and Bowser 1986).

2.2. Axonemal microtubule patterns

The axoneme consists of a longitudinal rod of Mts cross-linked by bridges which delineate adjacent microprisms or palisades. In cross sections these Mt-arrays show specific patterns that attain a great complexity in certain taxa (Cachon et al. 1973, 1990; Cachon and Cachon 1974; Bardele 1977a,b; Febvre 1986, 1990; Febvre-Chevalier 1982, 1990) (Fig. 1).

Fig. 1. Summary diagram of the structure of the microtubule organizing centers (MTOCs) (upper part of the figure) and the Mt-patterns in cross section among the four classes of Actinopoda: Heliozoa, Acantharia, Polycystina and Phaeodaria. First column: *Ciliophrys marina*. Tiny MTOCs scattered on the nuclear envelope; triangular pattern (angles between bridges around 60°. Second column: *Actinophrys* and *Echinosphaerium (Actinosphaerium)*. MTOCs scattered on the nuclear envelope; two interlocking coils of Mts; short and long links. Third column: *Dimorpha mutans*. Single massive MTOC inserted in a nuclear invagination (N= Nucleus). Quincunx pattern. Fourth column: Heliozoa *Heterophrys, Raphidiophrys, Acanthocystis*. Single MTOC including a tripartite disc or centroplast. Centered hexagons and triangles. Mts with 4 bridges forming two 60° angles, and two 106° and 134° angles respectively. Fifth column: Heliozoa *Gymnosphaera, Hedraiophrys, Actinocoryne, Sticholonche,* Acantharia. Single MTOC without inner differentiation (A=axoplast). Lengthened hexagons. Three links per Mt with 111°, 111°, 138° angles. In *Sticholonche* the MTOCs (not shown here) are scattered on the nuclear envelope, while in the Acantharia Chaunacanthida and Arthracanthida, they are apposed to the perispicular membrane. Sixth column: Polycystina. MTOCs apposed to the membrane limiting the capsular wall. They can also be included in a nuclear cup (Centroplastidiata) or apposed to the perispicular membrane (Acantharia). Dodecagonal Pattern. Mts with 2 or 3 links. Seventh column: Polycystina Single axoplast in a nuclear invagination. Pseudo "X" pattern delineating curved palisades. Eight column: Phaeodaria. Hemispheric MTOC just below the capsular wall. No observed bridges

2.2.1. Heliozoa

Five types of architecture have been reported among the Heliozoa.

Two interlocking coils of Mts. Cross sections through *Actinophrys* and *Echinosphaerium (Actinosphaerium)* show two interlocking coils of Mts cross-linked by two types of bridges, short links connecting successive microtubules in each spiral and long fine strands uniting the Mts in the adjacent spirals. The overall pattern resembles a spider's web which can be divided into twelve adjacent triangular sectors. (Kitching 1964, Tilney and Porter 1965, McDonald and Kitching 1967, Ockleford and Tucker 1973). A model of pattern formation detailed below was proposed by Roth and coworkers (Roth et al. 1970).

Equilateral triangle. The simplest arrangement was found in the tiny helioflagellate *Ciliophrys marina* (Davidson 1975). Each axopod comprises a single microprism in which only three Mts are linked to one another by bridges (15 μm long) forming 60° angles.

Centric hexagonal patterns. These are built from a structural unit consisting of a microtubule capable of binding a maximum of four linkers. They have been described in several species of heliozoans (O. Phaneraxohelida). In *Heterophrys marina* (Davidson 1975; Bardele 1975, 1977a,b), *Oxnerella maritima* (personal data) and *Chlamydaster fimbriatus* (Dürrschmidt and Patterson 1987) there are only six Mts per axoneme delineating a single slightly distorted hexagon with angles close to 106° and 134°. In other species of *Heterophrys* 6 additional Mts define equilateral triangles forming a star-like pattern (Bardele 1977a,b). In the related heliozoans *Raphidiophrys* and *Acanthocystis* the number of Mts in each axoneme is about a hundred. They are arranged in a lattice of hexagons and equilateral triangles that connect with each other at their corners (Bardele 1977a, Tilney 1971, Dürrschmidt and Patterson 1986-87). Mixed patterns with a single central hexagon and additional Mts delineating other polygons are found in some Heterophryiidae. In *Heterophrys magna* the central hexagon is surrounded by pentagons (Bardele 1977a) while in *Cienkowskya* it is surrounded by a complex system of curved palisades which participate in the formation of triangles, heptagons, enneagons or even larger irregular polygons at the periphery of the rod (Febvre-Chevalier and Febvre 1984).

Using high voltage electron microscopy, a filament (20 nm in diameter) has been visualized in the center of each microprism in *Acanthocystis*. This filament is short and terminates at the periphery of the MTOC. It is connected by electron opaque linkage material to the Mts forming the hexagonal microprisms (Rieder 1979). A similar structure can also be visualized at the base near the MTOC in most other heliozoans.

Hexagonal flooring patterns. In *Sticholonche, Hedraiophrys, Gymnosphaera* and *Actinocoryne* the Mts and the linkers (3 per Mt forming 138°, 111°, 111°) define in cross sections adjacent lengthened hexagons arranged in parallel rows (Hollande et al. 1967; Febvre-Chevalier 1973a, 1975, 1980; Jones 1975; Cachon and Cachon 1978). In *Sticholonche*, the long medians of the hexagons are oriented to the same direction, while in the three other genera the pattern resembles a floor, the long medians in one row of hexagons forming a constant 111° angle with the long medians in the adjacent rows.

A quincunx architecture with 4 long links per Mt *oriented* at 90° has been described in *Dimorpha*. In contrast, irregular patterns have been reported in the three other helioflagellates *Clathrulina, Tetradimorpha* and *Hedriocystis* (Bardele 1972; Brugerolle and Mignot 1983, 1984a,b, 1985).

2.2.2. Polycystina

In the polycystines, two types of arrangements were described:

A dodecagonal pattern was found in the Proaxoplastidiata (O. Nassellarida) (Cachon and Cachon 1971), Periaxoplastidiata (O. Spumellarida, F. Sphaerellarina) (Cachon and Cachon 1972a) and Exo-axoplastidiata (O. Spumellarida, Sphaerocollina) (Cachon and Cachon 1976). In these radiolarians, the first central microtubule links with three neighbor Mts. Then, three divergent primary palisades consisting of the alternation of Mts with two linkers and Mts with three linkers are formed. From the edges of these palisades, secondary identical palisades are generated so that the axial region of the axoneme is constituted of adjacent dodecagons while the palisades are incomplete at the periphery (Cachon and Cachon 1974, Cachon et al. 1990).

X-patterns with only 10 Mts have been described in Cryptoaxoplastidiata (O. Spumellarida, Sphaerellarina) and Exocryptoaxoplastidiata (O. Spumellarida, Sphaerocollina) (Cachon and Cachon 1972a, 1974; Cachon et al. 1990). They are formed from two initial microtubules with three links surrounded by 4 Mts with two bridges attached to four terminal Mts.

A closely related pattern was described in the Centroaxoplastidiata (O. Spumellarida, Sphaerellarina; O. Spu-

mellarida, Sphaerocollina) (Cachon and Cachon 1972b, 1974, 1976a, 1977a). It differs only by the presence of several hundreds of Mts which are arranged around the central pseudo X pattern forming concave primary and secondary palisades.

In the Polycystines, the cytoplasm (endoplasm) being limited by a thick central capsule, the Mt-arrays pass across this barrier via fusules. These special organelles consist of a narrow gullet which is filled with a dense substance and pierced by thin parallel channels (Hollande et al. 1965).

2.2.3. Phaeodaria

Equilateral triangles. In the Phaeodaria, the axonemes consist of Mt-arrays arising from two large pores through the capsular wall named parapyles. Although cross bridges have not been observed, the Mts are very numerous and roughly distributed at the apex of equilateral triangles (Cachon and Cachon 1973).

2.2.4. Acantharia

In the Acantharia two patterns were reported.

Dodecagonal pattern found in *Acanthochiasma,* similar to that described in the Polycystines.

Hexagonal architecture similar to that found in the heliozoans *Sticholonche, Gymnosphaera* and *Actinocoryne.* However, only one or two rows of hexagons are alternating (Febvre 1986, 1990).

2.3. Axopodial organelles

The axopodial cytoplasm can contain membrane-bound organelles, such as dense granules, kinetocysts and mucocysts referred to as extrusomes, mitochondria, "X" bodies, coated or smooth vesicles and tubes of endoplasmic reticulum.

The extrusive organelles, kinetocysts, mucocysts and dense granules shuttle back and forth with uniform velocity in a saltatory motion, as examined below (Fitzharris et al. 1972; Edds 1975a, 1981; Troyer 1975, 1976; Bardele 1976; Suzaki and Shigenaka 1982). These organelles are involved in secretion of mucus and/or enzymes used for food capture, cell-recognition and protection.

The fine structure of the kinetocysts has been studied in detail in several heliozoans. They originate in the endoplasm (Golgi, endoplasmic reticulum) and differentiate an internal dense missile-like structure while they are transported towards the cell membrane (Bardele 1969, 1975). They link to the cell membrane via a rosette of 8-transmembrane particles (Bardele 1976, Davidson 1976). Larger extrusive organelles resembling kinetocysts are also present in the Acantharia and the Radiolaria (Cachon et al. 1990, Febvre 1990). Electrondense bodies are found in Actinophryid heliozoans that apparantly play a role similar to the kinetocysts and mucocysts. Mitochondria are generally scarce in the axopodial cytoplasm. Vesicles are found in the hyaloplasm. They are attached by "arms" to the peripheral microtubules or included within the Mt-microprisms in the acantharians and the radiolarians. In *Thalassicola* these arms measure 15 nm long and consist of a tail (10 nm long) and a head (5 nm in diameter), suggesting that they are mechanoenzymes (Cachon and Cachon 1975, 1976b, 1977b; Febvre 1986). These vesicles appear to be intensely labelled after treatments that precipitate intracellular Ca^{2+}; they may represent internal Ca^{2+} stores (Febvre and Febvre-Chevalier 1989). Tubular filaments (10-27 nm in diameter) arranged in bundles named "X" bodies or morulate bodies have been described in actinophryid heliozoans. They were first thought to sequester excretion products (Tilney and Porter 1965), then, either as artifactual features (Patterson and Hausmann 1982) or as contractile bundles (Suzaki et al. 1980, Ando and Shigenaka 1989). Although filament bundles lying parallel to the Mt-arrays have not been described in the axopodia of other Actinopoda, it is presumed that a thin fibrillar network is present between the Mt-arrays and plays a part in axopodial functions.

2.4. Microtubule organizing centers

Microtubule organizing centers (MTOCs) with different appearances and positions exist in all eukaryotic cells. They are sites from which cytoplasmic and nuclear Mts assemble. The number, distribution, length and polarity of Mts are considered to be partially controlled by the MTOCs (Tucker 1984, Brinkley 1985). Although the centrosome is by far the most ubiquitous MTOC, other related structures can be recognized, especially among Protists. In Actinopoda, MTOCs can be roughly divided into two major types: multiple discrete clumps of granular-fibrillar material closely associated with membranes or single central or subcentral spherical masses (Fig. 1).

2.4.1. MTOCs scattered on the nuclear envelope or attached to cytoplasmic membranes

Heliozoa. Multiple MTOCs are generally scattered at the surface of the nuclear envelope or closely apposed to cytoplasmic membranes.

Several tiny clumps are visible on the outer nuclear membrane from which axonemal Mts extend in Heliozoa Cryptaxohelida such as *Ciliophrys* (Davidson 1982), *Echinosphaerium* (Tilney and Porter 1965), *Clathrulina* (Bardele 1972) and *Hedriocystis* (Brugerolle and Mignot 1985). Although in *Actinophrys,* the Mts assemble obviously from the nuclear envelope, no visible differentiation except a dense substance can be seen in the perinuclear space (Ockleford and Tucker 1973, Patterson 1979). Small patches were also seen along the sides of axonemes near their proximal ends in *Echinosphaerium.* After cold treatment these patches were much larger and numerous than in the untreated specimens. Ultrastructural data suggested that they were involved in nucleating Mt-assembly (Jones and Tucker 1981). MTOCs consisting of large, dense stratified plaques at the base of each axopod and articulated in caveolae of the nuclear envelope are observed in *Sticholonche zanclea* (Hollande et al. 1967, Cachon et al. 1977, Cachon and Cachon 1978).

Polycystines. In some polycystines (Cryptaxoplastidiata), the nuclear envelope is extremely thick and lined with a saccule of endoplasmic reticulum. The membrane of the saccule facing the cytoplasm bears tiny MTOCs from which the axonemes arise. The proximal part of the axoneme called the "colonnette axopodiale" is so dense that the Mts are indistinguishable (Cachon and Cachon 1972a, 1974). In other polycystines such as *Thallassicolla* (O. Spumellarida, Exoaxoplastidiata) and *Thalassolampe* (O. Spumellarida, Exocryptaxo-plastidiata) the MTOCs are either fitted to the cell membrane which covers the capsular wall or are located at the base of each fusule. The MTOCs are external so that the axonemes can be reconstituted when the ectoplasm is removed (Cachon and Cachon 1976a).

Acantharians. In this Class the axonemes are generated from tiny MTOCs apposed to the membrane of a large vacuole including the mineral skeleton. These MTOCs consist of thin homogeneous dense plaques scattered on the perispicular membrane near the base of the spicules (Febvre 1990).

2.4.2. Single dense MTOCs localized in the cell center

Heliozoa and polycystines. A single central or subcentral MTOC from which all the axonemes radiate is observed in some heliozoans and polycystines (Febvre-Chevalier and Febvre 1984, Febvre-Chevalier 1990, Cachon and Cachon 1974, Cachon et al. 1990). Since this organelle is very conspicuous, it can be distinguished by light microscopy (Zuelzer 1909, Dobell 1917).

Two distinct categories of massive MTOCs have been recognized on the basis of electron microscopical data, one including a tripartite disc, the other in which this feature is lacking.

MTOCs including a centroplast. The centroplast is a central tripartite disc (0.2-1.5 μm in diameter) sandwiched between two hemispheres of dense material. This centroplast is surrounded by two concentric layers, a clear exclusion zone and a peripheral interaxonemal substance in which the bases of the axonemes are rooted. Such MTOCs were found in *Heterophrys, Oxnerella, Cienkowskya* and *Chlamydaster* (Family Heterophryidae) (Bardele 1975; Davidson 1975, 1982; Febvre-Chevalier and Febvre 1984; Dürrschmidt and Patterson 1986-87), and *Acanthocystis, Raphidiophrys, Raphidocystis* (Family Acanthocystidae sensu Dürrschmidt and Patterson 1987) (Tilney 1971; Bardele 1977a,b; Rieder 1979; Dürrschmidt and Patterson, 1987).

MTOCs without central disc. These consist of a central or subcentral large spherical mass of fibrillar-granular material. This type of MTOC called an axoplast is located either in the cytoplasm or in a nuclear invagination. The first situation is found in *Gymnosphaera, Hedraiophrys* and *Actinocoryne* (sub-Order Axoplasthelida) (Febvre-Chevalier 1973a,b; 1975, 1980). In the second case, the axonemes pass across channels limited by the nuclear envelope. This organization is observed in the helioflagellates *Dimorpha* and *Tetradimorpha* (sub-Order Endo- and Exoaxoplasthelida) (Brugerolles and Mignot 1983, 1984a,b) and the Polycystina Centroplastidiata and Periaxoplastidiata belonging to the orders Spumellarida and Nassellarida (Cachon and Cachon 1972a,b, 1973, 1974; Cachon et al. 1990).

Phaeodaria. There are two axoplasts from which two very large Mt-bundles are generated. These MTOCs form hemispherical masses located under the central capsule membrane just in front of two large apertures named parapyles (Cachon and Cachon 1978).

2.5. How are Mt-patterns generated ?

Electron microscopical observations have shown that:(1) the axopodial arrays of microtubules are polar structures with their proximal minus ends attached to discrete or obvious clumps of a dense morphoplasmic material forming the MTOC. (2) The architecture of the Mt-arrays is species-specific. It is defined precisely by the number of protofilaments forming the Mt-wall, the distribution of linkers on the Mt-wall and the values of angles between successive links. (3) Axonemal Mts are

partially or completely disassembled when the cell is submitted to external agents. (4) The Mt-pattern is strictly rebuilt after axopodial recovery. (5) An axial fibrillar rod and cross-bridging contacts with the surrounding Mts are seen near the MTOC in the polygon-forming pattern.

The main question suggested by these observations was to know whether the information depended on the geometry of the Mt-pattern itself or was included in a species-specific template located in the MTOC. First attempts at understanding how nucleation, distribution and bridging of Mts are controlled resulted from experiments using destabilizing effects of external agents and further analysis of the axonemal geometry during recovery (Tilney 1968, Tilney and Porter 1967, Tilney and Byers 1969, Shigenaka et al. 1971). In *Raphidiophrys,* Tilney (1991) suggested that the pattern resulted from a self-linkage mechanism. This hypothesis was supported by the fact that in developing axonemes initial microtubules did not reappear in the axonemal pattern but as doublets or Y's and X's clusters. Furthermore, no structure was present that could be interpreted as a template and the pattern appeared first at a distance from the MTOC. Further examination of pattern formation after cold treatment showed that microtubules were randomly scattered around dense clumps acting as MTOCs and interconnected by filamentous meshworks (Jones and Tucker 1981). These observations appeared to confirm that the double spiral Mt-pattern may be established by a self linkage mechanism, the final positioning of Mts taking place via a "zipper-like" procedure (Ockleford and Tucker 1973).

Regarding the exact position and the number of links attached to one Mt, it was suggested that once a Mt binds to another Mt, some conformational change appears to act through several subunits to produce a long distance allosteric gradient or "gradion" which specifies the position of the other links (Roth et al. 1970, Roth and Pihlaja 1977). Although the allosteric model for Mt-patterning allowed Roth and coworkers to reconstitute the double spiraling arrangement seen in Actinophryidae, it is inadequate to explain complex arrangements with more than one linkage pattern (Cachon and Cachon 1973; Bardele 1977a,b).

A linker nucleation hypothesis was thus proposed which suggested that "graded" conformational changes in the Mt subunits not only specify the binding position of the next linker but also that this linker through linkage induces secondary Mt-nucleation (Bardele 1977a). This model allowed the reconstitution of closed and mixed polygonal patterns made of a limited number of Mts and polygons. However, it was less adequate for large mixed patterns containing a wide diversity of polygons as in *Cienkowskya* (Febvre-Chevalier and Febvre 1984). Since the distribution of Mts is generally less strictly ordered at the periphery than in the center of the array, factors controlling pattern formation presumably reside primarily in the axis of the array.

A 10 nm fibrillar rod positioned in the center of each microprism and associated with both the MTOC and the Mts may be involved in forming and maintaining the Mt-pattern (Rieder 1979). First detected in the hexagonal microprisms of *Raphidiophrys* using high voltage electron microscopy, this scaffold structure exists in other polygon-based axonemes, as revealed in micrographs from the literature (Febvre-Chevalier 1973a, Bardele 1975, Jones 1975, Cachon et al. 1977a, Brugerolle and Mignot 1983).

3. PHYSIOLOGICAL BASIS OF AXOPODIAL DYNAMICS

3.1. Involvement of axopodia in physiological functions

Axopodia are used for diverse cellular activities, such as contraction and extension, locomotion, feeding, secretion and excretion, fission and fusion.

Contraction of the axopodia (and of the stalk when present) and subsequent regrowth are one of the most striking characteristics of actinopoda (Porter 1966). Contraction is very rapid and is accompanied by profound remodeling of the axopodial cytoskeleton. This activity will be discussed in a separate section.

Locomotion takes place in response to local environmental change. Planktonic actinopods are passive protozoa which use their axopodia as a regulatory system of buoyancy (Cachon and Cachon 1984a, Febvre-Chevalier and Febvre, in press). In the Polycystines e.g. *Thalassicola, Thalassolampe* or *Thalassophysa,* active transport of large vesicles containing substances of lower density than seawater accumulate at the cell surface. They form a thick layer which can be dispersed and reconstituted periodically (Cachon and Cachon 1976b; 1977b).

Locomotion studied in heliozoans includes a rolling motion as well as horizontal and vertical displacements. Although active bending may be partially involved, locomotion may result from forces generated between

the cell body and the substratum via attached axopodia undergoing retraction (Watters 1968). An exception is the remarkable marine planktonic heliozoan *Sticholonche zanclea*, which uses its stiff axopodia as oars to perform a rowing motion. The mechanism of metachronal beating of axopodia involves bundles of nonactin filaments which are inserted in caveolae of the nuclear envelope at the base of each axopod (Hollande et al. 1967, Cachon and Cachon 1978, Cachon et al. 1977).

Food capture and ingestion involve a complex pattern of reactions including chemosensitivity, exocytosis of mucus, toxins and enzymes at the axopodial surface, and diverse movements such as axopodial contraction, bidirectional transport of extrusomes along the axopodia, formation of a food vacuole and retrograde cytoplasmic flow. These processes are obvious in the heliozoans, while in the polycystines and the acantharians food particles have not been observed in the axopodia, suggesting that phagocytosis may occur in the ectoplasm (Cachon and Cachon 1976b). In the phaeodarians, the axopodia are probably not involved in feeding and a large conical gullet, the astropylum is regarded as a cytopharynx (Cachon and Cachon 1973).

In the heliozoans, a very rapid contraction is triggered when a prey organism touches the tip of an axopod. This motion conveys the prey to the cell center where a food vacuole is formed. When a prey organism collides with an axopod it is liable to stick to the membrane as the result of exocytosis of muciferous bodies and/or kinetocysts. Then, it follows a unidirectional path toward the cell body without eliciting a visible change in the Mt-axis. A food vacuole is formed, and cytoplasmic droplets flow along the axopod (Ockleford and Tucker 1973, Suzaki et al. 1980, Patterson and Hausmann 1981).

Intracellular traffic along the Mt-arrays is associated with secretion of mucopolysaccharides used for formation of the mucous coat (Hollande and Hollande 1975) and regeneration of the extracapsular cytoplasm in Polycystines (Cachon and Cachon 1976b, 1977b). In the heliozoan *Cienkowskya*, a hollow stalk is also formed via exocytosis of mucocysts. These organelles are transported along the cytoplasm of a multiple bundle of axopodia directed toward the substrate. The stalk secreted around these axopodia elongates while the bundle of axopodia shortens (unpublished observations).

Axopodia are actively involved in cell fission and cell fusion. Two distinct models have been proposed for their role in fission. When a heliozoan divides close to the bottom of a Petri dish, the axopodia at the periphery of the presumptive daughter cells are attached to the bottom. Adhesion is accompanied by shortening of the supporting axopodia, while the cell elongates in the mid-region (Suzaki et al. 1978). This observation supports the hypothesis that active pulling force exerted by shortened axopodia moves the cells apart. When heliozoans float freely in the water, stiff axopodia grow between the prospective daughter cells. A pushing force might be exerted by the daughter cells against each other (Ockleford 1974). In most heliozoans, sexual reproduction takes place within a cyst (progamic cyst). Formation of this progamic cyst is preceded by axopodial retraction (Mignot 1979, Patterson 1979). Cell fusion is a common tendency in heliozoa. It can be induced repeatedly by treatments which elicit axopodial contraction and their subsequent regrowth in the presence of divalent cations (Vollet and Roth 1974, Shigenaka et al., 1979).

3.2. Axopodial transport

Three types of axopodial transport have been observed in Actinopoda: (a) extracellular membrane-mediated translocation of organic or inorganic particles, (b) unidirectional displacement of larger elements such as cytoplasmic droplets and food vacuoles, (c) intracellular saltatory motion of tiny particles such as organelles and small vesicles (Fig. 2). These different forms of axopodial motility are important for most cellular activities. They involve cell-environment and cell-cell recognition associated with signaling pathways and activation of internal motor systems.

3.2.1. Axopodial surface motility

External translocation of particles has been studied in *Echinosphaerium nucleofilum* (Bloodgood 1978) and *E. akame* (Suzaki and Shigenaka 1982) using extracellular markers (polystyrene microspheres, carbon or carmine particles, squid ink and motionless bacteria). In both species particles were found to be transported along the surface of the axopodia with constant velocity (1.8 ± 0.1 μm sec^{-1} or 155 mm day^{-1}) in an unidirectional movement directed toward the tip of the axopod. In *Actinosphaerium,* colchicine was found to impede cell surface motion (Suzaki and Shigenaka 1982). In *Actinocoryne contractilis*, Ca^{2+} and Na^{+} free artificial media and inhibitors of Ca^{2+} pathways (Co^{2+}, Mn^{2+}, La^{3+}, caffeine, theophylline, quercetin) inhibit adhesion of particles to the axopodial membrane and the slow surface transport of prey (Febvre-Chevalier 1987). Inhibitors of ATP production from mitochondrial oxidative

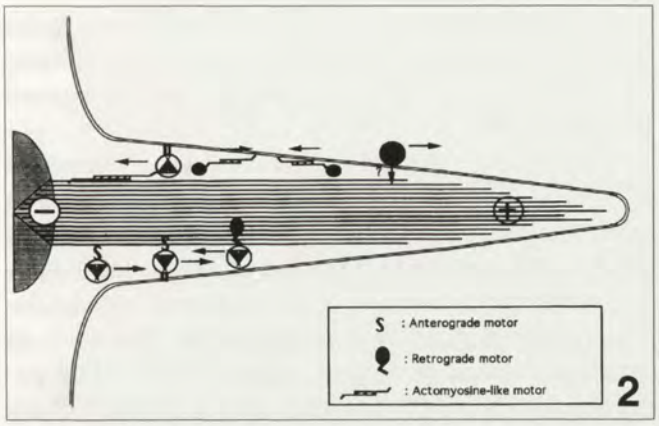

Fig. 2. Different types of extracellular and intracellular axopodial transport and possible motor systems. Polarity of the axonemal Mts is indicated by the signs "+" and "-"

phosphorylation (potassium cyanide, sodium azide) and the alternative pathway (Sham) produced no noticeable effect on this motion. Although data are qualitative and require further experiments, they raise questions about the possible mechanism of external transport. As noted by Bloodgood (1978), membrane lipid flow is too slow (3 μm min^{-1}) to account for the external surface transport. The fact that this motion is blocked or slowed in Ca^{2+}-free media or in the presence of inhibitors of the Ca^{2+} pathway suggests that some active Ca^{2+}-mediated process may be involved.

3.2.2. Unidirectional fast transport

Unidirectional transport of material consisting of large vacuoles (food vacuoles, excretory vesicles and cytoplasmic droplets) consisting of a local accumulation of membrane-bound organelles takes place along the axopodia of heliozoans (Ockleford 1974, Suzaki et al. 1980, Patterson and Hausmann 1981, Hausmann and Patterson 1982, Febvre-Chevalier 1987).

In the stalked heliozoan *Actinocoryne,* prey organisms are captured in the axopodia. Food vacuoles are formed near a spherical head from which the axopodia diverge. They are conveyed via the stalk to a flat base where they are digested. This transport (0.8-2.5 μm sec^{-1} or 70-200 mm day^{-1}) follows a unidirectional path over several hundred micrometers (Febvre-Chevalier 1987). Excretory vacuoles follow the opposite way and are released at the tip of the axopodia.

3.2.3. Bidirectional particle transport

Vectorial bidirectional transport of intracellular particles in Actinopoda fulfills several characteristics of the saltatory motion found in other cell types and diverse protists (Rebhun 1972, Allen et al. 1982, Schliwa 1984, Bowser and Delaca 1985, Koonce and Schliwa 1985, Koonce et al. 1986). Although vectorial particle transport exists in all the Actinopoda, it has mainly been studied in the heliozoans. These have thin and very long axopodia containing extrusomes, that shuttle back and forth for several micrometers in the cytoplasm close to the axoneme.

Size, velocity and pathlengths of the moving particles have been identified in four genera, *Echinosphaerium* (Fitzharris et al. 1972, Edds 1975a, Suzaki and Shigenaka 1982), *Raphidiophrys* (Bardele 1976), *Heterophrys* (Davidson 1975; Troyer 1975, 1976) and *Actinocoryne* (Febvre-Chevalier 1987).

Fitzharris and co-workers indicated that in *Echinosphaerium nucleofilum* the motion of electron dense granules (0.4-0.6 μm in diameter) was rectilinear, the average excursion in one direction or the opposite direction was 14 ± 8.5 μm and the movement occurred at uniform velocity (0.5-5 μm s^{-1}; 43-430 mm day^{-1}). In the same species, Edds (1975a) obtained similar results (average velocity: 49.2 mm day^{-1}). In *Heterophrys* and *Raphidiophrys* the refractile particles (kinetocysts, also called conicysts 0.30-0.38 μm in diameter) followed linear slightly oblique paths (1-15 μm) in one direction, stopped, then reversed at a velocity of 0.5-3 μm s^{-1} (43-260 mm day^{-1}). This alternation was stochastic. The velocity was independent of the mass and density of the particle. However, both the velocity of particles and the distance followed were strongly correlated with the physiological condition of the living specimen (Bardele 1976). The number of extrusomes along the axopodia was shown to decrease drastically after introduction of prey organisms, while their mobility increased up to 5-10 μm s^{-1} (430-860 mm day^{-1}). The mean velocity reported in heliozoans is slower than in foraminiferans (640 mm day^{-1}) (Bowser and Delaca 1985) and amoebae (2160 mm day^{-1}) (Koonce and Schliwa 1985) and may correspond to groups I and II of the axonal transport (Schliwa 1984). Using freeze fracture procedures, Bardele (1976) and Davidson (1976) showed that the kinetocysts are attached to the cell membrane via rosettes of 6-9 membrane particles. Davidson showed in *Ciliophrys* that muciferous bodies link to the axopodial membrane by rectangular arrays of particles.

3.2.4. How are organelles transported ?

What role do Mts or other cytoskeletal structures play in saltatory motion ? Fitzharris et al. (1972) observed

particle motion in zones apparently lacking Mts and considered that they were not necessary. In support of this, Edds (1975a) substituted a glass needle for the Mt-axoneme in *Echinosphaerium* treated with colchicine to promote Mt disassembly and showed that particle transport was maintained and indistinguishable from that observed in natural conditions. This idea that in normal axopodia the Mts may be not involved in force production was supported by the fact that the Mt-inhibitor vinblastine did not stop intra-axopodial particle movement (Troyer 1975, Suzaki and Shigenaka 1982). Actin filaments in the cell body of *Echinosphaerium* could be involved in cytoplasmic streaming (Edds 1975b, Bardele 1976). However, microfilaments were never detected in the axopodia, and axopodial transport was not inhibited by cytochalasin B a potent disrupter of actin filaments (Troyer 1976, Suzaki and Shigenaka 1982).

The discovery of rosettes of particles linking the membrane of kinetocysts to the plasmalemma suggested that these highly ordered membrane domains might be transported by some filament-based motor (Bardele 1976, Davidson 1976). Arrest of the saltatory motion in the presence of anesthetics that disconnect dense granules from the cell membrane seemed in agreement with this hypothesis (Suzaki and Shigenaka 1982). The recent identification in a variety of eukaryotic cells of two classes of soluble mechanochemical transducers associated with Mt-transport (kinesins, cytoplasmic dyneins) opens new perspectives. Evidence for a role of a variant of cytoplasmic dynein in bidirectional transport of organelles has been recently obtained in the Myxamoeba *Reticulomyxa* (Euteneur et al. 1988, 1989). However, motor molecules responsible for bidirectional organelle transport in axopodia have still to be identified among Actinopoda.

3.3. Axopodial sensitivity

In the last 30 years, several works have shown that the axopodia are sensitive to a variety of chemical or physical factors which perturb both membrane electrogenesis and structure of the Mt-cytoskeleton (Fig. 3). As a consequence, motility and other functions are also modified. Depending on the factor, the place where it is applied, and the dose used for the experiments, the response may be an immediate or delayed, partial or complete, reversible or irreversible contraction of axopodia accompanied with Mt-remodeling. Unstimulated Actinopoda are immobile in water or are attached to aquatic plants by the tip of one or a few stiff axopodia. In such unperturbed conditions no obvious change in the length of axopodia could be seen. Neither cytoplasmic transport along their axis nor other activity could be seen (Bardele 1976).

In some cases, the cell membrane is poorly sensitive to external factors, while in others the response is a noticeable change in motile activities. In the heliozoans *Echinosphaerium nucleofilum* and *E. akame*, the axopodial membrane is insensitive to mechanical shocks delivered with a glass or a metal needle. However, as mentioned above, when prey organisms or carbon panicles coated with albumin touch the tip or length of the axopod, feeding reaction occurs, suggesting the presence of chemoreceptors on the axopodial membrane (Suzaki et al. 1980). In *Sticholonche* no change was observed in the axopodial aspect upon mechanical stimulation (300 shakes/min for 5 min) but the rowing motion was more vigorous than normal (Cachon and Cachon 1981). In the remarkably sensitive heliozoan *Actinocoryne*, when the tip of one axopod is stimulated with a glass needle a rapid contraction is triggered, while no change occurs in the neighbor axopodia. When 5-10 axopodia are stimulated at the same time, they contract simultaneously. A complete contraction of the axopodia and the stalk can be elicited by stimulating a greater number of arms. Thus, there is a threshold number of axopodia, above which complete contraction was elicited. Mechanical stimulation of the head or the base produced an all or none contraction of the axopodia, the head and the stalk (Febvre-Chevalier 1981).

We have shown in this species that graded mechanical stimulations elicit graded depolarizations which correspond to Na^+-dependent receptor potentials. Above a threshold level up to 50 mV a firing action potential

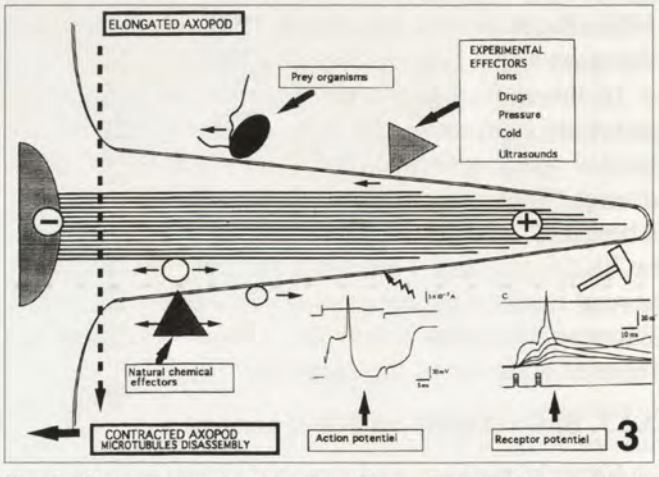

Fig. 3. Diagram summarizing the effects of external factor on the axopodia

occurrs followed by rapid repolarization and a catastrophic contraction of the axopodial system accompanied by Mt-disassembly (Febvre-Chevalier et al. 1986, 1990; Febvre-Chevalier and Febvre 1992).

In *Echinosphaerium* electrical stimulation between two wire electrodes produces a contraction of the axopodia extending toward the cathode when the current is turned on, while those oriented to the anode contract when the current is turned off (Shigenaka et al. 1989). In the marine stalked heliozoan *Actinocoryne*, the response to electrical stimulation in a DC field is an all or none synchronous contraction of all the axopodia and the stalk into the base (Febvre-Chevalier 1981).

Electrophysiological studies with intracellular electrodes have been made in only two heliozoans (Febvre-Chevalier et al. 1989). In *Echinosphaerium*, Ca^{2+}-dependent action potentials were found to correlate with the vacuolar contraction but not the axopodial contraction (Nishi et al. 1986). In *Actinocoryne contractilis*, the action potential was found to be associated with contraction (Fig. 3). The resting membrane potential (-78 mV S.D.=8) was potassium dependent. Overshooting action potentials of high amplitude (110-134 mV; overshoot: 28-50 mV) could be elicited by current injection. As for the mechanical stimulation, the response was very rapid (duration at half spike amplitude 0.5 ms). Analysis of the ionic dependence of action potential, using Ca^{2+}-EGTA buffers, Na^{+}-free media and Ca^{2+} channel inhibitors showed that action potential was mainly Na^{+}-dependent but involved a minor Ca^{2+}-dependence. The repolarization was followed by a very rapid contraction which depended only on external Ca^{2+} (Febvre-Chevalier et al. 1986).

3.4. Effects of external factors on axopodial microtubule-arrays

3.4.1. Effects of physical factors

Low temperature, high pressure and ultrasound produce complete or partial retraction of axopodia. Stiffness and birefringence of axonemes disappear and Mts become segmented or disrupted after cooling, forming sheet-like arrays (Tilney and Porter 1967; Tilney et al. 1966; Cachon and Cachon 1980, 1981).

The effect of cold treatment on the formation of polymorphic forms of Mts has been studied in *Actinophrys sol, Actinosphaerium eichhorni* and *Sticholonche zanclea*. In the two Actinophryid heliozoans, cold treatment induces axopodial retraction although short microspikes still project from the cell surface. The ectoplasm contains numerous macrotubules 40 nm in diameter (Tilney and Porter 1967) and it suggested that they may serve to maintain the pointed shape of they protuberances (Jones and Tucker 1981). Axonemal microtubules are relatively stable in the marine planktonic species *Sticholonche zanclea*, and different steps of Mt-remodeling after cold treatment can be distinguished by electron microscopy (Cachon and Cachon 1980). After a few minutes, local breaks are seen along the axonemes followed after 30 minutes by complete axonemal disorganization. Prolonged treatment results in the formation of zig-zag filamentous structures occupying almost the whole axopod. Curved macrotubules form when specimens are cooled for 90 min, while numerous arrays of macrotubules appear to be oriented in diverse directions through the axopodial cytoplasm after 4 h at 2°C. Mechanical shocks (5 Hz) and ultrasounds (up to 20 KHz) also produce partial or complete axopodial retraction accompanied by the formation of granules, Mt-segments or zig-zag filaments (Cachon et al. 1981). UV illumination produces axopodial shortening or amputation depending on where the UV light is applied (Ockleford 1975).

3.4.2. Effects of chemical agents on microtubule arrays

Effect of drugs. Chemical poisons, such as colchicine and its derivatives, vinca alkaloids, griseofulvin, podophyllotoxin, nocodazole, anaesthetic drugs, sulfhydryl blocking reagents, urea and metal ions are known to trigger slowed or rapid retraction of the axopods. Depending upon the concentration and duration of the treatment, slight or extensive changes are seen in the axonemal fine structure (Dustin 1978, 1984). After a short treatment with colchicine (Tilney 1968, Cachon and Cachon 1984b, Febvre-Chevalier and Febvre 1986), urea (Shigenaka et al. 1971), heavy metal ions (Shigenaka 1976), or sulfhydryl blocking agents (Shigenaka et al. 1979b), the linkers are broken and the Mts appear to be sinuous. Longer treatment induces the formation of incomplete C-shaped Mts. After prolonged treatment, transverse breakage of the Mt-arrays and an accumulation of granular material are visiblae long the axopodial axis. High concentrations of $MgCl_2$, vinblastine or the anaesthetic drug halothane, destroy the Mt-arrays and allotropic transformation of tubulin takes place. After these treatments or with the stabilizing agent polyethylene glycol, macrotubules or tubulin paracrystals, similar

to those formed after cold treatment, were reported in Heliozoans (Allison et al. 1970; Cachon and Cachon 1980, 1982, 1984b; Febvre-Chevalier and Febvre 1986).

The effects of the antitumor drug taxol were investigated in the heliozoans *Echinosphaerium* and *Heterophrys* (Hausmann et al. 1983, Hauser 1986). This Mt-promoter induced polymerization of tubulin and disturbed interactions between Mts and the long interhelix linkers in *Echinosphaerium*. In *Heterophrys*, the MTOC, the cross-bridging MAPs and the overall pattern were affected, leading to the formation of an asymmetrical thick axopodia. Longer treatment induced the formation of paracrystalline arrays (Hauser 1986).

Deuterium oxide (40-60%) was found to stabilize the axopodial microtubules, making them more resistant to solating effects of high pressure, low temperature, colchicine or fixatives (Marsland et al. 1971, Tilney and Byers 1969, Febvre-Chevalier 1980). At a higher concentration (65%) D_2O was also found to induce detachment of the axopodia (Sugiyama et al. 1992).

Effects of ions. Depending on their concentration, divalent light and heavy metal ions (Mg^{2+}, Ca^{2+}, Sr^{2+} and Zn^{2+}, Cd^{2+}, Hg^{2+}, Cu^{2+}, Ni^{2+}) were found to cause degradation or stabilization of the Mts in *Echinosphaerium* (Roth and Shigenaka 1970, Shigenaka et al. 1975, Shigenaka 1976). Evidence for a regulatory role of Ca^{2+} *in vivo* was provided by Schliwa (1976). Using Ca^{2+}-EGTA buffers and the ionophore A 23187, he showed that the axopodia shorten at a rate characteristic for the Ca^{2+} concentration. As detailed below, we have recently shown in *Actinocoryne contractilis* that the axonemes stiffening the stalk and the axopodia are sensitive to variations of intracellular Ca^{2+} concentration.

3.5. Extension and contraction of axopodia

3.5.1. Extension

In natural conditions, axopodia reform within a few minutes after a contraction elicited by chemical, mechanical or electrical stimulation. Their regrowth is accompanied by an increase of birefringence of the axonemes. In *Actinocoryne*, the result of rapid contraction is a complete collapse of the axopodia, the head and the stalk into the cytoplasmic base. Therefore, only a smooth convex area corresponding to the surface of the head is visible at the upper side of the base. The first indication of axopodial regrowth is the formation of short curved processes at the surface of the presumptive head. Segments of axonemes which were randomly scattered within the granular-fibrillar substance of the MTOC reorient themselves radially around the axoplast. All the axonemes are presumed to grow at about the same speed. Those oriented toward the upper side stiffen the microvilli, which become birefringent, while those oriented toward the base push the head over the base. This morphogenetic process is accompanied by an active anterograde cytoplasmic streaming along the developing axonemes. It takes 10 min for the stalk to elongate to 100 µm (Febvre-Chevalier 1987). When a Heliozoan is treated with Mt-destabilizing agents, the axopodia do not regrow until the cell is returned to natural conditions.

3.5.2. Rapid contraction and its ionic basis

Kinetics of shortening subsequent to stimulation were studied in *Echinosphaerium, Heterophrys* and *Actinocoryne*. In *Echinosphaerium akame* the axopodia shortened after chemical stimulation by 200-300 µm within 20-40 ms and the shortening velocity was around 2.5-5 mm sec^{-1} (Shigenaka et al. 1982, Ando and Shigenaka 1989, Suzaki et al. 1992). In *Heterophrys*, Davidson estimataed axopodial shortening subsequent to mechanical shocks at 50-100 lengths per second (Davidson 1975).

In *Actinocoryne*, the contraction is by far the most rapid. Using high speed cinematography we have shown that the length of the axopodia and stalk follow an exponential decrease (mean half time 4 ms) (Febvre-Chevalier 1981; Febvre-Chevalier and Febvre 1981, 1992). In natural conditions, both of them collapse during rapid shortening and appear to break.

Rapid contraction is controlled by the cytosolic concentration of calcium. In *Echinosphaerium nucleofilum* and *E. akame*, entry of extracellular Ca^{2+} into the cell was found to elicit axopodial retraction (Schliwa 1976, Matsuoka and Shigenaka 1985). In *Actinocoryne* the specimens were completely stabilized below a Ca^{2+} concentration of 4×10^{-9} M whatever the stimulation, and the Mt-arrays appeared to be uninterrupted. With Ca^{2+} concentrations in the range of 10^{-7}-10^{-6} M the contractile response was generally rapid. Above 10^{-6} M, catastrophic shortening of the cell was triggered by mechanical or electrical stimulation. Specimens fixed during slowed contraction showed folded regions resembling a bended knee. The Mt-arrays were interrupted by a single or multiple series of transversal bands consisting of a dense granular material, and polymorphic forms of Mt-disassembly were observed around the axonemes. Thin sections through the base of specimens fixed just after rapid contraction showed short segments

of axonemes scattered through the matrix of the MTOC (Febvre-Chevalier and Febvre 1992). Recent unpublished observations have been obtained with S. Inoué (MBL, Woods Hole, Mass, USA) using an ultra high speed framing streak videocamera (Hamamatsu Corp., USA) (Takeshita et al. 1991) and sensitive polarizing microscopy. Some change in the birefringence of the Mt-arrays seem to be visible during the very rapid contraction elicited by DC field electrical stimulation in natural seawater (results shown at the IX International Congress of Protozoology, Berlin, 1993 in the Poster session). Additional very preliminary data using recombinant aequorin suggest a remarkable (20 fold) increase in internal Ca^{2+} just after contraction, confirming the prominent role of calcium in the cellular contraction of *Actinocoryne* (unpublished results; collaboration with L. Jaffe and A. Miller).

3.5.3. Mechanisms of rapid microtubule disassembly and axopodial contraction

In the extended state, the Mt-arrays form a long cohesive building which must be disrupted within a few milliseconds upon stimulation of rapid contraction. If the Mt-arrays are stabilized (e.g. with D_2O) they cannot contract. Therefore, axopodial contraction poses two related though distinct questions: How can the Mts disassemble so quickly ? What forces drive such a rapid shortening?

Two basically different mechanisms have been proposed to explain how microtubules shorten before axopodial contraction. Suzaki and co-workers (1992) suggested that "the distal portion of the axonemal Mts slides rapidly into the proximal portion without distinct disassembly of the Mts themselves". Since in *Echinosphaerium* the microtubules are uninterrupted in the extended axopodia (Shigenaka et al. 1971), they must be broken before sliding. "Quantitative calculation suggested that the fractional volume occupied by the Mts increased at the proximal region". The Mt-arrays in the cell body should be several times larger after axopodial shortening than they were just before in the extended state. It would be interesting to know how the Mt-bundles are arranged in the cell body. The report of two bundles of axonemal microtubules crossed in the proximal region of axonemes (Suzaki et al. 1992) suggests that some breakage occurs rather than supporting the idea of a sliding mechanism.

In *Actinocoryne*, axopodial shortening is correlated with the formation of intercalary destabilization bands,

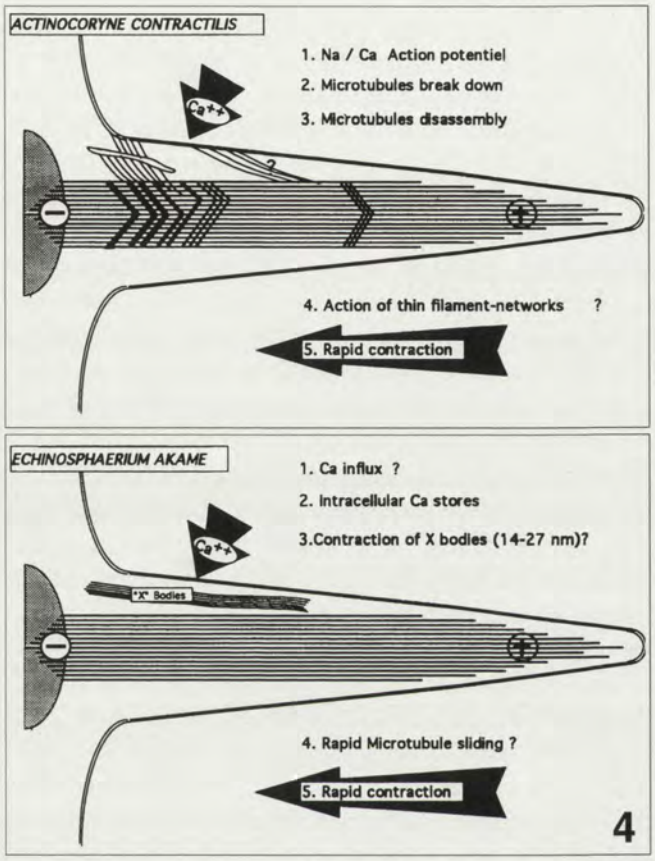

Fig. 4. Interpretative drawing of the possible mechanisms of axopodial contraction in *Actinocoryne contractilis* and *Echinosphaerium akame*. In the first species axopodial contraction may result from intercalary disassembly and fragmentation of Mts and action of tensile or contractile force due to filament networks. In the second species, contraction may result from rapid Mt-sliding and contraction of "X" bodies

breakage of Mts and polymorphic forms of Mt-disassembly (Fig. 4).

These data, and our kinetic analysis, imply that an endwise disassembly mechanism cannot account for the very rapid shortening observed in natural conditions, and that a mechanism of intercalary destabilization and fragmentation is involved. This may be accompanied by the loss of tubulin subunits from the ends of the newly formed segments (Febvre-Chevalier and Febvre 1992). This system of Mt-breakdown may also take place in many other actinopods exhibiting very rapid axopodial contraction.

Thus the forces driving the axopodial shortening remain a matter of debate.

The presence of moniliform structures or "X" bodies in relaxed specimens of *Echinosphaerium* and the formation of beads during axopodial shortening suggest that contraction could be caused by simultaneous disassembly of the axonemal Mts and conformational change

of the "X" body (Suzaki et al. 1980). In *Actinophrys*, morulate bodies, similar to the X-bodies of *Echinosphaerium*, were originally thought to be a fixation artifact associated with disassembly of axonemal Mts (Patterson and Hausmann 1982). However, recent reports suggest that the granulated form of the "X" bodies results from self-twisting and supercoiling taking place during contraction elicited by Ca^{2+} influx (Matsuoka et al. 1985, Matsuoka and Shigenaka 1984, Ando and Shigenaka 1989). Although no data on the biochemical composition of the "X" bodies are presently available, a mechanism similar to the antagonist systems of microtubule sheets and myoneme filaments described in the Heterotrich Ciliates (Huang and Pitelka 1973, Ishida and Shigenaka 1988) was suggested in *Echinosphaerium*. The force required for axopodial contraction was estimated to be very low (10^{-11} N) suggesting that the axopodial tension resulting from Mt-disassembly cannot be responsible for the contraction (Suzaki et al. 1992).

In *Actinocoryne*, there is no feature resembling "X" bodies or morulate bodies. Rapid contraction is an active process which can be completely inhibited in the presence of a mixture of poisons of ATP production from both the respiratory chain and the alternative pathway (Febvre-Chevalier and Febvre 1986). It is Ca^{2+} dependent and there are some indications that external Ca^{2+} passing across the cell membrane during action potential is directly responsible for activation of the contractile machinery. Since at the end of rapid contraction segments of axonemes are scarce, short and very thin, it is quite unlikely that the mechanism of rapid shortening involves sliding interactions as proposed by Ando and Shigenaka (1989) for *Echinosphaerium*. It may rather be caused in *Actinocoryne* by the joint effects of the synchronous breakdown of axonemal Mts and the sudden effect of tensile and/or motile forces exerted on the Mt-fragments by a thin meshwork of filaments linking the Mts to other cytoplasmic components, especially the cell membrane and the endoplasmic reticulum. The structural, behavioral and functional differences observed in *Echinosphaerium* and *Actinocoryne* may confirm that the Actinophryidae may have evolved separately from the other heliozoans (Patterson and Fenchel 1985).

In summary the axopodia of Actinopoda display distinct properties of structure, membrane sensitivity and motility. They are an exceptional system in which progressive or sudden remodeling of microtubules during morphogenesis and rapid motion can be studied. A stimulating challenge for the future concerns the motor proteins involved in the different kinds of Mt-transport and the contraction-extension process. What are the Ca^{2+} pathways responsible for Mt-disassembly and axopodial shortening? Is there some severing-like protein around the axonemes involved in Mt-breakdown? Is an annealing process involved in Mt-regrowth as recently shown in foraminiferans (Golz and Hauser 1991)? Answers to these questions will aid our understanding of why axopodial Mts are such versatile structures capable upon stimulation of being instantly converted from their tightly packed configuration used for maintenance of cell shape, into the fully disassembled form seen after contraction.

REFERENCES

Allen R.D., Allen N.S., Travis J.L. (1982) Video enhanced contrast differential interference contrast (AVEC-DIC) microscopy: A new method capable of analyzing microtubule related motility in the reticulopodial network of *Allogromia laticollaris*. Cell Motility 1: 291-302.

Allison A.C., Hulands G.H., Nunn J.F., Kitching J.A., MacDonald A.C. (1970) The effect of inhalational anesthetics on the microtubular system in *Actinosphaerium nucleofilum*. J. Cell Sci. 7: 483-499.

Ando M., Shigenaka Y. (1989) Structure and function of the cytoskeleton in Heliozoa: I. Mechanism of rapid axopodial contraction in *Echinosphaerium*. Cell Motil. Cytoskeleton 14: 288-301.

Bardele C.F. (1969) Ultrastruktur der Körnchen auf den Axopodien von *Raphidiophrys* (Centrohelida, Heliozoa). Z. Naturforsch. 24: 362-364.

Bardele C.F. (1972) Cell cycle, morphogenesis and ultrastructure in the Pseudoheliozoan *Clathrulina elegans*. Z. Zellforsch. 130: 219-242.

Bardele C.F. (1975) The fine structure of the Centrohelidian Heliozoan *Heterophrys marina*. Cell. Tis. Res. 161: 85-102.

Bardele C.F. (1976) Particle movement in Heliozoan axopods associated with lateral displacement of highly ordered membrane domains. Z. Naturforsch. 31: 190-194.

Bardele C.F. (1977a) Comparative study of axopodial microtubule patterns and possible mechanisms of pattern-control in the Centrohelidian Heliozoa *Acanthocystis, Raphidiophrys* and *Heterophrys*. J. Cell Sci. 25: 205-232.

Bardele C.F. (1977b) Organization and control of microtubule pattern in Centrohelidan Heliozoa. J. Protozool. 24: 9-14.

Bloodgood R.A. (1978) Unidirectional motility occurring in association with axopodial membrane in *Echinosphaerium nucleofilum*. Cell. Biol. Int. Rep. 2: 171-176.

Bowser S.S., Delaca T.E. (1985) Rapid intracellular motility and dynamic membrane events in an antarctic Foraminifer. Cell Biol. Int. Rep. 9: 901-910.

Brinkley B.R. (1985) Microtubule organizing centers. Ann. Rev. Cell Biol. 1: 145-172.

Brugerolle G., Mignot J.P. (1983) Caracteristiques ultrastructurales de l'Hélioflagellé *Tetradimorpha* (Hsiung) et leur intérêt pour l'étude phylétique des Héliozoaires. J. Protozool. 30: 473-480.

Brugerolle G., Mignot J.P. (1984a) Les caractéristiques ultrastructurales de l'Hélioflagellé *Dimorpha mutans* Gruber (Sarcodina, Actinopoda) et leur intérêt phylétique. Protistologica 20: 97-112.

Brugerolle G., Mignot J.P. (1984b) The cell characters of two Helioflagellates related to the Centrohelidian lineage: *Dimorpha* and *Tetradimorpha*. Origins of life. 13: 305-314.

Brugerolle G., Mignot J.P. (1985) Ultrastructure d'*Hedriocystis pellucida* (Heliozoa, Desmothoracida) et de sa forme migratrice flagellée. Protistologica 21: 259-265.

Cachon J., Cachon M. (1971) Le système axopodial des Nassellaires. Origine, organisation et rapports avec les autres organites cellu-

laires. Considérations générales sur l'organisation macromoléculaire du stéréoplasme chez les Actinopodes. Arch. Protistenk. 113: 80-97.
Cachon J., Cachon M. (1972a) Le système axopodial des Radiolaires Sphaeroidés. I.Centroaxoplastidiés. Arch. Protistenk. 114: 51-64.
Cachon J., Cachon M. (1972b) Le système axopodial des Radiolaires Sphaeroidés. II. Les Périaxoiplastidiés. III. Les Cryptoaxoplastidiés (Anaxoplastidiés). IV. Les fusules et le systme rhéoplasmique. Arch. Protistenk. 114: 291-307.
Cachon J., Cachon M. (1973) Systèmes microtubulaires de l'astropyle et des parapyles de Phaeodariés. Arch. Protistenk. 115: 324-335.
Cachon J., Cachon M. (1974) Les systèmes axopodiaux. Ann. Biol. 13: 523-560.
Cachon J., Cachon M. (1975) Rôle des microtubules dans les courants cytoplasmiques des axopodes. C. R. Acad. Sc. Paris 280: 2341-2343.
Cachon J., Cachon M. (1976a) Le Système axopodial des Collodaires. I. Les Exoaxoplastidiés. Arch. Protistenk. 118: 227-234.
Cachon J., Cachon M. (1976b) Les axopodes de Radiolaires dans leur partie libre et ectoplasmique. Structure et fonction. Arch. Protistenk. 118: 310-320.
Cachon J., Cachon M. (1977a) Le Système axopodial des Collodaires (Radiolaires, Polycystines). II. *Thalassolampe margarodes* Haeckel. Arch. Protistenk. 119: 401-406.
Cachon J., Cachon M. (1977b) Intracellular transfer of membranes and its relation to the microtubular axopodial system. J. Biol. Cellulaire 30: 137-140.
Cachon J., Cachon M. (1978) *Sticholonche zanclea* Hertwig: Reinterpretation of its phylogenetic position based upon new observations and its ultrastructure. Arch. Protistenk. 120: 148-168.
Cachon J., Cachon M. (1980) Polymorphism of tubulin reassembly: I. Different aspects of allotropic transformations induced by low temperature. J. Biol. Cellulaire 37: 23-34.
Cachon J., Cachon M. (1981) Polymorphism of tubulin reassembly in the microtubular system of a Heliozoan. II. Cytochemical effects of mechanical shocks and ultrasounds. Biol. Cell. 40: 23-32.
Cachon J., Cachon M. (1982) Induction of unusual structures after a microtubule disassembly in the Protozoan *Sticholonche zanclea*. In: Microtubules in microorganisms. (Eds. P. Cappuccinelli, N.R. Morris). M.Dekker. New York, 325-339.
Cachon J., Cachon M. (1984a) Adaptative evolution of Protists to planktonic life. Ann. Inst. Oceanogr., Paris, 60: 105-114.
Cachon J., Cachon M. (1984b) Various effects induced by chemical microtubule inhibitors and neurodrugs on the microtubular system of the Heliozoan *Sticholonche zanclea*. Arch. Protistenk. 128: 25-35.
Cachon J., Cachon M., Bruneton J-N. (1981) An ultrastructural study of the effects of a very high frequency ultrasounds on a microtubular system (axopods of a Heliozoan). Biol. Cell. 40: 69-72.
Cachon J., Cachon M., Estep K.W (1990) Phylum Actinopoda, Class Polycystina, (=Radiolaria) and Phaeodaria. In: Handbook of Protoctista. (Eds. L. Margulis, J.O. Corliss, M. Melkonian, D. Chapman) Jones and Batlett, Inc. Boston, Ma. 334-346.
Cachon J., Cachon M., Febvre-Chevalier C., Febvre J. (1973) Déterminisme de l'édification des systèmes microtubulaires stéréoplasmiques d'Actinopodes. Arch. Protistenk. 115: 137-153.
Cachon J., Cachon M., Tilney L.G., Tilney M. (1977) Interactions between microtubules and nonactin containing microfilaments in *Sticholonche zanclea*. J. Cell Biol. 72: 314-338.
Davidson L.A. (1975) Studies of the Actinopods *Heterophrys marina* and *Ciliophrys marina*. Energetics and structural analysis of their contractile axopodia. General ultrastructure and phylogenetic relationships. PhD. Thesis. University of California, Berkeley.
Davidson L.A. (1976) Ultrastructure of the membrane attachment sites of the extrusomes of *Ciliophrys marina* and *Heterophrys marina* (Actinopoda). Cell Tiss. Res. 170: 353-365.
Davidson L.A. (1982) Ultrastructure, behavior and algal flagellate affinities of the Helioflagellate *Ciliophrys marina* and the classification of the Helioflagellates (Protista, Actinopoda, Heliozoa). J. Protozool. 29: 19-29.
Dobell C. (1917) On *Oxnerella maritima* nov gen. nov. sp., a new Heliozoan, and its methods of division with some remarks on the centroplast of the Heliozoa. Quart. J. Microsc. Sci. 62: 515-538.
Dürrschmidt M., Patterson D.J. (1986-87) On the organization of the Heliozoa *Raphidiophrys ambigua* Penard and R. pallida Schulze. Ann. Sci. Nat., Zool., Paris. 8: 135-I55.
Dürrschmidt M., Patterson D.J. (1987) A light and electron microscopic study of a new species of Centroheliozoon, *Chlamydaster fimbriatus*. Tiss. & Cell. 19: 365-376.
Dustin P. (1978) Microtubules. Springer Verlag, Berlin.
Dustin P. (1984) Microtubules. 2 ed. Springer Verlag, Berlin, Heidelberg, New-York.
Edds K.T. (1975a) Motility in *Echinosphaerium nucleofilum*. I. An analysis of particle motions in the axopodia and a direct test of the involvement of the axoneme. J. Cell Biol. 66: 145-I55.
Edds K.T. (1975b) Motility in *Echinosphaerium nucleofilum*. II. Cytoplasmic contractility and its molecular basis. J. Cell Biol. 66: 156-164.
Edds K.T. (1981) Cytoplasmic streaming in a Heliozoan. Biosystems. 14: 371-376.
Euteneur U., McIntosh J.B. (1981) Polarity of some motility-related microtubules. Proc. Natl. Acad. Sci. USA. 78: 372-376.
Euteneur U., Koonce M.P., Pfister K.K., Schliwa M. (1988) An ATPase with properties expected for the organelle motor of the giant amoeba, *Reticulomyxa*. Nature 332: 176-178.
Euteneur U., Johnson K.B., Schliwa M. (1989) Photolytic cleavage of cytoplasmic dynein inhibits organelle transport in *Reticulomyxa*. Eur. J. Cell Biol. 50: 34-40.
Febvre J. (1986) Les Acanthaires (Protozoa, Actinopoda) Ultrastructures. Mècanismes cellulaires d'un système primitif de motilité: le myonème. Thèse Doctorat d'Etat, Juin 1986, Nice. Office des Thèses, Grenoble.
Febvre J. (1990) Phylum Actinopoda, Class Acantharia. In: Handbook of Protoctists. (Eds. L. Margulis, J.O. Corliss, M. Melkonian, D. Chapman) Jones and Batlett, Inc. Boston, Ma. 347-362.
Febvre J., Febvre-Chevalier C. (1989) Motility processes in Acantharia (Protozoa). III . Calcium regulation of the contraction-relaxation cycles of *in vivo* myonemes. Biol. Cell. 67: 251-261.
Febvre-Chevalier C. (1973a) Un nouveau type d'association des microtubules axopodiaux chez les Héliozoaires. Protistologica 9: 35-43
Febvre-Chevalier C. (1973b) *Hedraiophrys hovassei*, Morphologie, Biologie et cytologie. Protistologica 9: 503-520.
Febvre-Chevalier C. (1975) Etude cytologique de *Gymnosphaera albida*, Sassaki, 1894 (Héliozoaire Centrohélidié). Protistologica 11: 331-344.
Febvre-Chevalier C. (1980) Behaviour and cytology of *Actinocoryne contractilis* nov. gen., nov. sp. A stalked Heliozoan (Centrohelidia). Comparison with other related genera. J. Mar. Biol. Ass U.K. 60: 909-928.
Febvre-Chevalier C. (1981) Preliminary study of the motility processes in the stalked Heliozoan *Actinocoryne contractilis*. Biosystems 14: 337-343.
Febvre-Chevalier C. (1982) Revision of the taxonomy of the Heliozoa with attention to electron microscopical criteria. Ann. Inst. Océanol., Paris 57(S): 173-178.
Febvre-Chevalier (1987) Ultrastructure et critères taxonomiques. Excitabilité et motilité cellulaire d'Héliozoaires marins. Thèse Doctorat d'Etat, Juin 1987, Nice. Office des Thèses, Grenoble.
Febvre-Chevalier C. (1990) Phylum Actinopoda, Class Heliozoa. In: Handbook of Protocists. (Eds. L. Margulis, J.O. Corliss, M. Melkonian, D. Chapman) Jones and Batlett, Inc. Boston, Ma. 347-362.
Febvre-Chevalier C., Febvre J. (1981) Cytophysiologie de la motilité. Film S.F.R.S., Paris.
Febvre-Chevalier C., Febvre J. (1984) Axonemal microtubule pattern of *Cienkowskya mereschkovskyi* and a revision of Heliozoan taxonomy. Origins of Life 13: 315-338.
Febvre-Chevalier C., Febvre J. (1986) Motility mechanisms in the actinopods (Protozoa): A review with particular attention to axopodial contraction-extension, and movement of nonactin filament systems. Cell Motil. Cytoskeleton 6: 198-208.

Febvre-Chevalier C., Febvre J. (1992) Microtubule disassembly in vivo: Intercalary destabilization and breakdown of microtubules in the Heliozoan *Actinocoryne contractilis*. J. Cell Biol. 118: 585-594.

Febvre-Chevalier C., Febvre J. (0000) Buoyancy and Swimming in marine planktonic Protists. J. Mar. Biol. Ass., UK (in press).

Febvre-Chevalier C., Bilbault A., Bone Q., Febvre J. (1986) Sodium-calcium action potential associated with contraction in the Heliozoan *Actinocoryne contractilis*. J. Exp. Biol. 122: 177-192.

Febvre-Chevalier C., Bilbault A., Febvre J., Bone Q. (1990) Membrane excitability and motile responses in the Protozoa, with particular attention to the Heliozoan *Actinocoryne contractilis*. In: Evolution of the first nervous systems. (Ed. P.A.V. Anderson), Plenum Press, New-York, 237-253.

Fitzharris T.P., Bloodgood R.A., McIntosh J.R. (1972) Particle movement in the axopodia of *Echinosphaerium:* Evidence concerning the role of the axoneme. J. Mechanochem. Cell Motility 1: 117-124.

Golz R., Hauser M. (1991) Direct evidence for the occurrence of simple MTOCs and for end to end joining of microtubules with modified ends in the reticulopodia of *Allogromia laticollaris* (Foraminifera). Eur. J. Protistol. 27: 357-364.

Haeckel E. (1862) Radiolarien (Rhizopoda Radiaria). Eine Monographie. 1-572. Mit einem atlas mit 35 kupfertafeln. Reimer. Berlin, 1862.

Hauser M. (1986) Taxol affects both the microtubular arrays of heliozoan axonemes and their microtubule-organizing center. Eur. J. Cell Biol. 42: 295-304.

Hausmann K. and Patterson (1982) Pseudopod formation and membrane production during prey capture by a Heliozoon (Feeding by *Actinophrys II)*. Cell. Motil. 2: 9-24.

Hausmann K., Linnenbach M., Patterson D.J. (1983) The effects of taxol on microtubular arrays: *In vivo* effect on Heliozoan axonemes. J. Ultrastr. Res. 82: 212-220.

Heidemann S.R., McIntosh J.R. (1980) Visualization of the structural polarity of microtubules. Nature 286: 517-519.

Hoffman E.J., Price D.A., Krumpelman J.A. (1983) Isolation of axopodial axonemes from mass cultured *Echinosphaerium nucleoflum*. J. Protozool. 30: 371-375.

Hollande A., Hollande E. (1975) Appareil de Golgi et glycocalyx des Radiolaires. Visualisation de mucosubstances acides, APS posirives, l'aide du complexe amines d'osmium-OS2. Protistologica 10: 279-292.

Hollande A., Cachon J., Cachon-Enjumet M. (1965) Infrastructure des axopodes chez les Radiolaires Sphaerellaires Périaxoplastidiés. C. R. Acad. Sci. Paris 261: 1388-1391.

Hollande A., Cachon J.M., Valentin I. (1967) Infrastructure des axopodes et organisation générale de *Sticholonche zanclea* Hertwig (Radiolaire Sticholonchidé). Protistologica 3: 155-169.

Huang B., Pitelka D.R. (1973) The contractile process in the ciliate *Stentor coeruleus*. I. The role of microtubules and filaments. J. Cell Biol. 57: 704-728.

Hyams J.S., Stebbings H. (1977) Microtubule associated cytoplasmic transport. In: Microtubules. (Eds. K.Roberts, J.S. Hyams). London, 487-530.

Ishida H., Shigenaka Y. (1988) Cell model contraction in the Ciliate *Spirostomum*. Cell Motil. Cytoskeleton. 9: 278-282.

Jones W.C. (1975) The pattern of microtubules in the axonemes of *Gymnosphaera albida* Sassaki. J. Cell Sci. 18: 133-155.

Jones C.R., Tucker I.B. (1981) Microtubule-organizing centres and assembly of the double-spiral microtubule pattern in certain Heliozoan axonemes. J. Cell Sci. 50: 259-281.

Kitching I.A. (1964) The axopods of the sun animalcule *Actinophrys sol* (Heliozoa). In: Primitive Motile Systems in Cell Biology. (Eds. R.D. Allen, N. Kamiya). Acad. Press Inc, New York, 445-465.

Koonce R.P., McIntosh J.R. (1990) Identification and immunolocalization of a cytoplasmic dynein in *Dictyostelium*. Cell Motil Cytosk. 15: 51-62.

Koonce R.P., Schliwa M. (1985) Bidirectional organelle transport can occur in cell processes that contain single microtubules. J. Cell Biol. 100: 322-326.

Koonce R.P., Euteneur U., McDonald K.L., Menzel D., Schliwa M. (1986) Cytoskeletal architecture and motility in a giant freshwater Amoeba *Reticulomyxa*. Cell Motil. Cytosk. 6: 521-533.

Little M., Quinlan R.A., Hoffman E.J., Luduena R.F. (1983) Identification and characterization of axopodial tubulins from *Echinosphaerium nucleofilum*. J. Cell Biol. 31: 55-61.

Macdonald A.C., Kitching J.A. (1967) Axopod filaments of Heliozoa. Nature 215: 99-100.

Mandelkow ? , Mandelkow E. (1989) Tubulin, microtubules and oligomers: molecular structure and implications for assembly. In: Cell movement II. (Eds. F.R. Warner, J.R. MacIntosh) Alan R. Liss Inc. 3: 23-45.

Marsland D., Tilney L.G., Hirshfeld M. (1971) Stabilizing effect of D_2O on the microtubular component and needle-like form of Heliozoan axopods: a pressure-temperature analysis. J. Cell Physiol. 77: 187- 194.

Matsuoka T., Shigenaka Y. (1984) Localization of calcium during axopodial contraction in Heliozoan *Echinosphaerium akame*. Biomed. Res. 5: 425-432.

Matsuoka T., Shigenaka Y., Naitoh Y. (1985) A model of contractile tubules showing how they contract in the Heliozoan *Echinosphaerium akame*. Cell Struct. Funct. 10: 63-70.

Mignot J-P. (1979) Etude ultrastructurale de la pédogamie chez *Actinophrys sol* (Héliozoaire). I. La division progamique. Protistologica 15: 387-406.

Mitchison T., Kirschner M. (1984) Dynamic instability of microtubule growth. Nature (Lond.) 312: 237-242.

Nishi T., Kobayashi M., Shigenaka Y. (1986) Membrane activity and its correlation with vacuolar contraction in the Heliozoan Echinosphaerium. J. Exp. Cell Biol. 239: 175-182.

Ockleford C.D. (1974) Cytokinesis in the Heliozoan *Actinophrys sol*. J. Cell Sci. 16: 499-517.

Ockleford C.D (1975) Ultraviolet light microbeam irradiation of the microtubules in single Heliozoan axopodia. Exp. Cell Res. 93: 127-135.

Ockleford C.D., Tucker J.B (1973) Growth, breakdown, repair and rapid contraction of microtubular axopodia in the Heliozoan *Actinophrys sol*. J. Ultrastr. Res. 44: 369-387.

Patterson D.J. (1979) On the organization and classification of the Protozoon, *Actinophrys sol* Ehrenberg, 1830. Microbios 26: 165-208.

Patterson D.J., Fenchel T. (1985) Insights into the evolution of heliozoa (Protozoa, Sarcodina) as provided by ultrastructural studies on a new species of flagellate from the genus *Pteridomonas*. Biol. J. Lin. Soc. 34: 381-403.

Patterson D.J., Hausmann K. (1981) Feeding by *Actinophrys sol* (Protista, Heliozoa): I. Light microscopy. Microbios 31: 39-55.

Patterson D.J., Hausmann K. (1982) Morulate bodies in Actinophryid Heliozoa: A fixation artefact derived from microtubules ? Cell Struct. Funct. 7: 341-348.

Pickett-Heaps J.D. (1969) The evolution of the mitotic apparatus: an attempt at comparative ultrastructural cytology in dividing plant cells. Cytobios 3: 257-280.

Porter K.R. (1966) Cytoplasmic microtubules and their functions. In: Principles of biomolecular organization. (Eds. G.E.W. Wolstenholme, M. O'Connor). J.& A. Churchill Ltd. London, 308-345.

Rebhun L.I. (1972) Polarized intracellular particle transport, saltatory movement and cytoplasmic streaming. Intern. Rev. Cytol. 32: 97-137.

Rieder C.L. (1979) High-voltage electron microscopy reveals new components in the axonemes and centroplast of the centrohelidian *Raphidiophrys ambigua*. J. Cell Sci. 40: 215-234.

Rose M.D., Biggins S., Satterwhite L.L. (1993) Unravelling the tangled web at the microtubule-organizing center. Curr. Opin. Cell Biol. 5: 105-115.

Roth L.E., Pihlaja D.J. (1977) Gradionation: Hypothesis for patterning. J. Protozool. 24: 2-9.

Roth L.E., Shigenaka Y. (1970) Microtubule in the Heliozoan axopodium. II. Rapid degradation by cupric and nickelous ions. J. Ultrastr. Res. 31: 356-374.

Roth L.E., Pihlaja D.J., Shigenaka Y. (1970) Microtubule in the Heliozoan axopodium. I. The gradion hypothesis of allosterism in structural proteins. J. Ultrastr. Res. 30: 7-37.

Schliwa M. (1976) The role of divalent cations in the regulation of microtubule assembly. In vivo studies on microtubules of the Heliozoan axopodium using the ionophore A23187. J. Cell Biol. 70: 527-540.

Schliwa M. (1984) Mechanisms of intracellular organelle transport. In: Cell and muscle motility. (Ed. J. Chay), Plenum. 5: 1-82.

Schewiakoff W. (1926) Die Acantharia des Golfes von Neapel. In: Fauna e Flora del Golfo di Napoli, Monographie 37. G. Bardi, Roma; R. Friedlander u Sohn, Berlin.

Shigenaka Y. (1976) Microtubule in Protozoan cells. II. Heavy metal ion effects on degradation and stabilization of the Heliozoan microtubules. Annot. Zool. Jap. 49: 164-176.

Shigenaka Y., Roth L.E., Pihlaja D.J. (1971) Microtubule in the Heliozoan axopodium. III. Degradation and reformation after dilute urea treatment. J. Cell Sci. 8: 127-151.

Shigenaka Y., Todokoro Y., Kaneda M. (1975) Microtubule in Protozoan cells. I. Effects of light metal ions on the Heliozoan microtubules and their kinetic analysis. Annot. Zool. Jap. 48: 227-241.

Shigenaka Y., Yano K., Imada M. (1989) Axopodial contraction evoked by electrical stimulation and its ultrastructural analysis in a Heliozoan *Echinosphaerium*. Zool. Sci. 6: 45-54.

Shigenaka Y., Maruoka T., Toyohara A., Suzaki T. (1979a) Studies on the cell fusion of Heliozoans. V. Cell membrane fluidity and surface coat in close relation to the fusion reaction. Annot. Zool. Jap. 52: 163-178.

Shigenaka Y., Maruoka T., Toyohara A., Suzaki T. (1979b) Microtubules in Protozoa. IV. Effects of sulfhydryl-blocking reagents on axopodial degradation and reformation in Heliozoa. Cell Struct. Funct. 4: 23-34.

Shigenaka Y., Yano K., Yogosawa R., Suzaki T. (1982) Rapid contraction of the microtubule-containing axopodia in a large Heliozoan *Echinosphaerium*. In: Biological Functions of Microtubules and related Structures. (Eds. H. Sakai, H. Mohri, G.G. Borisy) Acad. Press, Inc. 105-114.

Sugiyama M., Ikegawa S., Masuyama T., Ishida M., Shigenaka Y. (1992) Isolation and properties of the axopodial cytoskeleton of a Heliozoan *Echinosphaerium akame*. Eur. J. Protozool. 28: 214-219.

Suzaki T., Shigenaka Y. (1982) Intra-axopodial particle movement and axopodial surface motility in *Echinosphaerium akame*. In: Biological functions of microtubules and related structures. (Eds. H. Sakai, H. Mohri, G.G. Borisy). Acad Press, New York, 91-103.

Suzaki T. Shigenaka Y., Takeda Y. (1978) Studies on the cell division of Heliozoans. II. Active role of axopodia on division process and transformation of remnants of cytoplasmic connecting bridge to new axopodia. Cell. Struct. Funct. 3: 209-218.

Suzaki T., Shigenaka Y., Watanabe S., Toyohara A. (1980) Food capture and ingestion in the large Heliozoan *Echinosphaerium nucleofilum*. J. Cell. Sci. 42: 61-79.

Suzaki T., Ando M., Ishigame K., Shigenaka Y., Sugiyama M. (1992) Structure and function of the cytoskeleton in Heliozoa. 2. Measurement of the force of rapid axopodial contraction in *Echinosphaerium*. Eur. J. Protistol. 28: 430-433.

Takeshita T., Suzaki K., Takahashi A., Koishi M. (1991) Framing streak camera. Ultrahigh-speed photography, videography and photonics. SPIE 1539:1-10.

Tilney L.G. (1968) Studies on the microtubules in Heliozoa IV. The effect of colchicine on the formation and maintenance of axopodia in *Actinosphaerium nucleofilum* (Barrett). J. Cell Sci. 3: 549-562.

Tilney L.G. (1971) How microtubule patterns are generated. The relative importance of nucleation and bridging of microtubules in the formation of the axoneme of *Raphidiophrys*. J. Cell Biol. 51: 837-854.

Tilney L.G., Byers B. (1969) Studies on the microtubules in Heliozoa. V. Factors controlling the organization of microtubules in the axonemal pattern in *Echinosphaerium*. J. Cell Biol. 43: 148-163.

Tilney L.G., Porter K.R. (1965) Studies on the microtubules in Heliozoa. I. Fine structure of *Actinosphaerium* with particular reference to axial rod structure. Protoplasma 60: 317-344.

Tilney L.G., Porter K.R. (1967) Studies on the microtubules in Heliozoa. II. The effect of low temperature on these structures in the formation and maintenance of the axopodia. J. Cell Biol. 34: 327-343.

Tilney L.G., Hiramoto Y., Marsland D. (1966) Studies on the microtubules in Heliozoa. III. A pressure analysis of the role of these structures on the formation and maintenance of the axopodia of *Actinosphaerium nucleofilum*. (Barrett). J. Cell Biol. 29: 77-97.

Tilney L.G., Bryan J., Bush D.J., Fujiwara K., Mooseker M.S., Murray D.B., Snyder D.H. (1973) Microtubules: evidence for 13 protofilaments J. Cell Biol. 59: 267-275.

Travis J.L., Bowser S.S. (1986) A new model of reticulopodial motility and shape. Evidence of a microtubule-based motor and an actin cytoskeleton. Cell Motil. Cytoskeleton 6: 2-14.

Troyer D. (1975) Possible involvement of plasma membrane in saltatory particle movement in heliozoan axopods. Nature 254: 696-698.

Troyer D. (1976) Untersuchungen an saltatischer Partikelbewegung bei *Heterophrys*. Dissertation. Ruhr Universität, Bochum: 1-105.

Tucker J.B. (1984) Spatial organization of microtubule-organizing centers and microtubules. J. Cell Biol. 99: 55-62.

Vale (1990) Microtubule-based motor proteins. Current Opinion Cell Biol. 2: 3-9.

Vollet J.J., Roth L.E. (1974) Cell fusion by nascent-membrane induction and divalent-cation treatment. Cytobiol. 9: 249-262.

Watters (1968) Studies on the motility of the Heliozoa. I. The locomotion of *Actinophaerium eichhorni* and *Actinophrys* sp. J. Cell Sci. 3: 231-244.

Zuelzer (1909) Bau und Entwicklung von *Wagnerella borealis* Mereschk. Arch. Protistenk. 17: 135-202.

Received on 3th August, 1993

ACTA
PROTOZOOLOGICA

Acta Protozoologica (1993) 32: 229 - 236

Swimming Velocity of *Paramecium* under the Conditions of Weightlessness

Ruth HEMMERSBACH-KRAUSE[1], Wolfgang BRIEGLEB[1], Kurt VOGEL[2] and Donat-P. HÄDER[2]

[1]DLR, Institute of Aerospace Medicine, Köln; [2]Institute for Botany and Pharmaceutic Biology, Friedrich-Alexander-University, Erlangen, Germany

Summary. During the 6 min-lasting "free-fall conditions" (4×10^{-6} g) of the parabolic flight of a sounding rocket *Paramecium aurelia* cells showed an increase of 7.5 % in their mean swimming velocity. A detailed analysis revealed that the kinetic response was transient: after 3 min the velocity decreased to the speed of the former horizontal swimming at 1 g. Control experiments simulating the influence of vibration and hypergravity during launch of the rocket lead to the conclusion that the increase of the velocity during the parabolic flight was exclusively induced by the transition to 0 g. An increased velocity was also observed under the condition of simulated weightlessness on a fast-rotating clinostat microscope.

Key words. Gravitaxis, gravikinesis, ciliates, clinostat, sounding rocket.

INTRODUCTION

It is still an open question how gravity as a permanent and constant background force influences the behavior of biological systems at the cellular level. Recent investigations have demonstrated that the gravity-dependent behavior of *Paramecium* includes tactic as well as kinetic responses (Hemmersbach-Krause et al. 1991a; Machamer and Bräucker 1992; Machemer et al. 1991, 1992). In addition, changes in the swimming behavior give us hints about the status of the membrane potential. Other authors have shown that hyperpolarization of the cell membrane results in a faster forward swimming whereas ciliary reversals resulting in backward swimming are caused by depolarization of the membrane (for review see Eckert and Brehm 1979, Kung and Saimi 1982, Preston and Saimi 1990, Machemer 1988).

The swimming behavior of *Paramecium* was investigated under the conditions of weightlessness during a parabolic flight of a payload of a sounding rocket. The experiment was supported by ground-experiments in a horizontal microscope, on a fast-rotating clinostat (60 rpm) and on a low-speed centrifuge microscope (up to 5 g). In a previous paper we investigated orientation and course of swimming tracks (Hemmersbach-Krause et al. 1993). The fact that after onset of 'free-fall' conditions as well as during functional weightlessness on a fast clinostat paramecia performed no phobic responses, lead us to the conclusion that no action potential was generated across the ciliate's excitable membrane. Swimming paths of the individual cells remained more or less straight demonstrating that the

Address for correspondence: R. Hemmersbach-Krause, DLR, Institute of Aerospace Medicine, P.O. Box 906058, 51140 Köln, Germany.

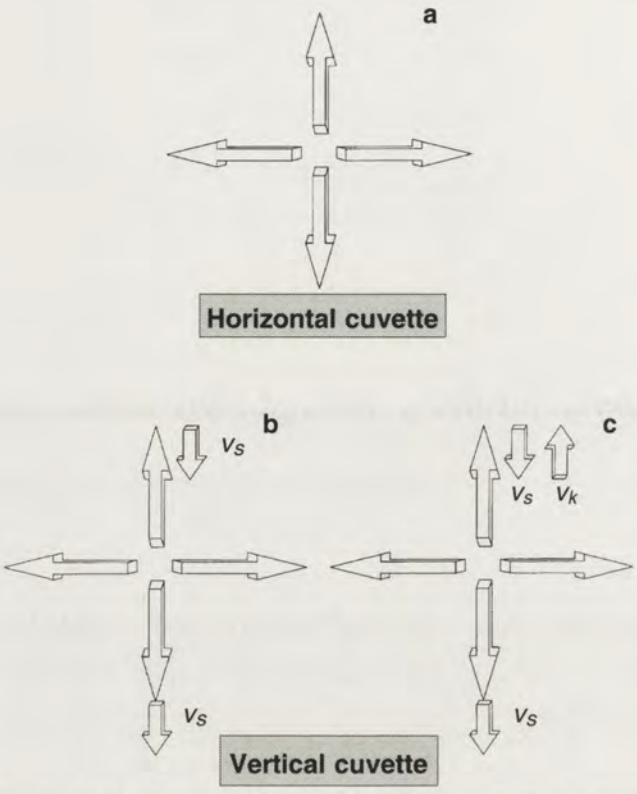

Fig. 1. Scheme for swimming velocities in horizontally and vertically positioned flat cuvettes. If a horizontal cuvette (a) is turned vertically (b, c) one would expect that sedimentation (v_S) adds to downward and subtracts from upward swimming velocities (b). However, in case of *Paramecium* sedimentation is compensated by a component v_K due to faster upward swimming, a behavior called "gravikinesis" (c)

control of the ciliary beat is not directly influenced by gravity otherwise an uncontrolled movement should occur. Due to the fact that *Paramecium* regulates its vertical swimming velocity at 1 g, resulting in an faster upward swimming than calculated from sedimentation and horizontal swimming (gravikinesis, see Fig. 1) (Machemer et al. 1991) we expected changes under 0 g conditions. The results are presented and discussed.

MATERIALS AND METHODS

Cell culture

Paramecium aurelia cells, (wild type) were cultivated with *Enterobacter* as a food source in phosphate-buffered straw medium (pH 7.2, 22° C). All experiments were carried out with cells in the stationary growth phase in their growth medium. Cells were enriched without centrifugation to exclude acceleration effects before the onset of the experiment. For this reason, cell suspensions were filled into special flasks, where they accumulated in the narrow neck of the flask due to negative gravitaxis and positive aerotaxis. Cells were placed in an observation chamber (∅ 30 mm; depth 0.5 mm) and temperature was controlled (via Peltier elements). The chamber consisted of two frames of titanium, in which two pieces of glass (RG 645, Schott & Gen., Mainz, FRG) were inserted. The cylindrical wall of the chamber was formed by titanium. The temperature was measured by temperature sensor within the titanium chamber. Evaluation of the flight-temperature data showed that the temperature was constant at 22° C within the observation chamber during the observation time.

Sounding Rocket

During the parabolic flight of the payload of a sounding Skylark rocket TEXUS 27 (TEXUS - Technologische Experimente unter Schwerelosigkeit), 6 min free-fall condition, with a quality of 4×10^{-6} g, was achieved. In the course of the 50 s ascent of the rocket two accelerations were effective; (1) the thrust acceleration with a mean of 5 g and (2) a centrifugal (spin) acceleration for space-stabilization of the rocket. Within the last phase of the ascent the spin acceleration alone was effective for 6.6 s and increased to 6.4 g at the site of the observation chamber. Within 1 s the spin was stopped by a "yo-yo-despin" mechanism meaning that the diameter of the rocket's payload was increased by releasing ropes tethering a mass. When the video signal was received from the rocket 60 s after lift-off, the residual radial acceleration was 2.6×10^{-4} g and declined to 4×10^{-6} g further on. Measurements of the residual accelerations were performed by Kayser-Threde (München, FRG) using micro-g sensors at the position of the sample (for further flight characteristics see Hemmersbach-Krause et al. 1993).

During the "late access" period (45 min before lift-off) the observation chamber was mounted on the stage of a horizontal microscope which was part of an experimental module (TEM 06-19) developed by MBB-ERNO (Bremen, FRG). Within this module the microscope objective is mounted tangentially to the cross section of the rocket. Therefore, the optical axis is perpendicular to the resultant vector which is varied by the increasing thrust and spin accelerations (see Fig. 2). The swimming cells were observed in dark field mode with a 1.6 x objective and a tube length of 130 mm (deflected 90°, 85 + 45 mm) providing an observation area of 2 mm in diameter. Video recording was performed by a CCD camera (Aqua TV, Kempten, FRG) from the time of insertion of the sample into the rocket until lift-off and continued after onset of 0 g. Images of the swimming cells were transmitted by a wireless TV-system (MORABA - Mobile Rocket Basis, DLR, Oberpfaffenhofen, FRG) to the ground and stored on video tapes.

Clinostat microscope

A fast-rotating clinostat microscope, developed by Briegleb and coworkers (Briegleb 1983, 1988; Block et al. 1986; Hemmersbach-Krause et al. 1991b) was used to cancel the influence of gravity. The clinostat microscope is a horizontal microscope which can be rotated about its optical axis (modified Zeiss AC body with Zeiss optics, Zeiss, Oberkochen, FRG) and which is equipped with a video camera (LDH 26 with Newvicon tube, Philips, Hamburg, FRG) for

direct observation. Special care was taken that the rotation axis is identical (± 0.2 mm) with the optical axis of the light microscope. For calculation of the residual acceleration during rotation of the clinostat, the maximum radii of the observation chamber and the observation field, as well as the speed of clinostat rotation were taken into account. In the case of our observation chamber different accelerations must be considered. At 60 rotations per min a maximal centrifugal force of 3×10^{-3} g is calculated for the border of the observed field (radius 1 mm ± 0.2 mm) and 4×10^{-2} g for the border of the whole chamber (radius 15 mm ± 0.2 mm).

180° reorientation

The influence of gravity was inverted by turning a vertically positioned cuvette 180 degrees about a horizontal axis within 5 s. Observations were made using a horizontal microscope.

Centrifuge microscope

Experiments under accelerations of up to 5 g were performed in a slow-rotating centrifuge microscope (NIZEMI) designed by Briegleb and coworkers (Hemmersbach-Krause et al. 1991c) and constructed by Dornier (Friedrichshafen, FRG). The NIZEMI is a horizontal microscope (Axioplan, Zeiss, Oberkochen, FRG) mounted tangentially on a circular platform belt-driven by an electric motor. During rotation, the optical axis is perpendicular to the resultant vector of gravity and centrifugal acceleration. With a radius of 170 mm (distance between center of focal plane and rotation axis) and 163 rotations per minute a centrifugal force of 5 g is achieved. Acceleration to 5 g took 15 s, stopping of the centrifuge 5 s.

Vibration test

Cells were exposed to a vibration test (5.5 g, 20 - 2000 Hz for 1 min) simulating the worst case of vibration during launch of the Skylark rocket. A vibration test facility from MBB ERNO, Bremen, FRG was used.

Computer analysis

Real time image analysis was performed on-line or during playback using video recorded sequences (Häder and Lebert 1985, Häder and Vogel 1991), tracking about 70 ciliates simultaneously. The technique is based on on-line digitization of four frames taken at 80 ms intervals and stored in a video memory. Position and outline of the individual cells are determined by chain coding and are further followed through the recorded series of images. The movement vectors of all cells tracked are stored by the distance an organism has moved in the time interval determined by the video frame and by deviation angles from the predefined stimulus direction (gravity). Note that one cell may be represented by more than one track. Under worst case conditions a cell may have been tracked up to 3 times when entering the observation field; this value, however, is usually smaller. Sectors of ± 30° were chosen for registration of upward (0°), downward (180°) and horizontal (90°; 270°) swimming velocities. In order to test for statistically significant differences experimental data sets were compared using the F-test or Welch-test (95 % confidence level) (Batschelet 1981).

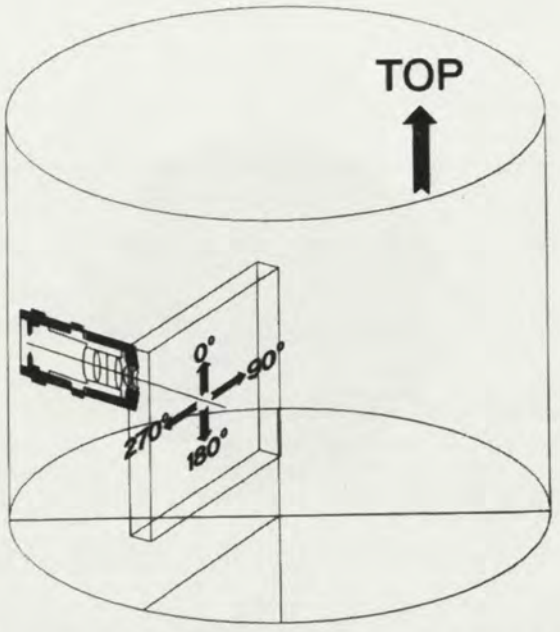

Fig. 2. Arrangement of recording optics and observation chamber within payload of the rocket

RESULTS

Swimming velocity in the TEXUS 27 experiment

Before lift-off paramecia swam 15 % faster downwards than upwards as indicated in the circular histogram (Fig. 3a; small shift of the histogram downwards). Differences between the velocities in dependence from the swimming directions are significant. Sedimentation velocities of $NiCl_2$-immobilized cells (N=2010 tracks) revealed a mean value of 81.5 ± 22 µm s^{-1}. With the values of the mean upward swimming velocity (U) (655 µm s^{-1} ± 113 µms^{-1}; N=1639), the downward velocity (D) (773 µm s^{-1} ± 135 µm s^{-1}: N=317) and the sedimentation velocity (S) a gravikinetic value of - 23 µm s^{-1} (Δ) was calculated according to Machemer et al. (1991) (D-U/2 = S+Δ). The velocity histogram of the flight sequence is radially symmetric (Fig. 3b), significant differences between the former horizontal and vertical swimming directions have disappeared (compare also Fig. 5a).

The velocities under 1 g as well as under the flight conditions have a Gaussian distribution (Fig. 4). The quotient of range and standard deviations is 6.03 (1 g) and 6.81 (0 g) that means it lies within the range of a

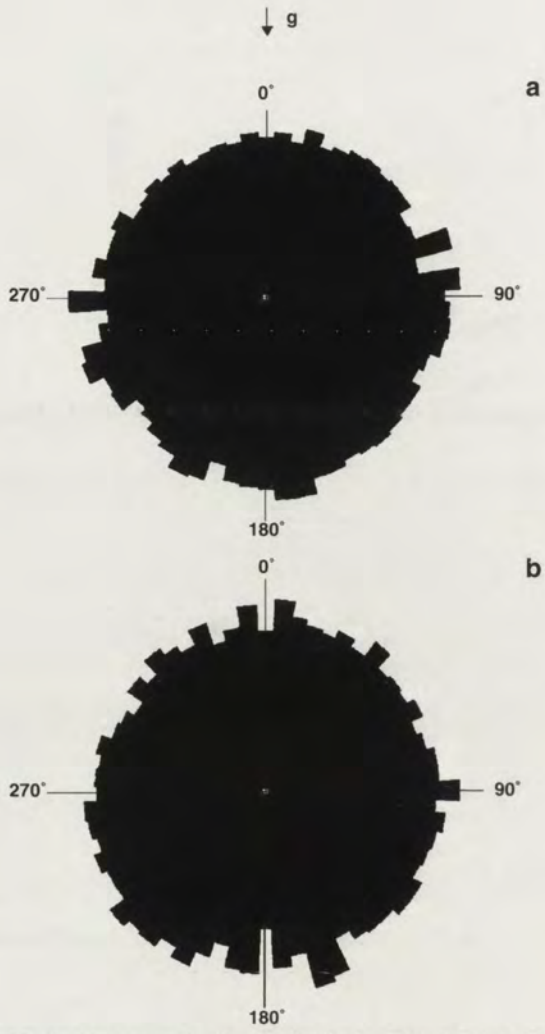

Fig. 3. Circular histograms showing the distribution of swimming velocities within the population: a - before lift-off (5 min measurement) cells swam slightly faster downwards than upwards (N=3223); b - after 3.5 min under the condition of weightlessness till up to the end of the free-fall period of the rocket a homogeneous velocity distribution was registered (N=2893). Calibration: a - sector 36.4° corresponds to 685 µm s^{-1}; b - sector 95.6° to 703 µm s^{-1}

Gaussian distribution. Compared to the mean swimming velocity at 1 g (685 µm s^{-1} ± 138 µm s^{-1} (N=3223) the mean velocity of the total flight sequence increased 7.5 % to 736 µm s^{-1} ± 208 µm s^{-1} (N=7936 tracks) (Fig. 5a). Mean values and median values under both conditions have only a small difference (8 µm/s^{-1}). According to the F test a variation coefficient of 2.27 was calculated indicating a significant difference between the two data sets. The Welch test (comparing mean velocities) also shows a significant value of 15.13. Besides that, standard deviations under 0 g increased significantly.

As a next step of evaluation, the flight sequence was subdivided into 1 min intervals (Fig. 6). Comparison of the mean swimming velocities during these time segments with the mean swimming velocities before lift-off revealed a transient increase in velocity. After 4 min under 0 g the mean swimming velocity approached the value of the former horizontal swimming velocity. The mean swimming velocity of the last 2.5 flight minutes (703 µms^{-1} ± 225 µms^{-1}; N=2893) was not significantly different to the former horizontal swimming velocity (713 µm s^{-1} ± 156 µm s^{-1}; N=319) but significantly decreased/increased compared to the former downward velocity (773 µm s^{-1} ± 135 µm s^{-1}: N=317) and the former upward velocity (655 µm s^{-1} ± 113 µms^{-1}; N=1639). 45 min after touch-down (time required for transfer of the rocket module back to the laboratory), the mean swimming velocity had further decreased and the former relationship (before lift-off) between the upward, downward and horizontal swimming directions was reestablished.

In a further step of evaluation, the time before, during and after the flight was divided in segments of 20 s each (Fig. 7). Comparison of the mean swimming velocities during these segments demonstrated first the increase and after 4 min the adaptation of the swimming velocity under free-fall conditions.

Hypergravity

For simulating the effect of linear acceleration during the rocket start on the swimming velocity of paramecia, a cell culture was exposed for 1 min to 5 g. Comparison of the mean swimming velocities before (731 µm s^{-1} ± 211 µm s^{-1}; N=2534) and after (707 µm s^{-1} ± 204 µm s^{-1}; N=3487) exposure to hyper-gravity (measurements of 6 min each) showed that the mean swimming velocity had significantly decreased, while the relationship between the rates of up, down and horizontally swimming cells had not been affected by the intervening hypergravity (Fig. 5b).

Vibration

Exposure to a 1 min-lasting vibration, comparable to that one during launch, did not produce a significant change in the mean swimming velocities before (976 µm s^{-1} ± 183 µm s^{-1}; N=1772) and after (970 µm s^{-1} ± 303 µm s^{-1}; N=2900) vibration, however, the standard deviation increased (Fig. 5c).

Functional weightlessness

During a 2 h-lasting experiment on a fast-rotating clinostat (60 rpm) the behavior of the cells was analyzed

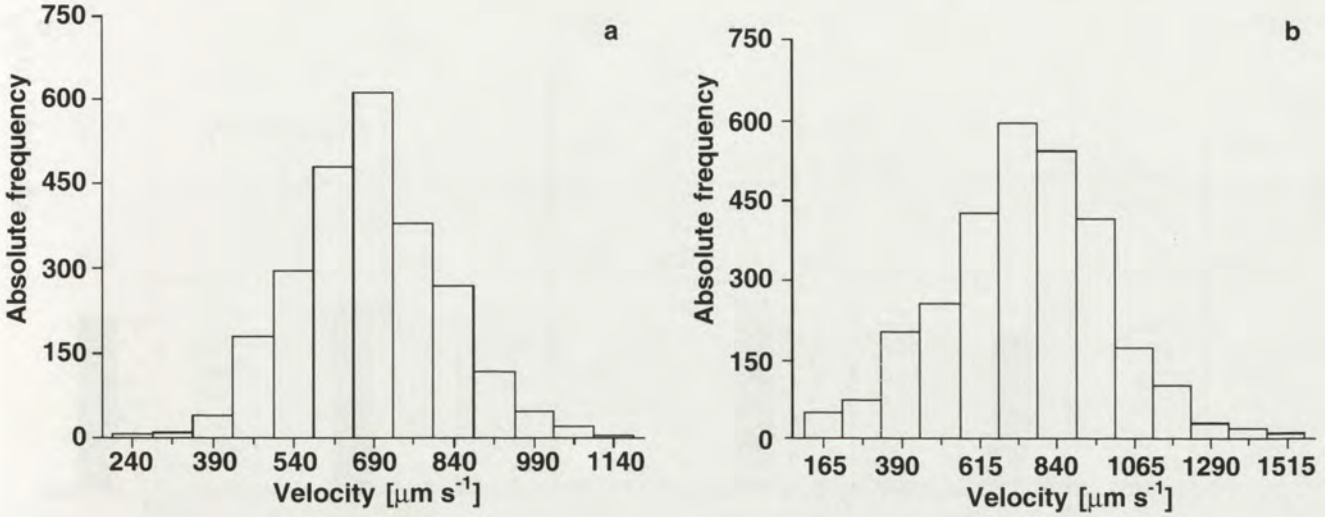

Fig. 4. Near Gaussian distribution of the swimming velocities: a - before lift-off (mean swimming velocity 683 ± 138 μm s^{-1}, N=2478) and b - during the flight (mean swimming velocity 738 ± 236 μm s^{-1}, N=2818)

(Figs. 5d, 8). Comparing the mean swimming velocities of the last 5 min before starting the clinostat (499 μm s^{-1} ± 114 μm s^{-1}; N=1395) with the first 6 min on the rotating clinostat (543 μm s^{-1} ± 131 μm s^{-1}; N=2317), showed that (a) the cells swam significantly faster (+ 8.8 %) on the clinostat and (b) that the differences observed in the non-rotating clinostat at 1 g between the velocities in up, down and horizontal swimming directions disappeared under simulated 0 g in the rotating clinostat (Fig. 5d).

Significant increases in the former upward as well as in the horizontal velocities (upward +64 μm s^{-1}, horizontal +72 μm s^{-1}), and a significant decrease of the former downward velocity (-84 μm s^{-1}) resulted in an increased mean swimming velocity over all directions in the running clinostat. After 1 h in the clinostat the swimming velocity decreased but remained even after stopping the clinostat higher than before starting the clinostat experiment, 2 hours before (Fig. 8). In addition, the directional differences between the swimming velocities were reestablished comparable to before starting the clinostat. In order to test the influence of shear forces of the fluid during start of rotation on the velocity of the paramecia, a vertically oriented flat chamber was turned (180° within 5 s) about its horizontal axis. Comparison of the mean velocities before (584 μm s^{-1} ± 133 m s^{-1}; N=1969) and after the turn (537 μm s^{-1} ± 124 μm s^{-1}; N=1744) (5 min measurements each) revealed that the mean swimming velocity was significantly reduced, whereas the relationships between the velocities of the different directions remained unaffected.

DISCUSSION

Under the conditions of gravity paramecia showed "gravikinesis" (Machemer et al. 1991) (Fig. 1) suggesting that the cells swim faster upwards than calculated from the horizontal swimming velocity in a flat cuvette and the sedimentation velocity (Hemmersbach-Krause et al. 1991a). Thus upward swimming cells compensate their sedimentation velocity. Like Machemer et al. we isolated a negative gravikinetic value. Gravikinesis is a strong argument for a physiologically mediated mechanism because it occurs only if paramecia are able to "sense" the direction of gravity and modulate their velocity depending on swimming direction. During the 6 min free-fall condition of the TEXUS experiment, *Paramecium* showed a transient increase in mean swimming velocity which is presumably not induced by acceleration or vibration during launch of the rocket as concluded from simulation experiments. Before onset of free-fall most of the cells were swimming against the acceleration vector as indicated by the high r-values (0.55 at 1g; 0.95 after spin of the rocket) after stopping the spin of the rocket (Hemmersbach-Krause et al. 1992). Obviously their gravikinesis was not switched off immediately after removal of the gravity stimulus, because only after four min the mean swimming velocity under 0 g achieved the value of the former horizontal speed. Under completely different experimental conditions using drop tower facilities Mogami et al. (1988) observed during a 2.1 s lasting free-fall experiment (drop tower) with a residual acceleration of 10^{-2} g a "small tendency of reduction" of the mean swimming velocity

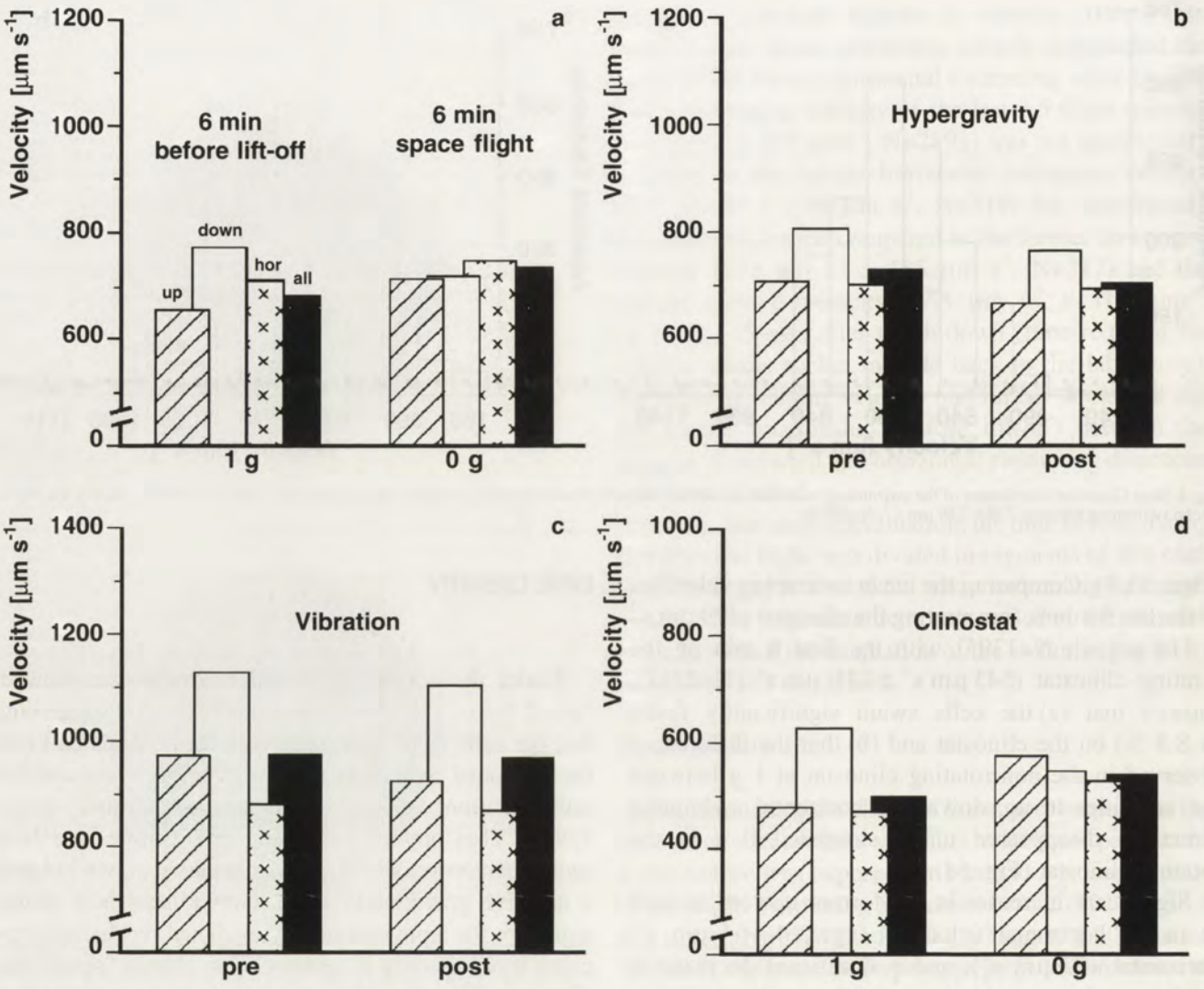

Fig. 5. Mean swimming velocities depending on direction: upward 0° ± 30° (hatched), downward 180° ± 30° (white), horizontal 90°; 270° ± 30° (crosses) and for all directions (0°- 360°, black): a - 5 min before lift-off (1 g) (N=3223) and during 6 min space flight (0 g) (N=7936); b - 6 min before (pre) (N=2534) and after (post) (N=3487) exposing cells for 1 min to hyper-gravity (5 g); c - 6 min before (pre) (N=1772) and after (post) (N=2900) exposing cells for 1 min to a vibration test; d - during the last 6 min before starting the clinostat (1 g) (N=1395) and during the first 6 min on the running clinostat (0 g) (N=2317). Notice that under reduced real (a) and simulated (d) gravity the mean swimming velocity increased and differences between the velocities of the three directions subsided. After exposing cells to hypergravity (b) and vibration (c) their mean swimming velocities tended to decrease (b) or were unchanged (c). The relationship between the velocities at horizontal and vertical directions persisted

(N=9). Murakami et al. (1990) stated from another drop tower experiment that "the vertical component of the swimming velocity changed" after the onset of 'free-fall' conditions and that the magnitude of change was larger than the "sinking" velocity at 1 g. Improved drop-tower experiments with 4.5 s free-fall at approximately 10^{-4} g revealed that within 4.5 s (total experimental time) upward and downward swimming velocities adjusted to a common value which corresponded to the horizontal swimming velocity at 1 g while full random orientation was not achieved during this time. Rocket and drop tower data support previous assumptions suggesting that the normal propulsive force of a cell, which can be measured only under the conditions of weightlessness, corresponds to the horizontal swimming velocity at 1 g (Machemer et al. 1991, 1992). However, identical swimming velocities must not reflect the same physiological status of the cell under both conditions. Due to the electrophysiological theory of gravikinesis it is assumed that bipolar membrane channel stimulation cancel under 1 g horizontal swimming (Machemer et al. 1992). However, if we postulate a distinct gravireceptor in interaction with cytoskeleton and membranes (comparable to the situation in plants; Sievers et al. 1991), no neutralisation in respect to gravity stimulation can be expected under 1 g independent from the cell's swimming direction.

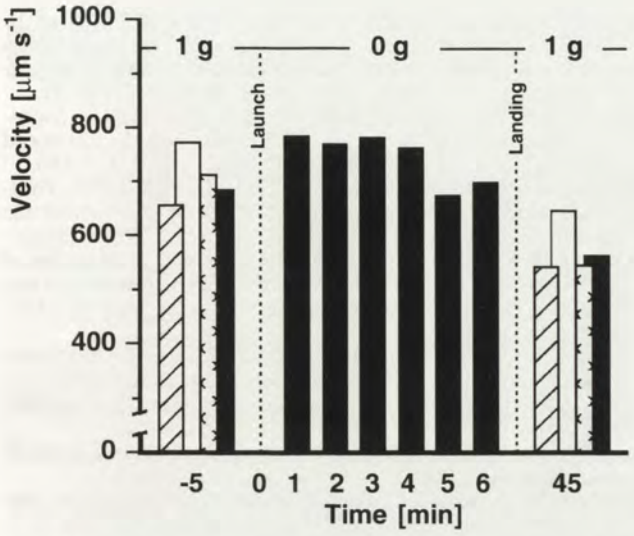

Fig. 6. Mean swimming velocities before (1 g), during (0 g) and after the flight (1 g). The flight sequence was divided into 1 - min intervals of evaluation and compared to measurements over a 5 min period before (-5) and after the flight (+45). Notice that after about 4 min the mean swimming velocity during the flight approached the speed of the former horizontal swimming (90°, 270° ± 30°). Black - mean swimming velocity over all directions (0°-360°); hatched - upward velocity (0° ± 30°); white - downward velocity (180° ± 30°); crosses - horizontal velocity (90°, 270° ± 30°)

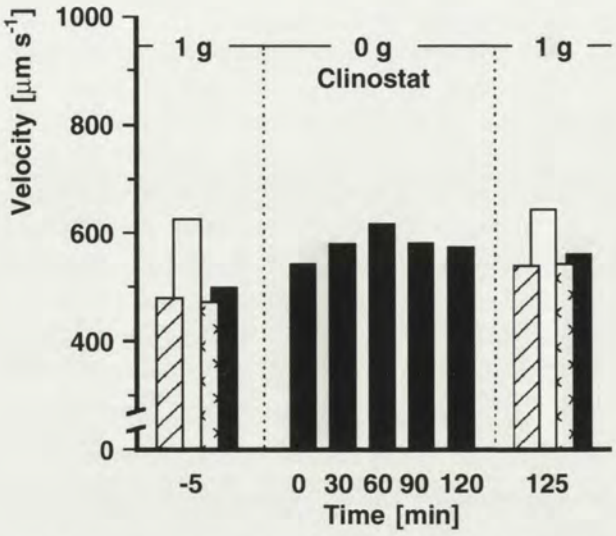

Fig. 8. Comparison of mean swimming velocities before (-5 min; 1 g), during 2 h of clinostatization (0 min - 120 min; simulated 0 g) and after stopping the clinostat (125 min; 1 g). For each of the 5min - lasting measurement more than 1800 tracks were registered. Notice that the mean swimming velocity under simulated weightlessness increased and that the relationship between the velocities in the different directions changed. Black - mean swimming velocity over all directions (0°-360°); hatched - upward velocity (0° ± 30°); white - downward velocity (180° ± 30°); crosses - horizontal velocity (90°, 270° ± 30°)

An increased swimming velocity was also measured during the whole experimental time on a fast-rotating clinostat. However, after 1 h a decrease in velocity was measured, indicating adaptation or energy loss due to the experimental conditions (closed cuvette).

The fact that a single 180° turn relative to gravity did not provoke an increase in the swimming velocity indicates that the mechanical disturbances caused by the moving fluid during the start of the clinostat are not responsible for the permanent increase in the swimming velocity during the 2 h - lasting experiment. It was observed that after 1 s, all layers within the medium and the chamber rotated with the same speed. However, due to the dimensions of the observation chamber, cells were swimming in a gradient of centrifugal forces between the center of rotation and the periphery of the chamber (4×10^{-2}g). The threshold for graviperception in *Paramecium* has not yet been determined. In the rotating clinostat the cells may experience transitions from super- to subthreshold accelerations, and vice versa which might induce a permanent increase in swimming velocity. For further consideration of this problem the threshold for graviperception of *Paramecium* must be determined. Such an experiment is planned for the IML-2 (International Microgravity Laboratory) mission scheduled for 1994.

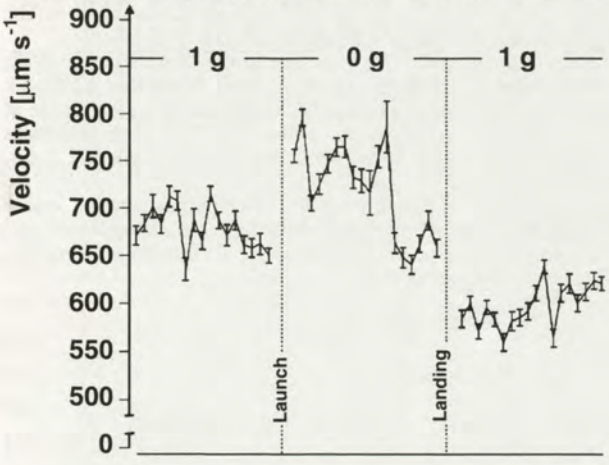

Fig. 7. Mean swimming velocities (line) (with standard error of the means) before (1 g), during (0 g) and after the flight (1 g). The transient increase of the mean velocity during 0 g associated with an increase in standard deviations. Successive measurements of 20 s intervals. Each point of measurement represents a mean value of more than 100 tracks. 15505 tracks were registered in total

Adaptation to weightlessness was accompanied by an increase in the standard deviations (Fig. 7). A similar phenomenon was observed in the case of *Physarum* after transition to simulated or near weightlessness (Block et al. 1986). However, in the case of *Paramecium* also vibration during launch could be a reason for the observed scatter but not for the increase in mean swimming velocity.

Direct effects of gravity on the membrane (Machemer et al. 1991, Schatz et al. 1992) as well as on the general metabolism (e.g., an increase in the amount of cAMP inside the cilia (Bonini et al. 1986)) as it was shown for

other cell types (Krasnov et al. 1975, 1977; Murakami et al. 1985; Hampp et al. 1992; Slenzka et al. 1992) could be a cause for an increase in the ciliary beat frequency and in turn an increase in the swimming velocity of the cell. Alternatively, an altered orientation of the power stroke towards the cell's long axis would also change its efficiency and result in an increased velocity (Naitoh and Eckert 1969). Further experiments should clarify whether the increase in the swimming velocity after onset of 0 g is a post-effect of gravikinesis at 1 g or whether it is a more general stimulation on the cellular level after transition to the conditions of weightlessness.

Acknowledgements. We thank our colleagues M. Köhler, A. Wolke, B. Bromeis and R. Donath (Space Biology, DLR), for their help, D. Franke, D. Grothe, I. Meyer, P. Kyr with the whole TEXUS-team of MBB-ERNO, Bremen, FRG and G. Schmitt and his team from Kayser-Threde, München, FRG, for their excellent work in conducting the TEXUS-system. We thank the German Minister for Research and Technology (BMFT), the German Space Agency (DARA) and the European Space Agency (ESA) for continuous support.

REFERENCES

Batschelet E. (1981) Circular statistics in biology. Academic Press, London.

Block I., Briegleb B., Wohlfarth-Bottermann, K.-E. (1986) Gravisensitivity of the acellular slime mold *Physarum polycephalum* demonstrated on the fast-running clinostat. Eur. J. Cell Biol. 41: 44-50.

Bonini N. M., Gustin M. C., Nelson D. L. (1986) Regulation of ciliary motility by membrane potential in *Paramecium*: A role for cyclic AMP. Cell Motil. Cytoskel. 6: 256-272.

Briegleb W. (1983) The clinostat - a tool for analyzing the influence of acceleration on solid-liquid systems. Proceedings of the Workshop on Space Biol, Cologne, FRG. ESA (Spec Publ) SP 206: 97-101.

Briegleb W. (1988) Ground-born methods in gravitational cell biology. The Physiologist 31: 44-47.

Eckert R., Brehm P. (1979) Ionic mechanisms of excitation in *Paramecium*. A. Rev. Biophys. Bioeng. 8: 353-383.

Häder D.-P., Lebert M. (1985) Real time computer-controlled tracking of motile microorganisms. Photochem. Photobiol. 42: 509-514.

Häder D.-P., Vogel K. (1991) Simultaneous tracking of flagellates in real time by image analysis. J. Math. Biol. 30: 63-72.

Hampp R., Naton B., Hoffmann E., Mehrle W., Schönherr K., Hemmersbach-Krause R. (1992) Hybrid formation and metabolism of plant cell protoplasts under microgravity. The Physiologist 35: 27-30.

Hemmersbach-Krause R., Briegleb W., Häder D.-P. (1991a) Dependence of gravitaxis in *Paramecium* on oxygen. Eur. J. Protistol. 27: 278-282.

Hemmersbach-Krause R., Briegleb W., Häder D.-P., Plattner H. (1991b) Gravity effects on *Paramecium* cells: an analysis of a possible sensory function of trichocysts and of simulated weightlessness on trichocyst exocytosis. Eur. J. Protistol. 27: 85-92.

Hemmersbach-Krause R., Briegleb W., Häder D.-P. (1991c) Swimming behavior of *Paramecium* - first results with the low-speed centrifuge microscope NIZEMI. Adv. Space Res. 3: 113-116.

Hemmersbach-Krause R., Briegleb W., Häder D.-P., Vogel K., Grothe D., Meyer I. (1993) Orientation of *Paramecium* under the conditions of weightlessness. J. Euk. Mickrobiol. 40: (in press).

Krasnov I. B. (1975) Quantitative cyto- and histochemical studies of the Deiters' Nucleus and nodular cortex of the cerebellum in rats exposed to weightlessness. Aviat. Space Environ. Med. 46: 1119-1122.

Krasnov I. B. (1977) Quantitative histochemistry of the vestibular cerebellum of the fish *Fundulus heteroclitus* flown aboard the biosatellite COSMOS-782. Aviat. Space Environ. Med. 48: 808-811.

Kung C., Saimi Y. (1982) The physiological basis of taxes in *Paramecium*. A. Rev. Physiol. 44: 519-534.

Machemer H. (1988) Motor control in cilia. In: *Paramecium* (Ed. H.D. Görtz). Springer Verlag, Berlin Heidelberg, 216-235.

Machemer H., Bräucker R. (1992) Graviperception and graviresponses in ciliates. Acta Protozool. 31: 185-214.

Machemer H., Bräucker R., Takahashi K., Murakami A. (1992) Short-term microgravity to isolate graviperception in cells. Micrograv. Sci. Technol. 5: 119-123.

Machemer H., Machemer-Röhnisch S., Bräucker R., Takahashi K. (1991) Gravikinesis in *Paramecium*: theory and isolation of a physiological response to the natural gravity vector. J. comp. Physiol. A 168: 1-12.

Mogami Y., Kimura T., Okuno M., Yamashita M., Baba S. A. (1988) Freefall experiment on swimming behavior of ciliates. In: Proceedings of the 16th Int. Symp. on Space Technology and Science, 2351-2354.

Murakami D. M., Miller J. D., Fuller C. A. (1985) Changes in functional metabolism in the rat central nervous system following spaceflight. The Physiologist 28: 143-144.

Murakami A., Yoshimura K., Takahaski K. (1990) Responses to gravity and gravitaxis in *Paramecium*. Sixty-first annual meeting of Zool Society Japan, Nigata, Japan, October 3-5, 1990, Zool. Sci. 7: 1046.

Naitoh Y., Eckert R. (1969) Ionic mechanisms controlling behavioral responses of *Paramecium* to mechanical stimulation, Science 164: 963-965.

Preston R. R., Saimi Y. (1990) Calcium ions and the regulation of motility in *Paramecium*. In: Ciliary and flagellar membranes (Ed. R.A. Bloodgood). Plenum Press, New York, 173-194.

Schatz A., Reitstetter R., Briegleb W., Linke-Hommes, A. (1992) Gravity effects on biological systems. Adv. Space Res. 12: 51-53.

Sievers A., Buchen B., Volkmann D., Hejnowicz Z. (1991) Role of the cytoskeleton in gravity perception. In: The cytoskeletal basis of plant growth and form (Ed.C.W Lloyd.). Academic Press, London, 169-182.

Slenzka K., Appel, R., Rahmann H. (1992) Brain creatine kinase activity during ontogeny of the cichlid fish *Oreochromis mossambicus* and the clawed toad *Xenopus laevis*, influence of gravity. Dev. Brain Res. (submitted).

Received on 7th January, 1993; accepted on 28th May, 1993

ACTA
PROTOZOOLOGICA

Acta Protozoologica (1993) 32: 237-243

Microarchitecture and Mineralization in Loricae of Phacotacean Flagellates

John R. DUNLAP and Patricia L. WALNE

Program in Microscopy and Department of Botany, University of Tennessee, Knoxville, TN, USA

Summary. The loricae of the phacotacean genera *Pteromonas*, *Phacotus* and *Dysmorphococcus* were examined by light, scanning and transmission electron microscopy, and analyzed by energy-dispersive X-ray spectroscopy. In general, all loricae consist of a meshwork of interwoven granulo-fibrillar components, many of which are subsequently mineralized. In *Pteromonas* and *Phacotus*, the major mineralizing element is calcium, which appears to be processed in the Golgi apparatus and transported to the cell surface via cytoplasmic vesicles. In contrast, in *Dysmorphococcus*, the major metals are iron and manganese, and there is no evidence thus far of active cellular involvement in their incorporation into the loricae. With respect to morphology, the loricae of both *Pteromonas* and *Phacotus* are bivalved, whereas the lorica of *Dysmorphococcus* is a single, porate unit. Lorica microarchitecture in *Dysmorphococcus* and *Phacotus* consists of granular and needle-like components, whereas the lorica of *Pteromonas* is composed primarily of electron-opaque calcium-containing granules associated with other less-dense fibrillar material.

Key words. Lorica, microarchitecture, mineralization, Phacotaceae, X-ray spectroscopy.

INTRODUCTION

An extracellular wall-like structure termed a lorica or an envelope characterizes members of the Phacotaceae, which have a chlamydomonad cellular organization. Historically used as a major taxonomic criterion, the lorica may vary in morphology and microarchitecture and has been shown to contain calcium (Ca), iron (Fe), manganese (Mn) and occasionally silicon (Si) in different amounts (Gerard and Walne 1979, Porcella and Walne 1980, Pocratsky and Walne 1981, Giering et al. 1990, Krienitz et al. 1990). The diversity of basic lorica morphology and ultrastructure, together with persisting questions about the extent of genetic control over its development and subsequent mineralization, point to the need for further study and clarification of loricae as tenable criteria in the systematics and phylogeny of the phacotacean flagellates.

Address for correspondence: P.L. Walne, Program in Microscopy and Department of Botany, University of Tennessee, Knoxville, TN 37996, USA.

MATERIALS AND METHODS

The organisms used in this investigation were obtained originally from the UTEX Culture Collection of Algae (Starr and Zeikus 1987): *Pteromonas protracta* (Stein) Lemm. (LB 647), *Phacotus lenticularis* Ehr. (LB 142), and *Dysmorphococcus globosus* Bold et Starr (LB 65). Cultures were maintained in a biphasic soil water medium (Starr 1978) on a 16:8 light/dark cycle under standard conditions. All samples were fixed in 0.05 M sodium-cacodylate-buffered 2% glutaraldehyde for 1 hour at 4°C. Some samples were post-fixed for 1 hour in buffered 2% osmium tetroxide, also at 4°C. After fixation, all samples were

dehydrated in alcohol and embedded in Spurr's low-viscosity resin. Thin sections were cut with a diamond knife on a Reichert OMU3 ultramicrotome and stained with uranyl acetate and lead citrate before being examined on an Hitachi H-800 transmission electron microscope operating at 200 kV. Energy dispersive X-ray spectra were collected from unstained thick sections of material, with a Link Pentafet X-ray detector and QX 2000 processing system attached to the Hitachi microscope.

RESULTS

The bivalved lorica of *Pteromonas* is compressed at the edges to form lateral wings that are slightly curved up or down, which cause the cell to gently rotate as it swims (Fig. 1). In surface view the mature lorica of *Pteromonas protracta* has a characteristic hexagonal periodicity (Fig. 1). Although this pattern is not obvious in sectioned material, the occurrence of regularly spaced electron-opaque material suggests a similar periodicity (Fig. 2). The ultrastructure of the cell is *Chlamydomonas*-like with a parietal chloroplast and a pyrenoid surrounded by large starch plates (Fig. 2). The Golgi apparatus appears to be actively involved in lorica development via the production of mucilaginous material and electron-opaque granules. Golgi saccules and cytoplasmic vesicles (Fig. 3) containing fibrillar and granular material similar to that found in the mature lorica (Fig. 4) are present in most actively growing cells. Chemical microanalysis of the electron-opaque deposits shows that calcium is the primary element (Fig. 5). These data suggest that the mucilaginous material found within such vesicles is also presumptive lorica material since the chemical composition is similar to that found in the mature lorica (Fig. 6). Once released from the cell, this material becomes part of a complex reticular network which characterizes the ultrastructure of the mature lorica.

Like *Pteromonas*, the lorica of *Phacotus lenticularis* is bivalved (Fig. 7), but the surface is rugose and lacks an hexagonal pattern. Lorica development begins with the production of a thin pliable matrix or "skin" around the cell (Fig. 8), typically before the daughter cell is released from the parent lorica. Ultrastructurally, the mature lorica is characterized by interwoven fibrillar material and associated electron-opaque deposits (Fig. 9). The Golgi apparatus is also implicated in lorica development since cytoplasmic vesicles contain densely stained material (Figs. 10, 11), similar to that seen in mature envelopes. Chemical analysis of such material shows that Ca is present (Fig. 12). Analysis of the lorica provides a similar spectrum (not shown).

Dysmorphococcus is similar cytologically to both *Pteromonas* and *Phacotus* (Fig. 13). Lorica development is also similar and begins with the production of a thin, filmy layer of mucopolysaccharides (Fig. 14). The mature lorica of *Dysmorphococcus* is, however, a single unit and more porate than the loricae of the other two genera (Fig. 15). Lorica microarchitecture is characterized by a complex network of fine fibrillar material and associated electron-opaque deposits. In *Dysmorphococcus*, iron and/or manganese are the primary mineralizing elements; calcium is a secondary element. The fine fibrillar material becomes complexed with electron-opaque granular (Fig. 16) and/or needle-like (Fig. 17) components. Via X-ray microanalysis, these components are shown to be iron enriched (Fig. 18) and manganese enriched (Fig. 19), respectively.

DISCUSSION

There are two basic components to the phacotacean lorica, one organic, the other inorganic. With electron microscopy the organic component appears as fine fibrillar material, and the inorganic component as electron-opaque granular or needle-like deposits. The microarchitecture of the mature (fully developed) lorica is usually characterized by a complex assemblage of both components. The initial stage of lorica development involves the production of a thin, pliable, unmineralized film of mucilaginous material surrounding the cell. This film has been suggested to serve as a template on or within which subsequent development and mineralization occur (Gerard and Walne 1979). Lorica development continues via the production and secretion of either mineralized or unmineralized mucilaginous material until a mature lorica, characteristic of the species, is formed (Gerard and Walne 1979, Pocratsky and Walne 1981,

Figs. 1-6. *Pteromonas protracta.* 1 - SEM frontal view shows bivalved, alate, mature lorica with hexagonal surface pattern. Anterior wedge-shaped lorica insert shows pores through which the two flagella emerge. Bar - 4.0 μm. 2 - TEM of portion of laterally compressed cell shows cup-shaped chloroplast with prominent pyrenoid surrounded by massive starch plates, Golgi apparatus and vacuoles containing electron-opaque lorica precursor material. Portion of lorica with lateral wing surrounds the cell. Bar - 1.0 μm. 3 - Golgi apparatus and derived vesicles near cell periphery contain electron-opaque lorica precursor material. Bar - 0.2 μm. 4 - portion of lorica wing (cf. Figs 1, 2) shows microarchitecture of electron-opaque regions interwoven with less-dense components. Bar - 0.1 μm. 5 - X-ray spectrum from Golgi-associated granules and vesicle material. 6 - X-ray spectrum from lorica shown in Fig. 4

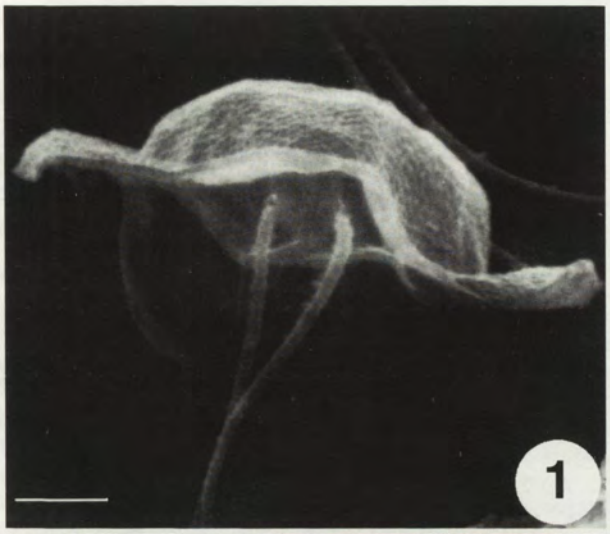

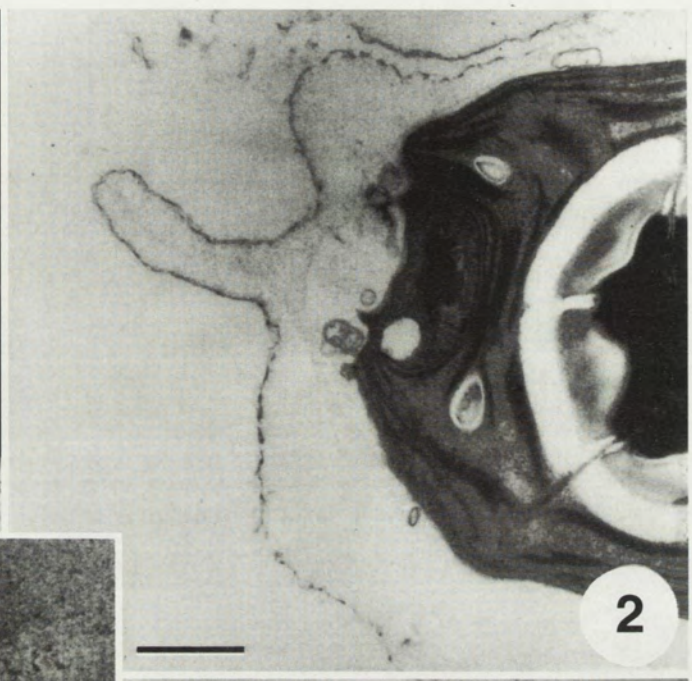

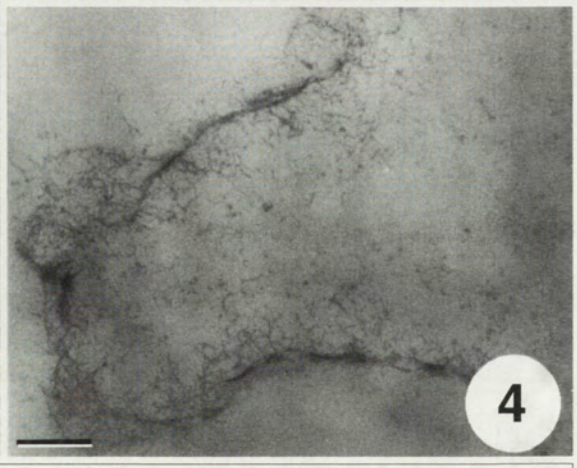

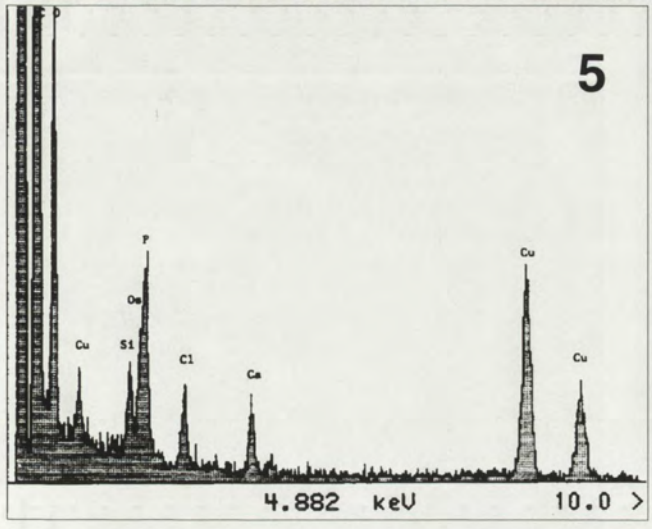

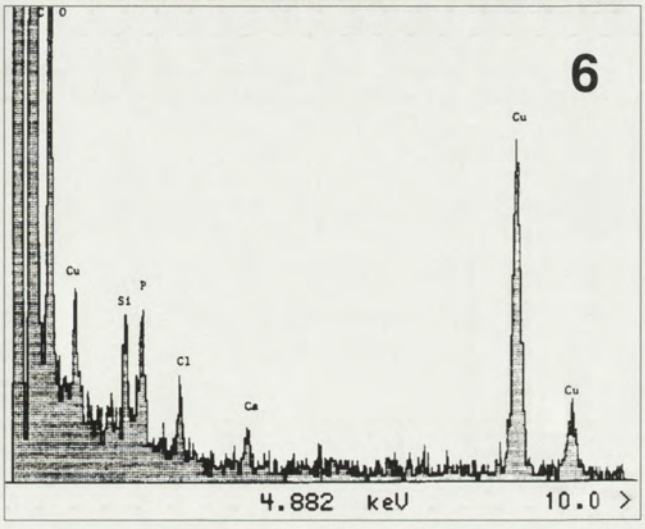

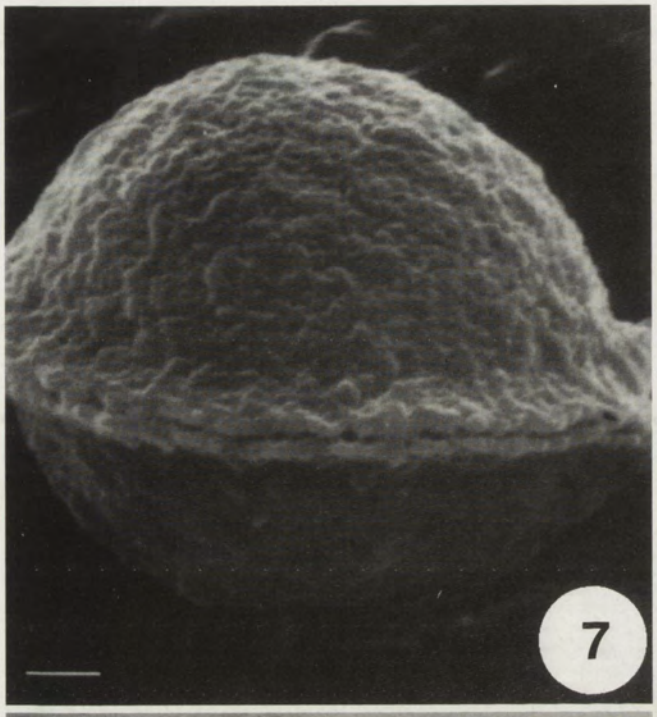

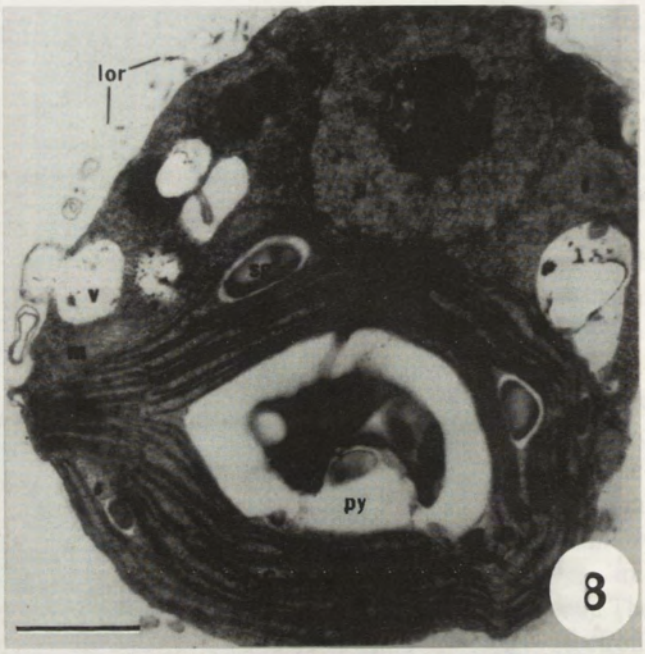

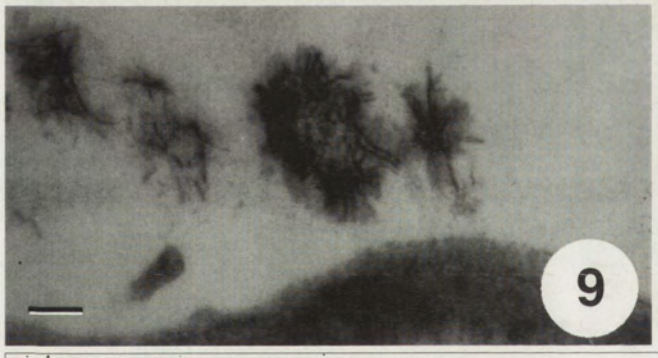

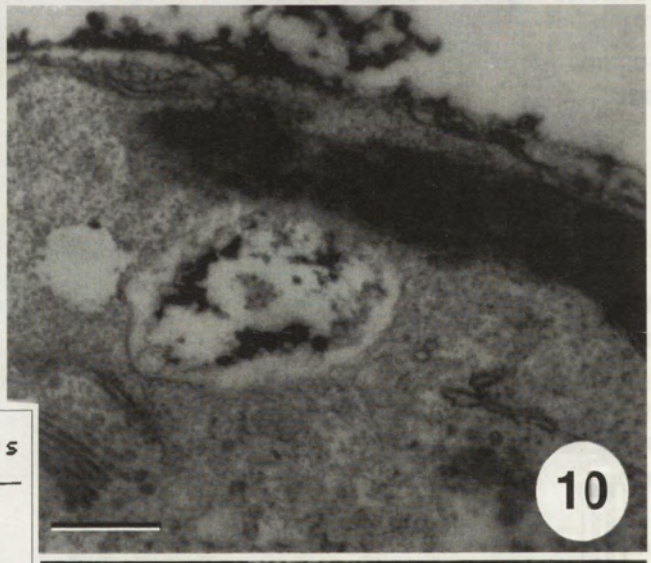

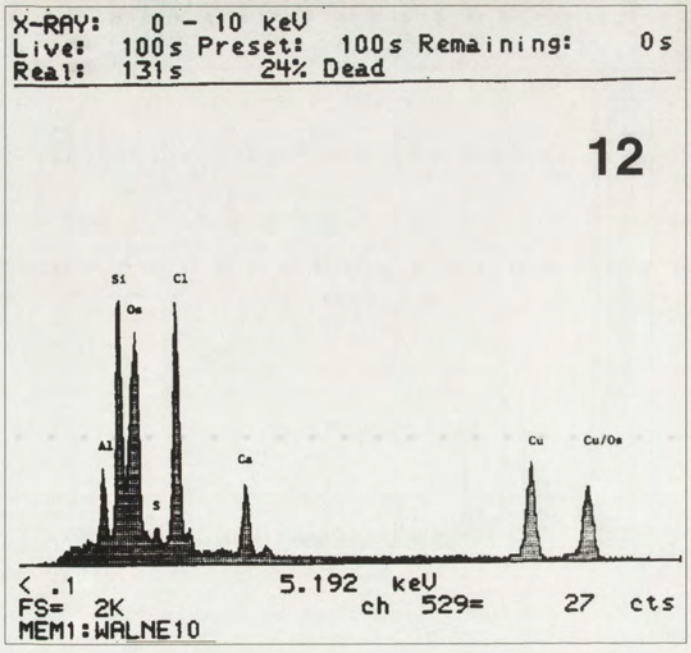

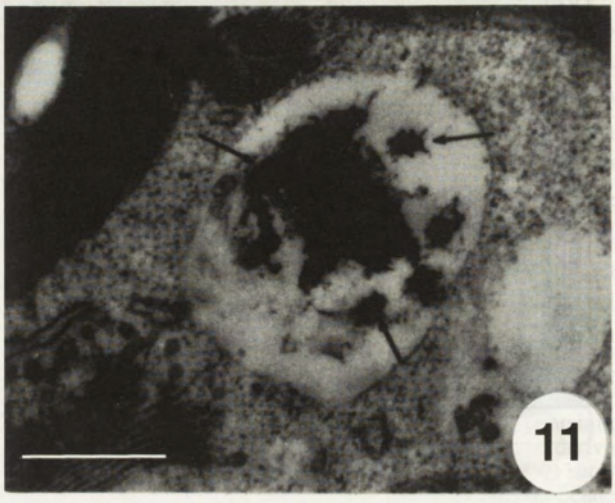

Giering et al. 1990). Although mucilage production and secretion may continue throughout the life of the cell, the lorica does not continue to grow, i.e., once the lorica has matured to its characteristic size, shape and degree of ornamentation, its development stops, a phenomenon suggesting that the cell has some control over the developmental process even though the lorica is physically remote from the cell. Giering et al. (1990) suggested that lorica development, structure and mineralization are under genetic control in *Phacotus lendneri*, an argument that is not contested thus far by any other studies on the loricate Phacotaceae or any other group of loricate algae.

The presence of calcite crystalline material in the loricae of *Phacotus*, another interesting phenomenon, was reported by Steinberg and Klee (1983), Heinrich et al. (1986), Koschel and Raidt (1988) and Giering et al. (1990), on the basis of SEM and X-ray or LAMMA microanalysis. Using laser microprobe mass analysis (LAMMA), Heinrich et al. (1986) reported the occurrence of Ca, Mn and Fe in the loricae of *P. lenticularis*, with considerably more Fe than either Mn or Ca. In their ecological investigations of a number of hardwater lakes in Germany, Koschel and Raidt (1988) compared autochthonous calcite precipitation in free water to the calcite surface structure and development of secondary or mature loricae in *Phacotus* and demonstrated a relationship between diverse hydrochemical conditions and microcrystalline structure. As part of a study on asexual reproduction and lorica formation in *Phacotus lendneri*, Giering et al. (1990) reported the first observations of the primary stages of calcite crystal formation in immature loricae.

Earlier investigations of *Phacotus lendneri*, using polarizing optics, indicated a rotational symmetry of calcite crystals on the lorica surface and a mirror symmetry in the center (Kamptner 1950). Similar results were reported by Müller and Oti (1981) from investigations of Pleistocene limestone deposits, termed "*Phacotus*-Kalk", near Hollerup, Denmark. In addressing the occurrence, distribution and geological implications of calcified nannoplankton, they used SEM, petrographic and polarizing microscopy to describe the structure and orientation of calcite microcrystals in fossil loricae of *Phacotus* (Müller and Oti 1981).

It is not yet clear why Ca is in the form of calcite in some but not all *Phacotus* species studied to date. For example, it was thought that calcite crystals occurred in *P. lendneri* and amorphous calcium in *P. lenticularis*; however, in their recent synonymization of *P. lendneri* with *P. lenticularis*, Giering et al. (1992) noted that the lorica can be composed of both amorphous and crystalline structures. Some of the apparent discrepancies may relate to whether analyses were carried out on organisms from natural populations or from laboratory cultures. Laboratory conditions may not support natural growth and development; thus, lorica mineralization patterns may be different. Environmental conditions may certainly play a role in the form of the metal being deposited. The relationship between ecological conditions and calcite crystalline structure and precipitation was clearly shown by Koschel and Raidt (1988), for example. In the case of the newly synonymized *P. lenticularis*, it would be interesting to know whether the calcite crystals are mediated through the Golgi apparatus and derived cytoplasmic vesicles and subsequently incorporated into the lorica, or whether the calcite precipitates extracellularly as a result of environmental pressures such as high calcium carbonate levels in the water (Giering et al. 1990). Similar arguments have been made by Conforti et al. (personal communication) for the euglenoid flagellates *Trachelomonas* and *Strombomonas*.

In the current study, calcium deposition was shown to occur intracellularly in *Pteromonas* and *Phacotus*. Thus, primary mineralization of lorica precursor material, i.e., calcium deposition on the fine fibrillar material, occurs intracellularly. The fact that iron is sometimes detected in the mature lorica, but has not been detected in intracellular vesicles suggests that secondary mineralization of the lorica may occur as an extracellular process. Similar passive types of mineralization phenomena are recognized in other loricate algae (Dunlap and Walne 1985) where mineralization is an extracellular process. This is considered a passive process since metal accumulation on lorica mucopolysaccharides occurs outside the cell membrane, results suggesting that the cell may not be directly involved in the mineralization process. In *Pteromonas* and *Phacotus*, lorica mineralization appears to be both passive and active, and as such at least partially under cellular (genetic) control.

Dysmorphococcus presents a somewhat different situation. Cellular morphology and ultrastructure are clearly *Chlamydomonas*-like (cf. Porcella and Walne 1980)

Figs. 7-12. *Phacotus lenticularis*. 7 - SEM, lateral view, shows bivalved lorica with rugose surface. Bar - 2.0 μm. 8 - TEM of cell surrounded by developing lorica. Golgi-derived cytoplasmic vesicles at cell periphery contain lorica precursor material. Nucleus and pyrenoid surrounded by starch plates are prominent. Bar -0.5 μm. 9 - TEM of portion of mature lorica showing interweaving of electron-opaque and other components. Bar - 0.1 μm. 10, 11 - cytoplasmic vesicle contain electron-opaque and more filmy lorica precursor material. Bars - 0.5 μm. 12 - X-ray spectrum from vesicle material like that shown in Figs. 10, 11

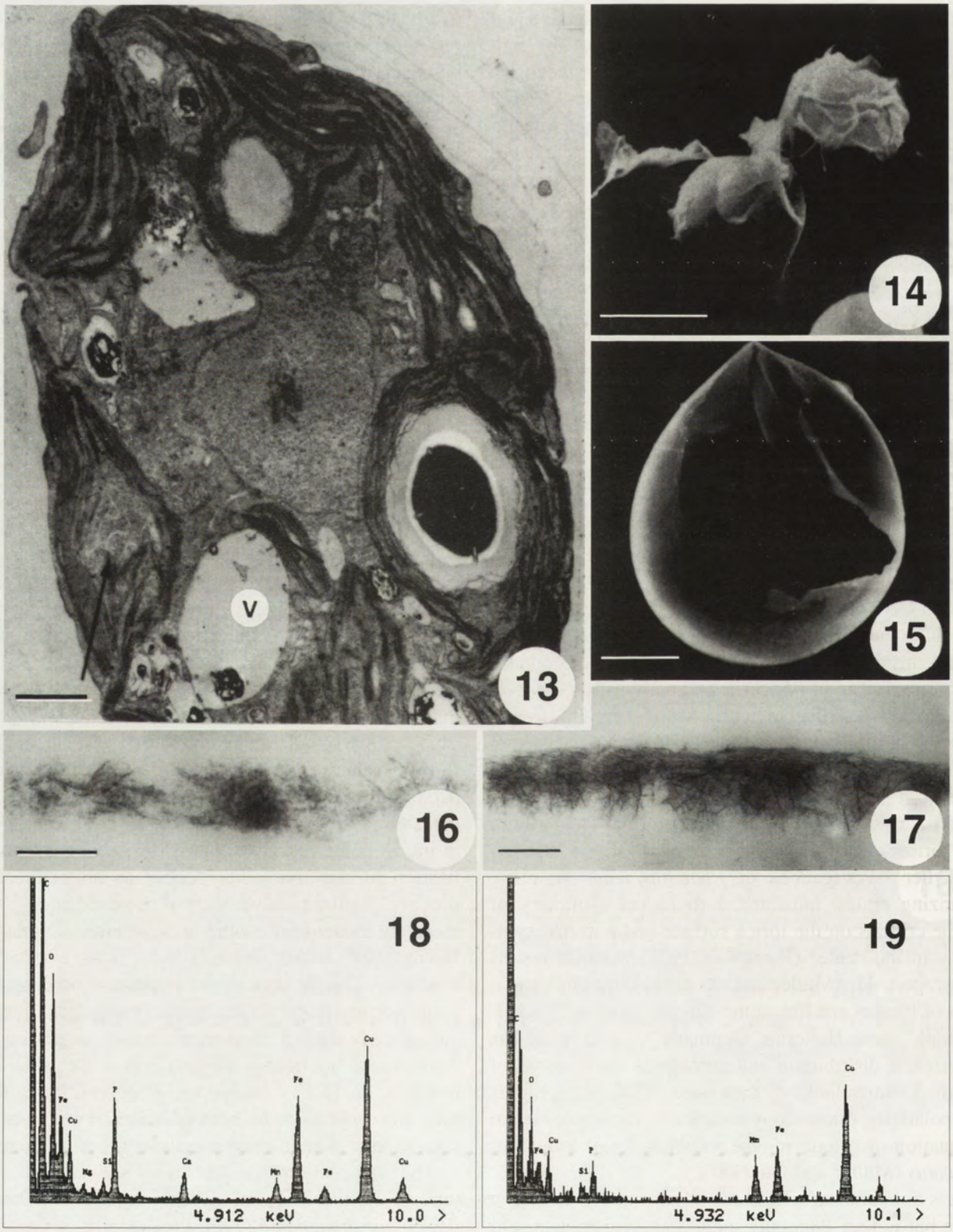

Figs. 13-19. *Dysmorphococcus globosus*. 13 - TEM of cell with incipient lorica. Cup-shaped chloroplast with pyrenoid, nucleus, and vesicles containing electron-opaque material are evident. Bar - 1.0 µm. 14 - SEM shows cell surface covered by incipient, filmy loricae. Bar - 10 µm. 15 - SEM of mature lorica showing posterior rupture associated with liberation of daughter cells. Bar - 3.0 µm. 16 -TEM of portion of mature lorica with granular subcomponents. Bar - 0.2 µm. 17 -TEM of portion of mature lorica with granular and fibrillar, needle-like components. Bar - 0.2 µm. 18 - X-ray spectrum from lorica shown in Fig. 16, shows Fe as the major mineralizing element. 19 - X-ray spectrum from lorica shown in Fig. 17; Fe and Mn are major mineralizing elements

and by these and other criteria appear to warrant inclusion in the Phacotaceae. Lorica morphology, microarchitecture and chemical composition, however, are very different from other phacotacean algae. Our data show that Fe and/or Mn are the primary mineralizing element(s) and that Ca is a secondary element, whereas in *Pteromonas* and *Phacotus* Ca is usually the primary mineralizing element. It should be noted, however, that Heinrich et al. (1986) reported the occurrence of high amounts of Fe, as well as lesser amounts of Mn and Ca, in the loricae of *P. lenticularis*. With respect to *Dysmorphococcus*, Ca, Fe or Mn have not been detected thus far in Golgi-derived cytoplasmic vesicles, results suggesting that these metals are added to the lorica matrix after it has been secreted from the cell.

Dysmorphococcus is not the only phacotacean alga in which Ca is not the primary mineralizing element in the lorica. Krienitz et al. (1990) reported that *Hemitoma* also has Fe as a primary mineralizing element. Morphologically, the two loricae are not similar, however. In *Dysmorphococcus* the lorica is a single unit of interwoven mucilaginous material, interrupted by many puncta, whereas the lorica of *Hemitoma* is bivalved (like *Pteromonas* and *Phacotus*) and bilayered, with an inner, highly porous or perforated component covered by an outer, irregular, open network of thick ridges. Since the SEM-EDS data indicate the presence of both Fe and Ca in the lorica (Krienitz et al. 1990), it would be of interest whether the two elements are segregated in the two layers, thus making *Hemitoma*, perhaps an intermediate between *Pteromonas/Phacotus* and *Dysmorphococcus*.

From these and other studies, it appears that the Phacotaceae are a diverse group of organisms. Those investigated thus far show a similar cellular morphology and ultrastructure; however, there is much variation in lorica structure and composition. The primary mineralizing elements are Ca and Fe, but there seems to be no correlation between lorica microarchitecture and elemental composition, as has been shown in some other mineralizing systems. Moreover, the diversity of lorica structure and composition raises questions about its validity as a taxonomic criterion above the generic level. Is there, for example, a need for subfamilies based on lorica characteristics, or does the family itself need to be more precisely circumscribed? Is it still useful to place all these loricate organisms in a single family? Before a massive systematic revision is undertaken, however, some of these issues may be resolved by the use of molecular biological approaches, including gene sequence data, that will either reaffirm the present situation or encourage us to reassess the systematic treatment of this interesting group of organisms.

Acknowledgements. Portions of this work were supported by NSF Grant BSR 8508483 and a University of Tennessee Faculty Research Grant to P.L.W. We thank Drs. D.A. Gerard, L. Pocratsky and R.A. Porcella for the use of unpublished Figures 1, 7-11 and 13-15, respectively.

REFERENCES

Dunlap J.R., Walne P.L. (1985) Fine structure and biomineralization of the mucilage in envelopes of *Trachelomonas lefevrei* (Euglenophyceae). J. Protozool. 32: 437-441.

Dunlap J.R., Walne P.L., Bentley J. (1983) Microarchitecture and elemental spatial segregation of envelopes of *Trachelomonas lefevrei* (Euglenophyceae). Protoplasma 117: 97-106.

Gerard D.A. (1980) Ultrastructure, development and elemental composition of the lorica of *Pteromonas protracta* (Stein) Lemm. Ph.D. Dissertation. The University of Tennessee, Knoxville.

Gerard D.A., Walne P.L. (1979) TEM and SEM-EDX of a loricate green alga (Volvocales). J. Phycol. 15: 15.

Giering B., Krienitz L., Casper S.J. (1992) Zur Taxonomie von *Phacotus lenticularis* (Ehrenberg) Stein (Chlamydophyceae, Phacotaceae). Nova. Hedw. 55: 367-380.

Giering B., Krienitz L., Casper S.J., Peschke T., Raidt H. (1990) LM and SEM observations on the asexual reproduction and lorica formation of *Phacotus lendneri* Chodat (Chlamydophyceae, Phacotaceae). Arch. Protistenk. 138: 75-88.

Heinrich G., Kies L., Schröder W. (1986) Eisen- und Mangan-Inkrustierung in Scheiden, Gehäusen und Zellwanden einiger Bakterien, Algen und Pilze des Süsswassers. Biochem. Physiol. Pflanzen 181: 481-496.

Kamptner E. (1950) Uber den Aufbau des Kalkgehuäses von *Phacotus lendneri* Chodat. Österr. Bot. Z. 97: 391-402.

Koschel R., Raidt H. (1988) Morphologische Merkmale der *Phacotus*-Hüllen in Hartwasserseen der Mecklenburger Seenplatte. Limnologica 19: 13-25.

Krienitz L., Peschke T., Giering B. (1990) Lichtmikroskopische, rasterelektronenmikroskopische und röntgenmikroanalytische Untersuchungen an *Hemitoma maeandrocystis* Skuja (Chlorophyta, Phacotaceae). Arch. Protistenk. 138: 159-170.

Müller G., Oti M. (1981) The occurrence of calcified planktonic green algae in freshwater carbonates. Sedimentology 28: 897-902.

Pocratsky L. (1982) Nutritional, chemical and ultrastructural characterization of the lorica and extracellular mucilage of *Phacotus lenticularis* (Phacotaceae, Volvocales). Ph.D. Dissertation. The University of Tennessee, Knoxville.

Pocratsky L., Walne P.L. (1981) Chemical, nutritional and ultrastructural characterization of the extracellular mucilage and lorica of *Phacotus lenticularis* (Chlorophyceae). J. Phycol. 17: 15.

Porcella R.A. (1976) Cellular organization and development of the envelope of *Dysmorphococcus globosus* Bold et Starr. Ph.D. Dissertation. The University of Tennessee, Knoxville.

Porcella R.A., Walne P.L. (1980) Microarchitecture and envelope development in *Dysmorphococcus globosus* (Phacotaceae, Chlorophyceae). J. Phycol. 16: 280-290.

Starr R.C. (1978) The culture collection of algae at the University of Texas at Austin. J. Phycol. 14: 47-100.

Starr R.C., Zeikus J.A. (1987) UTEX-The culture collection of algae at the University of Texas at Austin. J. Phycol. 23: 1-47.

Steinberg C., Klee R. (1983). Rontgenmikroanalyse der Schale einer einzelligen Grünalge. Mikrokosmos 72: 170-173.

Received on 30th June, 1993; accepted on 30th July, 1993

ACTA
PROTOZOOLOGICA

Acta Protozoologica (1993) 32: 245 - 253

On the Ultrastructure of the Adhesive Disc of *Trichodina xenopodos* Fantham, 1924 and *T. heterodentata* Duncan, 1977 (Ciliophora: Peritrichida)

Johlet KRUGER, Linda BASSON and Jo G. VAN AS

Department of Zoology and Entomology, University of the Orange Free State, Bloemfontein, South Africa

Summary. The ultrastructure of the adhesive disc elements of *Trichodina heterodentata* Duncan, 1977, an ectoparasite and *T. xenopodos* Fantham, 1924, an endoparasite, is compared using transmission (TEM) and scanning (SEM) electron microscopy. Until now studies carried out on these organisms, involved only TEM. In order to reveal the details of the adhesive disc elements by SEM, the soft tissue of the cells was dissolved. Although there are significant morphological differences between these two species, the functional morphology of the articulated internal skeleton is essentially the same. The endoparasite, *T. xenopodos*, is adapted for attachment by drawing epithelial cells into the adhesive disc, whilst the ectoparasite, *T. heterodentata* with a less flexible adhesive disc, is adapted for gliding on and attachment to the surface of the host.

Key words. Ultrastructure, adhesive disc, internal skeleton, *Trichodina heterodentata*, *T. xenopodos*.

INTRODUCTION

The peritrichian family Trichodinidae comprises genera with adhesive discs consisting of interlinking denticles. The genus *Trichodina* Ehrenberg, 1830 has complex denticles consisting of a blade, central part and ray. When silver impregnated, these form the basis for taxonomic evaluation. The structure and function of these denticles have long since intrigued workers, but remained unrevealed until the advent of modern technology. The first description of these internal structures was provided by Faure-Fremiet and Thaureaux (1944) who presented very accurate drawings of the denticles and how they were formed. They also determined that these are protein structures. With the availability of the electron microscope in later years, it was inevitable that these fascinating ciliophorans will have become the topic of serious investigations. The first transmission electron microscopical (TEM) account was provided by Favard, Carasso and Faure-Fremiet (1963), followed by various other accounts, which included Lom (1973), Hausmann and Hausmann (1981a, b) and Maslin-Leny and Bohatier (1984). These works were all based on TEM alone and did not include SEM studies. Wherever scanning electron microscopy (SEM) was used (Sirgel 1983, Arthur and Margolis 1984), the results proved unsatisfactory due to the fact that the pellicle covers the underlying structures in the adhesive disc. When we

Address for correspondence: J. G. Van As, Department of Zoology and Entomology, University of the Orange Free State, P.O.Box 339, Bloemfontein, 9300, South Africa.

initially set out to study the adhesive disc of trichodinids with the use of SEM this was exactly the problem we encountered (Hamilton-Attwell et al. 1981). Only after developing a technique by which the pellicle and soft material could be removed, were we able to expose the complexity of the underlying elements of the denticle ring (Van As and Basson 1989, 1990, 1993). A further limitation in studies of this nature is that large quantities of specimens are required as many specimens are lost during the preparation process. This requires the maintenance of a meaningful level of infection that could be harvested for preparation when required. The problem was overcome by maintaining infected *Xenopus* adults and larvae in the laboratory for more than three years.

This paper reports on a comparison of the ultrastructure of the adhesive disc elements of *Trichodina xenopodos* Fantham, 1924, a urinary bladder parasite in adult *Xenopus laevis laevis* and *T. heterodentata* Duncan, 1977, an ectoparasite of *X. l. laevis* tadpoles.

MATERIALS AND METHODS

Adult specimens of *X. l. laevis* infected with *T. xenopodos* were collected from localities in the vicinity of Bloemfontein (Kruger et al. 1991) and maintained in stainless steel containers in the laboratory for a period of three years. Tadpoles of *X. l. laevis* infected with *T. heterodentata* were collected from Zoo Lake in Bloemfontein and maintained in a plastic pond of two meter diameter in a protected area in the courtyard of the laboratory. In both cases the infections of trichodinids remained high and infected specimens were at our disposal at any time throughout the study. Specimens of *T. xenopodos* were collected by dissecting an adult *Xenopus*, removing the urinary bladder that provided sufficient material for electron microscopical preparation. *T. heterodentata* was collected by placing an infested tadpole in a block watch glass with a drop of water. Trichodinids were removed by brushing the tadpole with a fine sable brush.

For SEM studies specimens were fixed in 10% buffered neutral formalin, washed and dehydrated in ascending concentrations of ethanol, critical point dried and sputter coated with gold and studied in a Jeol Winsem JSM 6400 at 5 kV.

For TEM studies specimens were prepared in a standard way using 2.5% gluteraldehyde and 1% aqueous osmium tetra-oxide as fixatives, washed with phosphate buffer, dehyderated in ascending concentrations of ethanol, imbedded in Spurr's resin and studied by means of a Philips 300 TEM at 60 kV.

In order to study internal structures of trichodinids, the soft material was removed by dissolving specimens in a nitric acid solution normally used for softening chitin and keratin, whereafter specimens were prepared for SEM as described above.

RESULTS AND DISCUSSION

For taxonomic evaluations, specimens of trichodinids are impregnated with silver nitrate that will reveal some details of the adhesive disc as shown in Figs. 1 and 2. *T. xenopodos* has slender denticles of which the numbers vary between 46 and 55 (Kruger et al. 1991). The blades are straight with delicate central parts that fit tightly into the preceding denticle and thin rays directed in a slightly anterior direction. In the case of *T. heterodentata*, denticles are less in number, varying between 18 and 25, with a sickle-shaped blade, displaying a prominent apex and blade apophysis. The central part is broad and rays vary in thickness between specimens.

Based on electron microscopy the following morphological information was revealed. *T. xenopodos* has, unlike *T. heterodentata*, a high body with characteristic surface ridges forming a network of elongated shapes. In Fig. 3 *T. xenopodos* can be seen adhered to the urinary bladder epithelium, causing a swollen lesion where epithelium cells are sucked into the concave adhesive disc (Fig. 9). *T. heterodentata*, on the other hand, inhabiting the skin, fins and gills of the tadpoles, has a flattened body and adhesive disc (Fig. 4), but can also cause a swollen lesion (Fig. 10) though not to the same extent as in the case of *T. xenopodos*. The locomotary cilia of these two species show some differences. In both cases the compound wreath of cilia consists of diagonal rows which in the case of *T. xenopodos* vary between 11 and 15, with 7 to 10 in the case of *T. heterodentata* (Figs. 7 and 8). From available literature it appears that for all ectoparasites so far studied, the number of cilia rows in this compound wreath varies between 6 and 8 (Lom 1973, Maslin-Leny and Bohatier 1984, Hausmann and Hausmann 1981a), whilst the endoparasite *T. urinicola* also has 10 (Favard et al. 1963). In both *T. xenopodos* and *T. heterodentata* the inner rows are shorter, becoming progressively longer towards the outer rows (Figs. 5 and 6). The compound wreath is separated from the basal cilia by a continuous septum. In the case of *T. xenopodos* these cilia are free, attached only at their proximal base (Fig. 5), whilst in the case of *T. heterodentata* the proximal third is attached to the adoral side of the border membrane (Fig. 6) as was also the case in *T. urinicola* (Lom 1958). No marginal cilia were found in *T. xenopodos*, but in the case of *T. heterodentata* a row of well-spaced marginal cilia is present (Fig. 4). The absence of marginal cilia in *T. xenopodos* is in line with findings of Lom (1958) who is of the opinion that this is a characteristic of amphibian endoparasites.

The border membrane consists of tightly packed peripheral pins of equal length. In the case of *T. xenopodos* these pins are delicate and short (2 μm) (Fig. 13), whilst in *T. heterodentata* the pins are longer (6 μm) and of a

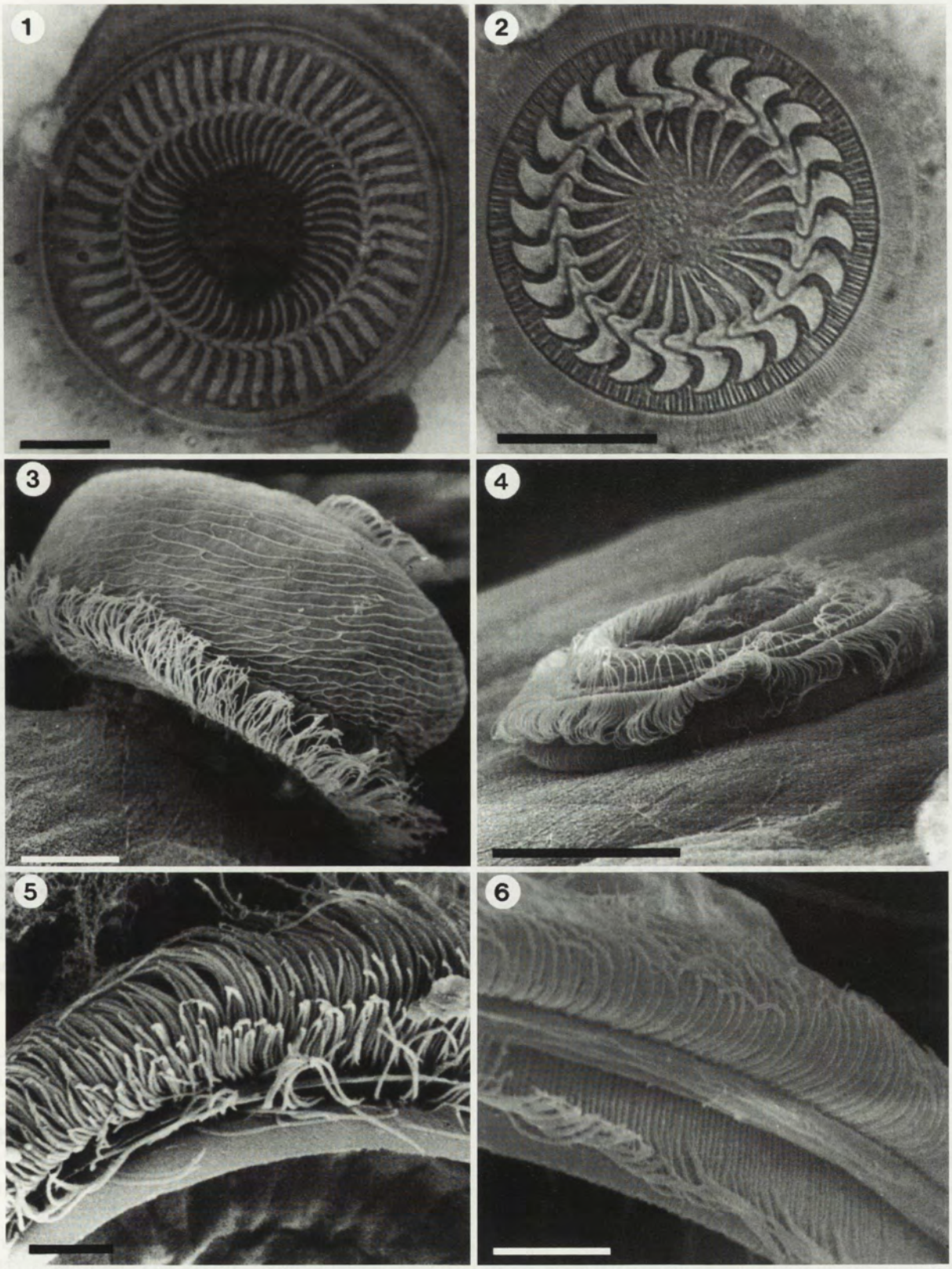

Figs. 1-6. Scanning electron micrographs (3-6) and photomicrographs (1, 2) of *Trichodina xenopodos* Fantham, 1924 (1, 3, 5) and *T. heterodentata* Duncan, 1977 (2, 4, 6) from the African clawed toad *Xenopus laevis laevis* (Daudin, 1802). 1 and 2 - silver impregnated adhesive discs. 3 - ciliate attached to bladder epithelium of host, body with characteristic cell-like striations. 4 - disc-shaped body of ciliate attached to skin epithelium of tadpole. 5 - ciliary wreath on aboral side of ciliate. 6 - ciliary wreath on aboral side of ciliate with inner row attached to border membrane for some distance. Bars - 20 µm (1-4), 2.5 µm (5), 5 µm (6)

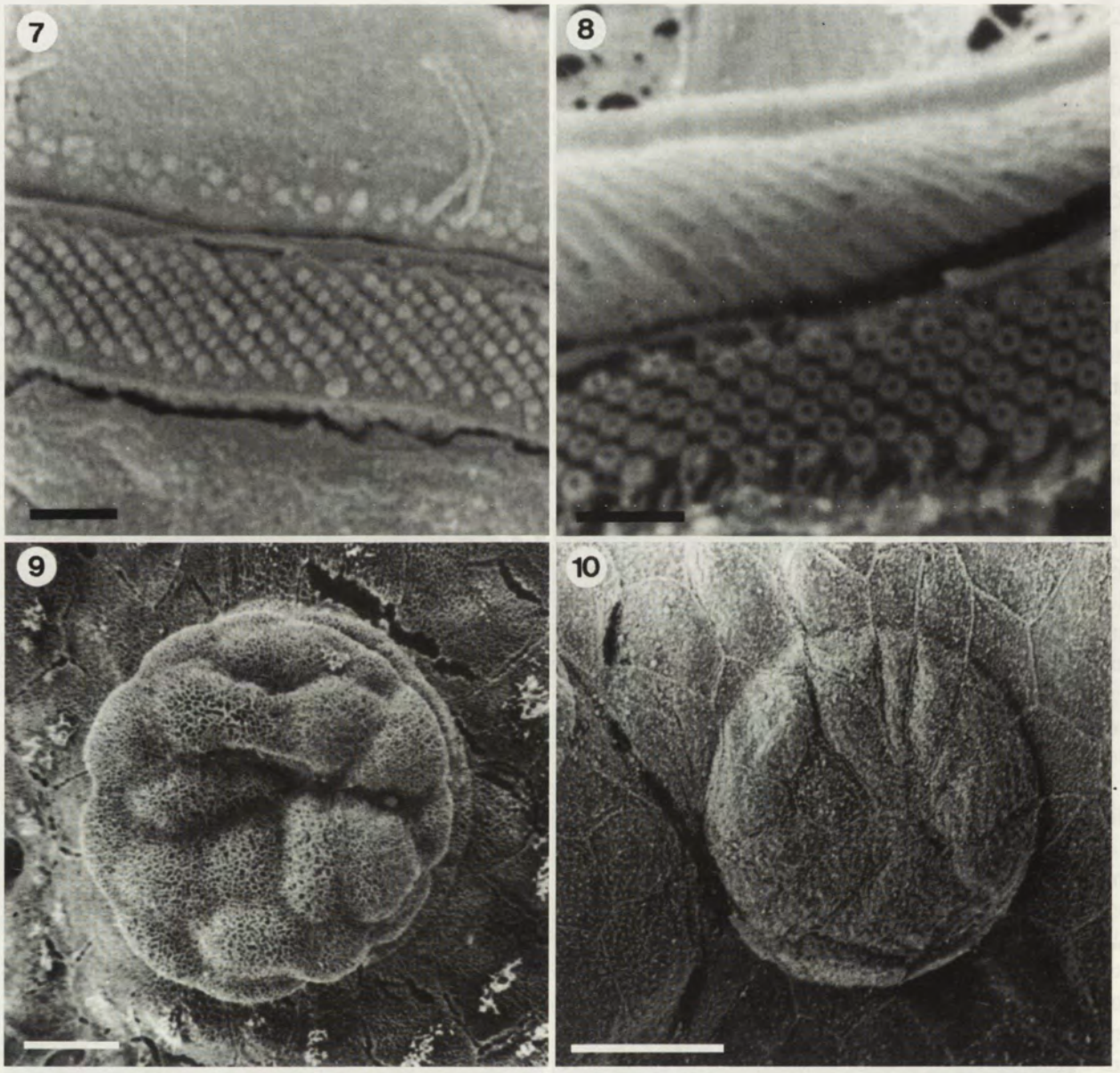

Figs. 7-10. Scanning electron micrographs of *Trichodina xenopodos* Fantham, 1924 (7 and 9) and *T. heterodentata* Duncan, 1977 (8 and 10). 7 and 8 - kinetosomes giving rise to cilia of the ciliary wreath. 9 and 10 - lesions caused by the adhesive disc during attachment of the trichodinids to the host epithelium. Bars - 1 μm (7 and 8), 20 μm (9 and 10)

more robust nature (Figs. 12 and 14). During the process of dissolving the soft material, we found that the pellicle covering the border membrane of *T. xenopodos* adhered more closely to the pins (Fig. 11) as was the case for *T. heterodentata* (Fig. 12). The pins taper from the hinge towards the distal rim. In the case of *T. xenopodos* the pins have an 8-shaped profile, which in *T. heterodentata* have an I-shaped profile. In Figs. 15 and 16 the border membrane and its hinge of these species can be seen. In both these micrographs the plane of the section was such that a number of different pins were sectioned to display the profile as it changes in a distal direction.

In both species the border membrane hinges on the radial pins to allow movement in an adoral-aboral direction. There is, however, a difference in the way these hinges are attached in these two species. In *T. xenopodos* the radial pins are flattened at their periphery where they wedge into a groove formed at the proximal edge of the border membrane (Figs. 11 and 15). This type of hinge corresponds to that found in *Trichodinella epizootica* (Raabe, 1953) Sramek-Husek, 1955 by Lom (1973) and *T. pediculus* by Hausmann and Hausmann (1981b). The hinge of *T. heterodentata* is formed by a groove in the distal periphery of the radial pins into which the pins of

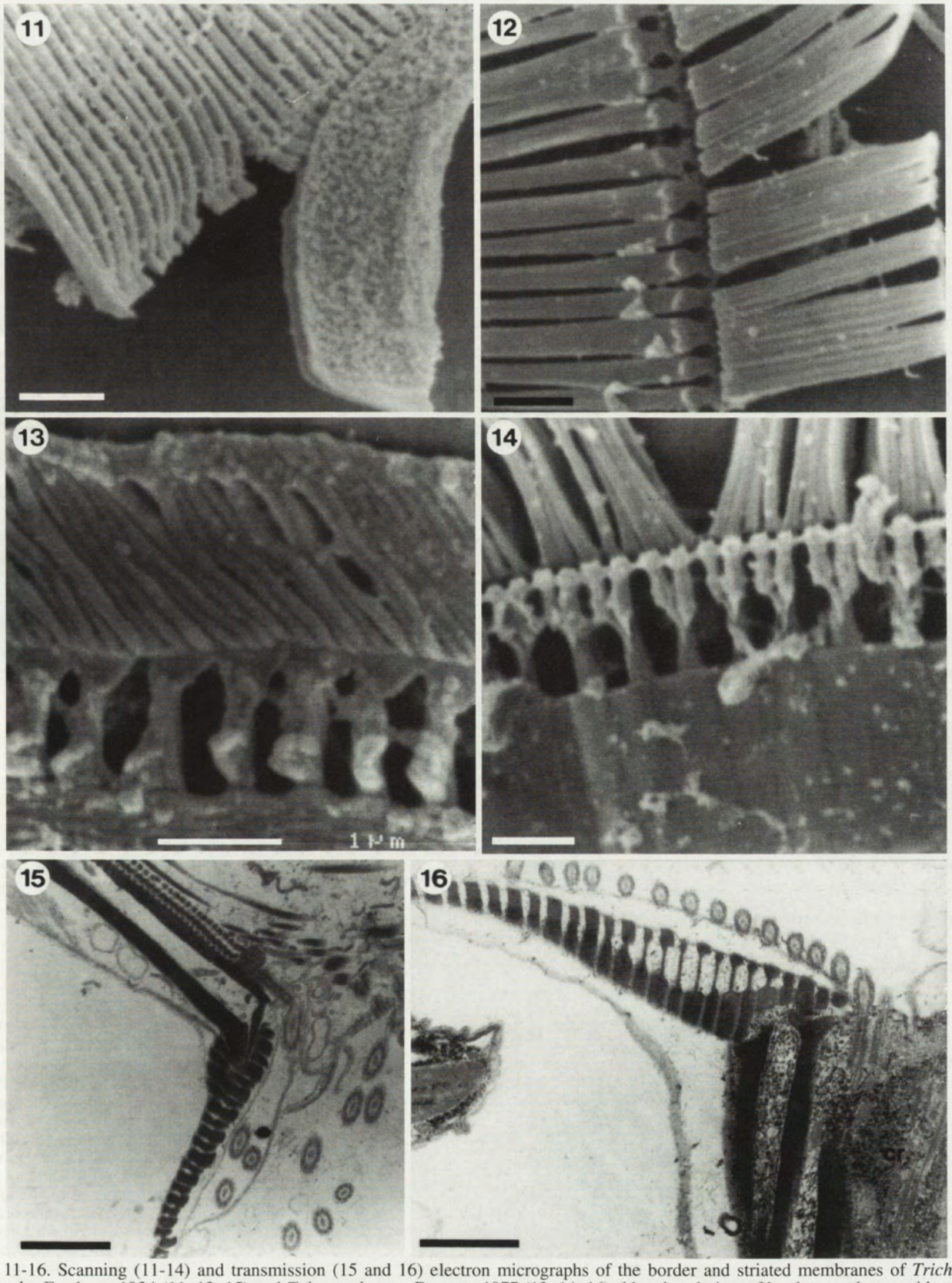

Figs. 11-16. Scanning (11-14) and transmission (15 and 16) electron micrographs of the border and striated membranes of *Trichodina xenopodos* Fantham, 1924 (11, 13, 15) and *T. heterodentata* Duncan, 1977 (12, 14, 16). 11 - aboral view of border membrane with pellicle still intact, partially detached from radial pins, 12 - radial pins and border membrane with pellicle dissolved (aboral view), 13 and 14 - adoral view of border membrane, hinge and thatched band, 15 and 16 - section through hinge and border membrane (cr - ciliary roots). Bars - 1 µm

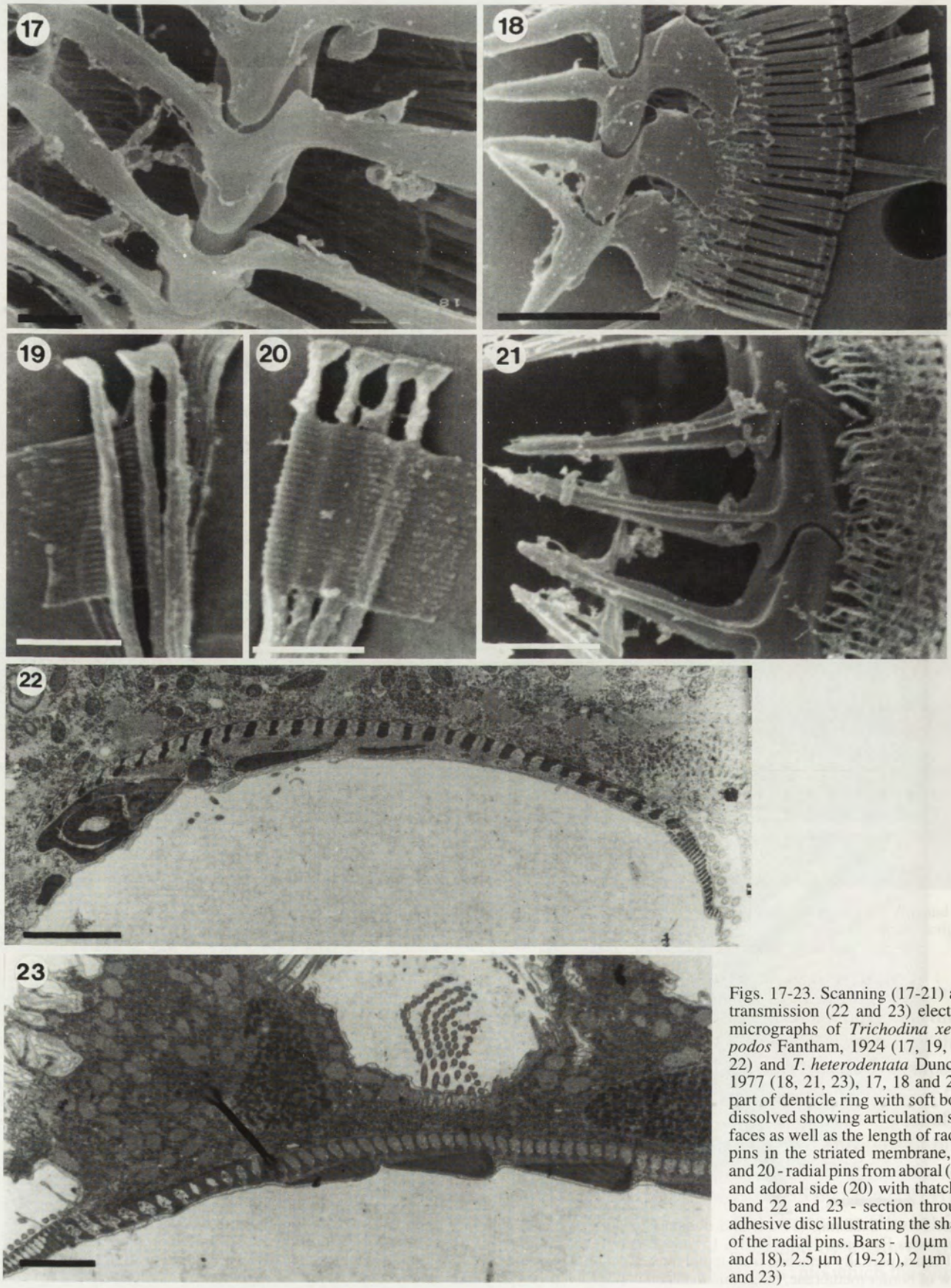

Figs. 17-23. Scanning (17-21) and transmission (22 and 23) electron micrographs of *Trichodina xenopodos* Fantham, 1924 (17, 19, 20, 22) and *T. heterodentata* Duncan, 1977 (18, 21, 23), 17, 18 and 21 - part of denticle ring with soft body dissolved showing articulation surfaces as well as the length of radial pins in the striated membrane, 19 and 20 - radial pins from aboral (19) and adoral side (20) with thatched band 22 and 23 - section through adhesive disc illustrating the shape of the radial pins. Bars - 10 µm (17 and 18), 2.5 µm (19-21), 2 µm (22 and 23)

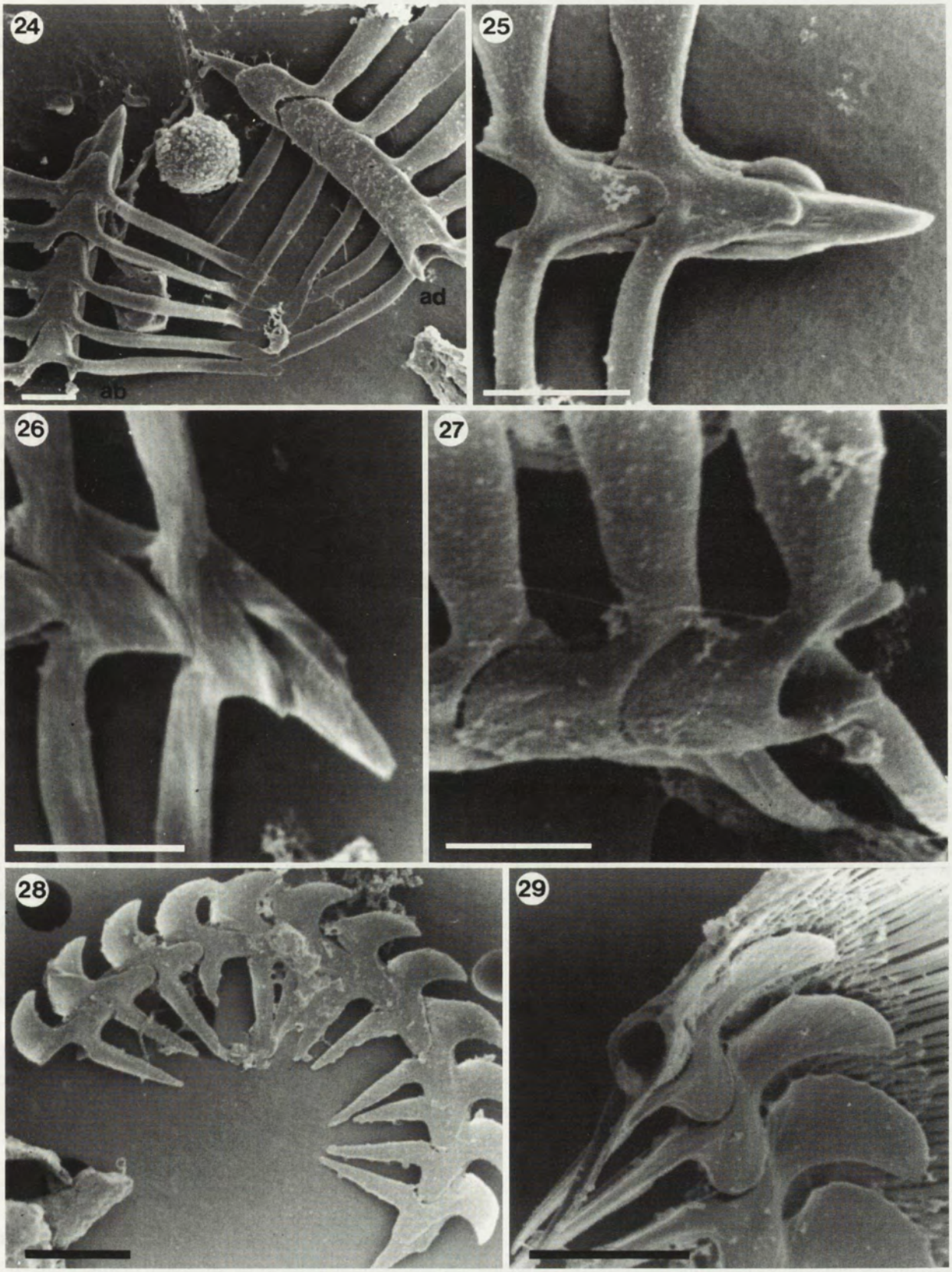

Figs. 24-29. Scanning electron micrographs of the denticles of *Trichodina xenopodos* Fantham, 1924 (24-27) and *T. heterodentata* Duncan, 1977 (28 and 29) with the soft part of the body dissolved. Adoral view (24 and 27). Aboral view (24-26, 28 and 29). Bars - 8 μm (24-28), 5 μm (29)

the border membrane fit (Figs. 12 and 16). This corresponds to Fig. 39 of Maslin-Leny and Bohatier (1984) for *T. nigra* Lom, 1961. On the aboral surface a trench-like groove can be seen between the radial and peripheral pins (Fig. 12). This facilitates movement in a aboral direction whilst most likely restricting movement in the opposite direction. Excessive movement in an aboral direction is prevented by the aboral protrusions on the distal edge of the radial pins (Fig 12). The extended and clearly flexible border membrane of *T. heterodentata* will ensure that the organism has the ability to glide over the host's surface whilst remaining adhered, much as the movements of a hover craft. In *T. xenopodos*, on the other hand, the border membrane most likely fulfills the function of the edge of a suction cup causing epithelial cells to be drawn into the concave adhesive disc as shown in Fig 3. The particular design of this hinge will allow relatively unrestricted movement of the border membrane in an adoral-as well as aboral direction.

As in the case of the peripheral pins, the radial pins of the striated membrane in *T. xenopodos* are also more delicate than those of *T. heterodentata* (Figs. 11 and 12). *T. xenopodos* has a total of between 350 and 450 radial pins in the circumference of the cell, whilst in *T. heterodentata* there are between 160 and 200. In *T. xenopodos* the radial pins extend to the rays (Fig. 17), whilst in *T. heterodentata* they only reach the central parts (Figs. 18 and 21). The profile of the radial pins changes throughout the length of the pin. At the point of the hinge, the radial pins of *T. xenopodos* is broad, flattened and spoon-shaped (Figs. 11, 19 and 20), whilst in the case of *T. heterodentata* the distal edge of the radial pin is bifurcated, each tip adorned with a kinetosome. The sequence of change can be seen in Figs. 22 and 23 where the section cuts different radial pins at different points throughout its length. These shapes correspond to those previously described by Hausmann and Hausmann (1981b), Lom (1973) and Maslin-Leny and Bohatier (1984). In both species in the present study the radial pins are interlinked by protruding filaments extending laterally to cover at least two other radial pins in the case of *T. xenopodos* (Figs. 19 and 20), whilst only one in *T. heterodentata* (Fig. 14). These protrusions form a thatched band at the distal edge of the denticles. This structure can sometimes be seen in silver impregnated specimens as a circle that impregnates in a different way than the rest of the adhesive disc (Fig. 1).

With all the soft material removed, the true denticle morphology is revealed. The denticle ring consists of individual denticles with tight articulation between the preceding and following denticles, in almost exactly the same way as the articulation between the vertebrae in the spinal column of vertebrates. Although there are significant differences between the denticle morphology of *T. xenopodos* and *T. heterodentata*, the functional articulation is exactly the same. The denticles fit into each other by an extended conical part that is rounded and tapers to a sharp point (Figs. 18, 24, 25, 26 and 28). This conical part fits into a smooth cavity (Figs. 27 and 29), which facilitates a turning movement on the axis so that the denticles can swivel in relation to one another. In the case of *T. xenopodos* the cavity extends to almost the tip of the conical part as the point of one denticle extends into two consecutive denticles, whilst in *T. heterodentata* the conical part is shorter, the tip is solid and extends only into the preceding denticle. The strength of the denticle ring is achieved by secure articulation facets of pressure and support levels (Figs. 17, 21, 24-27). These articulation facets restrict and guide the movement of individual denticles, so that coherent movements of the denticle ring will ensure that the shape of the organism is maintained while adhering to an uneven surface. The articulation levels, apophyses of the blade and ray (Van As and Basson 1989), slide on the support apophyses that are grooves formed in the central part separating the aboral-and adoral sides of the central part (Figs. 17, 21, 25, 26). In the case of T. xenopodos, the adoral central part is distinctly broader than the aboral side (Figs. 17 and 25), whilst in *T. heterodentata* the two sides of the central part are more or less of equal width (Fig. 18).

The slender shape of blades and rays of *T. xenopodos* suggests that these denticles are far more flexible, than in *T. heterodentata* where blades are broad and stout. In *T. heterodentata* the rays are reinforced on the adoral side by a rib extending throughout the length of the ray (Fig. 21).

Some of the features revealed by SEM, are not always shown in silver impregnation, i.e., features of the adoral sides of the central part which in the case of *T. xenopodos* is broader on the aboral side (Figs. 17 and 25). Other features that are sometimes obscured in certain species, are the blade and ray apophyses (Figs. 17, 25 and 28).

CONCLUDING REMARKS

The adhesive disc elements described above comprise the hard structures in the body of these species that consists of three rings: the first and outer ring is the border membrane with numerous individual pins, kept

in place by fine microfibrils and covered tightly by the pellicle to form a smooth flexible border membrane. This membrane articulates with the second ring, i.e., the striated membrane by means of an intricate hinge and is supported by the pellicle. The striated membrane comprises individual rods, the radial pins, which are linked by a membrane on the adoral side (Figs. 22 and 23) and are interconnected by means of microfibrils. The rods are individually linked to the cilia of the compound wreath by means of striated ciliary roots (Fig. 16). The third and most conspicuous ring is formed by interlinking denticles connected to the striated membrane by microfibrils.

These three rings form a coherent articulated internal skeletal system that provides body support and facilitate coordinated contractions of the body. In the case of *T. xenopodos* as shown in Fig. 3, the adhesive disc is in a deep concave shape that suggests that the position of the denticle elements to one another must follow the concave contours. The strong suction required by a specimen of *T. xenopodos* to attach to the bladder tissue and draw epithelial cells into the adhesive disc, requires considerable leverage that is facilitated by the internal skeletal structure. Skin parasites require a means of secure attachment with some suction abilities (Fig. 10), whilst allowing the possibility of hovering movements as often seen when these organisms are observed under a dissecting microscope. The denticle morphology of *T. heterodentata* suggests that these denticles are not capable of the same extent of articulation as is possible for the denticles of *T. xenopodos*.

REFERENCES

Arthur J.R., Margolis L. (1984) *Trichodina truttae* Mueller, 1937 (Ciliophora: Peritricha), a common pathogenic ectoparasite of cultured juvenile salmonid fishes in British Columbia: redescription and examination by scanning electron microscopy. Can. J. Zool. 62: 1842-1848.

Fauré-Fremiet E., Thaureaux J. (1944) Protéines de Structure et Cytosquelette chez les Urcéolarides. Biol. Bull. 78: 143-156.

Favard P., Carasso N., Fauré-Fremiet E. (1963) Ultrastructure de l'appareil adhesif des Urcéolaires (Ciliès, Pèritriches). J. Microsc. 2: 337-368.

Hamilton-Attwell V.L., Tiedt L.R., Van As J.G., Basson L. (1981) Ultrastructure of a trichodinid ciliate ectoparasitic on freshwater fish. Proc. Elec. Microsc. Soc. 11: 113-114.

Hausmann K, Hausmann E. (1981a) Structural studies on *Trichodina pediculus*. The locomotor fringe and the oral apparatus. J. Ultrastruc. Res. 74:131-143.

Hausmann K., Hausmann E. (1981b) Structural studies on *Trichodina pediculus*. The adhesive disc. J. Ultrastruc. Res. 74: 144-155.

Kruger J., Basson L., Van As J.G. (1991) Redescription of *Trichodina xenopodos* Fantham, 1924 (Ciliophora: Peritrichida), a urinary bladder parasite of *Xenopus laevis laevis* Daudin, 1802, with notes on transmission. Syst. Parasitol. 19: 43-50.

Kruger J., Basson L., Van As J.G. (1992) Ultrastructure of adhesive disc of a ciliated protozoan. Proc. Elec. Microsc. Soc. 22: 129-130.

Lom J. (1958) A contribution to the systematics and morphology of endoparasitic trichodinids from amphibians, with a proposal of uniform specific characteristics. J. Protozool. 5: 251-263.

Lom J. (1973) The adhesive disc of *Trichodinella epizootica* - ultrastructure and injury to the host tissue. Folia Parasitol. 20: 193-202.

Maslin-Leny Y., Bohatier J. (1984) Cytologie ultrastructurale de Trichodina et Tripartiella (Ciliès, Pèritriches) Protistol. 20: 113-132.

Sirgel W.F. (1983) A new ciliate genus *Trichodoxa* n.g. (Ciliata, Peritricha, Mobilina, Trichodinidae) with two new species from the genital system of terrestrial pulmonates. J. Protozool. 30: 118-125.

Van As J.G., Basson L. (1989) A further contribution to the taxonomy of trichodinid ciliophorans (Ciliophora: Peritrichia) and a review of the taxonomic status of some fish ectoparasites. Syst. Parasitol. 14: 157-179.

Van As J.G., Basson L. (1990) An articulated internal skeleton resembling a spinal column in a ciliated protozoan. Naturwiss. 77: 229-231.

Van As J.G., Basson L. (1993) On the biology of *Pallitrichodina rogenae* gen. nov., sp. n. and *P. stephanii* sp. n. (Ciliophora: Peritrichida) mantle cavity symbionts of the giant African snail *Achatina* in Mauritius and Taiwan. Acta Protozool. 32: 47-62.

Received on 21st May, 1993; accepted on 21st July, 1993

ACTA
PROTOZOOLOGICA

Acta Protozoologica (1993) 32: 255 - 259

Trichodina heterodentata Duncan, 1977 (Ciliophora: Peritrichida), an Ectoparasite on Larvae of the African Clawed Toad *Xenopus laevis laevis* (Daudin, 1802)

Johlet KRUGER, Jo G. VAN AS and Linda BASSON

Department of Zoology and Entomology, University of the Orange Free State, Bloemfontein, South Africa

Summary. *Trichodina heterodentata* Duncan, 1977, known only from cichlids and other freshwater fish, was found to occur widespread on the larvae of the African clawed toad *Xenopus laevis laevis* (Daudin, 1802) in southern Africa. In order to confirm this identification, a laboratory transmission experiment was carried out in which viable infestations were successfully transferred from *X. l. laevis* tadpoles to larvae of *Kassina senegalensis* (Duméril et Bibron, 1841), *Rana fuscigula* Duméril et Bibron, 1841 and freshwater fish. Comparative descriptions of *T. heterodentata* from tadpoles of *X. l. laevis* are provided.

Key words. *Trichodina heterodentata*, tadpole ectoparasite.

INTRODUCTION

The parasite fauna of the African clawed toad, *Xenopus laevis laevis* (Daudin, 1802) has been studied extensively by various authors since the early twenties. Amongst the parasites recorded from *Xenopus* is a trichodinid ciliophoran inhabiting the urinary bladder, i.e., *Trichodina xenopodos* Fantham, 1924. This parasite was originally described by Fantham (1924), later by Sandon (1965) and recently redescribed by Kruger et al. (1991) who also established that this parasite is widely distributed in southern Africa associated with different species of the genus *Xenopus*.

Address for correspondence: J. G. Van As, Department of Zoology and Entomology, University of the Orange Free State, P.O.Box 339, Bloemfontein, 9300, South Africa.

The first record of an ectoparasitic trichodinid from tadpoles of *X. laevis* was that by Sandon (1965) commenting on Dr. Thurston's finding of trichodinids on the tail of *Xenopus* larvae from Uganda. Sandon (1965) only examined gills of tadpoles without finding trichodinids. He expressed the opinion that the trichodinids on the tadpoles were probably a developmental stage of *T. xenopodos* which inhabits the urinary bladder. Later Thruston (1970) published her findings of a trichodinid on the body surface of *Xenopus* tadpoles. She unsuccessfully tried to demonstrate that these trichodinids migrate through the digestive system to the urinary bladder as suggested by Sandon (1965). None of these authors provided any taxonomic description or suggested any specific name. Tinsley and Whitear (1980) found a species of trichodinid on the skin of adult *Xenopus*, but provided no identification or description.

Tadpole trichodinids have been reported for the genera *Bufo* and *Rana* from various localities in Eur-Asia and the Americas by authors such as Diller (1928), Pai (1950), Lom (1961), Chen (1963), Kattar (1975), Arthur and Lom (1984) and Kazubski (1988). Those identified to species level all proved to be trichodinid species formally described from freshwater fish hosts.

During a survey carried out in southern Africa, adult *X. l. laevis* as well as larvae were collected and examined from various localities. The adults hosted *T. xenopodos* in the bladder, but had no infestation of ectoparasitic trichodinids on their skin. Populations of *Xenopus* larvae were infested with an ectoparasitic trichodinid on the skin, gills and fins. All these infestations from tadpoles proved to be the same species. A population of tadpoles maintained in the laboratory remained infested until the final stage of metamorphosis. No infestations were found on the skin of adults emanating from this laboratory population. The trichodinid is identified as *T. heterodentata* Duncan, 1977, a trichodinid commonly found associated with freshwater fish in various parts of the world. This finding, the first record of *T. heterodentata* on tadpoles, sheds new light on the current debate concerning host preference of this species. In order to confirm this identification, laboratory transmission experiments were carried out and to facilitate further faunistic evaluations, a comparative description of this trichodinid is provided.

MATERIALS AND METHODS

Tadpoles of *X. l. laevis* were collected from five different localities in southern Africa by means of beach-seine and electro-fishing. These specimens were transported to the laboratory in Bloemfontein where they were maintained separately in stainless steel holding tanks until they were anesthetized and dissected. Gill and skin smears, prepared separately were air dried. Taxonomic descriptions are based on material prepared by haematoxylin staining and silver impregnated specimens. All measurements given below are in micrometers and follow the uniform specific characteristic system proposed by Lom (1958). Minimum and maximum values are provided, followed in parentheses by the arithmetic mean and standard deviation. In the case of number of denticles and number of radial pins per denticle, the mode is given instead of the arithmetic mean. For fine details of denticle structure the method proposed by Van As and Basson (1989) was used and follows the sequence as indicated in Van As and Basson (1992). Body diameter is measured as the adhesive disc plus border membrane.

In order to study transmission, infested tadpoles of *X. l. laevis* were maintained together with tadpoles of *Rana fuscigula* Duméril et Bibron, 1841 and *Kassina senegalensis* (Duméril et Bibron, 1841), as well as specimens of the cichlids *Tilapia sparrmanii* Smith, 1840 and *Pseudocrenilabrus philander* (Weber, 1897) and the cyprinid *Cyprinus carpio* Linnaeus, 1758. After three, six and eleven days respectively, specimens of each species were examined for the presence of ectoparasitic trichodinids by preparing gill and skin smears which were processed as described above. After three days the original infested *Xenopus* larvae were removed from the containers and the rest of the animals under experimentation were maintained together.

RESULTS

The biometrical data of five populations of *T. heterodentata* collected from different localities in southern Africa are summarized in Table 1. Photomicrographs of specimens of some of these populations are presented in Figs. 1 to 4 and denticle drawings according to the method proposed by Van As and Basson (1989) are presented in Figs. 5 to 8.

Reference material of *T. heterodentata* from tadpoles of *X. l. laevis* is in the collection of the authors.

Reference Number: 89/03/07-03 for tadpoles of *X. l. laevis* from the Pony Club, Bloemfontein, South Africa.

Denticle description

Blade open sickle-shaped. Distal surface rounded, sloping downwards in anterior direction. Tangent point sharp, situated slightly below distal surface. Anterior surface with rounded apex, extending to and slightly beyond y+1 axis. Blade apophysis prominent, forming distinct indentation, on same level as deepest point of curve. Posterior surface with smooth, deep semi-lunar curve, deepest point of curve opposing blade apex. Blade connection thin and extended. Posterior projection not clearly visible. Central part robust with rounded tip extending more than halfway past y axis, fitting tightly into preceding denticle. Section above and below x axis similar. Ray connection short. Ray extends almost directly from central part. Ray apophysis not clearly visible in most specimens, no clear indentation corresponding to apophysis. Rays straight, sometimes slightly curved in posterior direction. Rays taper slightly to rounded points. Ratio of denticle above x axis to denticle below, less than one (0.7-0.8).

Transmission

All specimens of *R. fuscigula*, *K. senegalensis*, *T. sparrmanii*, *P. philander* and *C. carpio* hosted medium to high infestations of *T. heterodentata* after three days. After six days (three days after being removed

Table 1

Biometrical data (in µm) of different populations of *Trichodina heterodentata* Duncan, 1977 collected from *Xenopus laevis laevis* (Daudin, 1802) in southern Africa

Locality	Quarry north of Bloemfontein	Pony Club Pond, Bloemfontein	Hoedspruit Fish Farm, Transvaal	Zoo Lake, Bloemfontein	Oribi Gorge, Natal
Adhesive disc diameter	39.3-58.8 (46.3±4.7)	36.6-55.6 (45.5±5.1)	41.7-56.7 (50.4±4.6)	41.1-64.3 (49.3±5.6)	43.7-58.9 (51.8±5.0)
Denticle ring diameter	22.2-35.3 (28.2±3.5)	22.3-34.7 (28.5±3.3)	25.6-35.5 (30.9±2.4)	24.4-41.2 (31.4±3.8)	25.9-35.7 (32.2±3.8)
Border membrane width	1.4-5.5 (2.9±1.3)	3.9-6.2 (5.4±0.6)	4.0-6.3 (5.2±0.6)	3.5-6.1 (4.7±0.5)	3.0-6.1 (4.4±1.2)
Denticle number	18-25(20)	19-26(22)	20-22(21)	21-25(24)	19-22(21)
Radial pins per denticle	7-12(9)	6-10(7)	6-10(10)	7-13(11)	7-10(7)
Denticle span	10.1-16.5 (13.6)	11.2-17.7 (14.4)	11.5-17.8 (14.6)	11.6-18.7 (14.9)	12.6-18.4 (15.1)
Blade length	4.1-5.6 (4.8±0.5)	4.3-7.0 (5.4±0.7)	3.7-6.1 (4.9±0.7)	3.9-6.2 (5.1±0.6)	4.6-5.8 (5.3±0.5)
Central part width	1.9-3.6 (2.9±0.5)	2.3-3.5 (2.9±0.4)	2.1-3.2 (2.7±0.3)	1.8-3.3 (2.6±0.4)	2.6-3.6 (3.0±0.4)
Ray length	4.2-7.3 (5.9±0.9)	4.6-7.1 (6.2±0.7)	5.7-8.6 (7.1±0.8)	5.9-9.2 (7.2±0.8)	5.4-9.1 (6.9±1.5)
Denticle length	5.3-8.7 (7.3±0.9)	6.4-9.3 (7.7±0.9)	6.3-11.3 (9.2±1.1)	7.4-9.9 (8.4±0.8)	7.3-10.3 (9.0±1.1)
Number of specimens	25	14	18	35	6

from the original source of infestation) infestations persisted on all species. On day 11 fish and tadpoles still harbored viable populations of *T. heterodentata*. All host species used in the experiment remained infested with only one species of trichodinid, i.e., *T. heterodentata*.

DISCUSSION

The populations of *T. heterodentata* from tadpoles fall within the lower range of body dimensions known for this species from other hosts. The present populations appear to be more uniform and constant in denticle shape, in particular the shapes of the rays were less variable than normally encountered in populations from fish (Basson et al. 1983; Van As and Basson 1986, 1989, 1992; Basson and Van As in press). A similar trend was also noted in material collected during the transmission experiments. Specimens from the original stock of infestation, *X. l. laevis* tadpoles as well as *R. fuscigula* and *K. senegalensis* tadpoles subsequently infested, displayed a more uniform denticle shape than was the case for the three fish species used in the experiment. The typical denticle shape of trichodinids occurring on tadpoles is consistently found within populations of trichodinids found on fish and corresponds to descriptions of trichodinids previously published from fish populations (Van As and Basson 1989, see Fig. 5C). Typical shapes normally associated with *T. heterodentata* from fish was also found on tadpoles (See Fig. 2).

Although *T. heterodentata* was originally described from cichlids in the Philippines, this species has been found widespread on various fish species throughout the world (Duncan 1977; Basson et al. 1983; Van As and Basson 1986, 1989, 1992; Bondad-Reantaso and Arthur 1989; Albaladejo and Arthur 1989; Basson and Van As in press). In our previous evaluations of the host range and origin of *T. heterodentata* we came to the conclusion that *T. heterodentata*, although having a wide host range, was most likely a cichlid parasite originating from Africa, owing its world wide distribution to the translocation of cichlids for the purpose of aquaculture. The present information expands the host list of *T. heterodentata* to also include tadpoles of *X. l. laevis*. It is generally accepted that the genus *Xenopus* is a very primitive genus and most likely inhabited southern Afri-

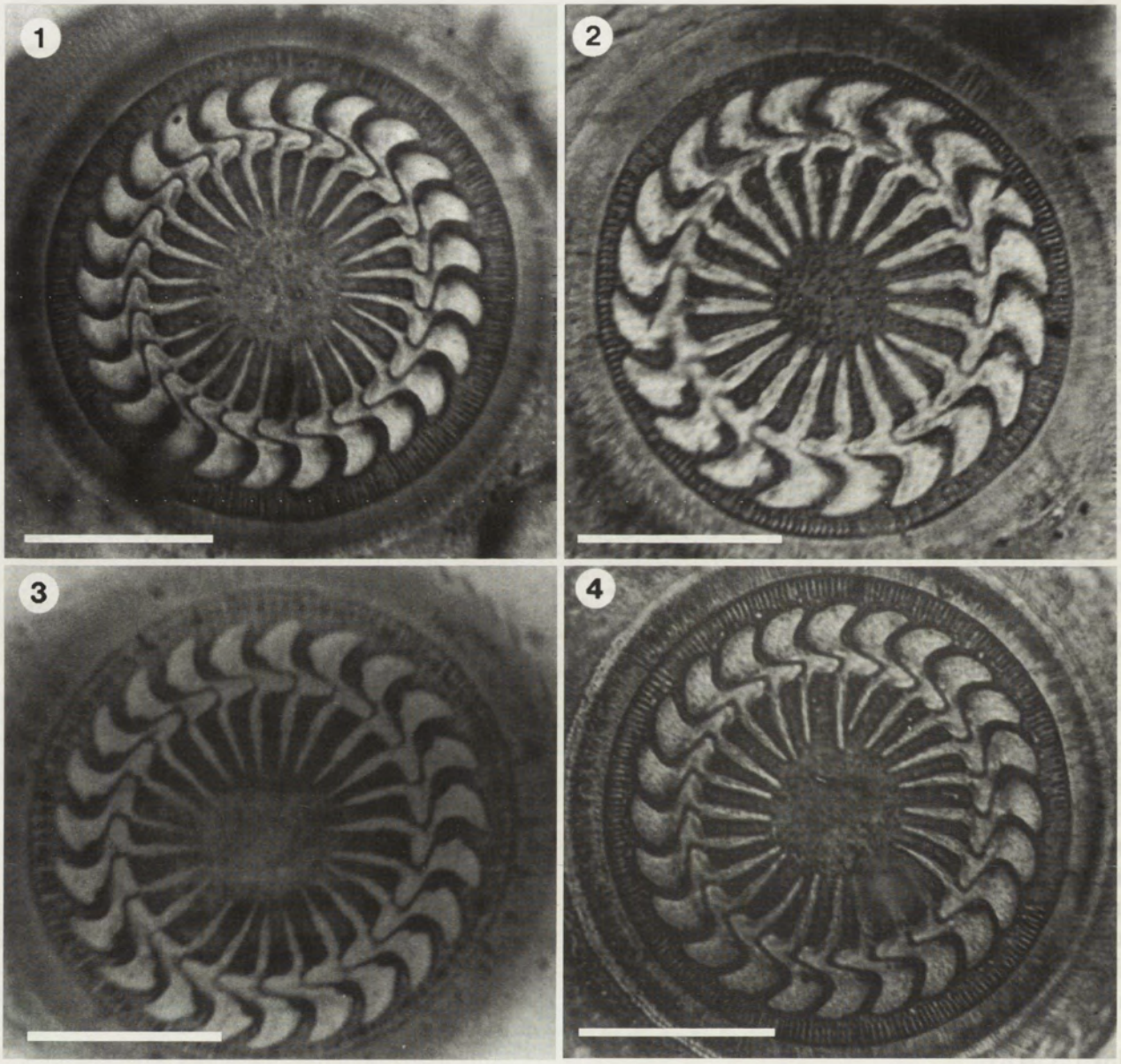

Figs. 1-4. Photomicrographs of silver impregnated specimens of *Trichodina heterodentata* Duncan, 1977 from skin, fins and gills of tadpoles of the African clawed toad *Xenopus laevis laevis* (Daudin,1802). 1 and 4 - from a quarry north of Bloemfontein; 2 - from Hoedspruit Farm, Eastern Transvaal; 3 - from transmission experiment, originally from the Zoo Lake of Bloemfontein. Bars - 20 µm

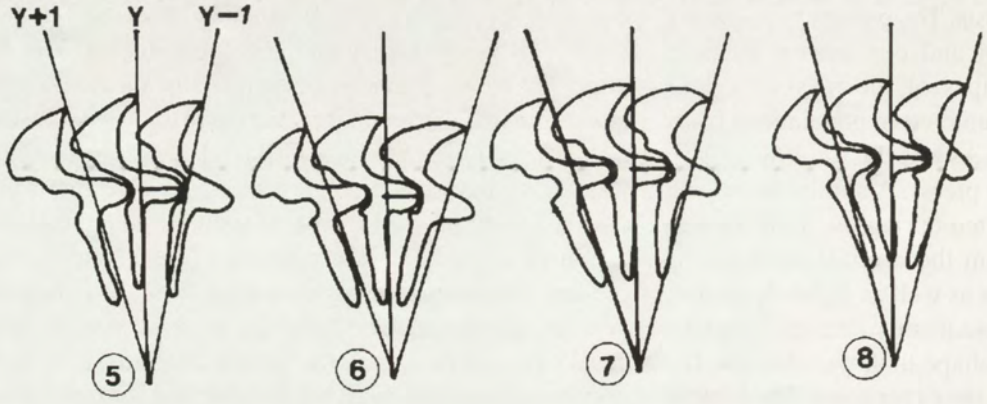

Figs. 5-8. Diagrammatic drawings of denticles of *Trichodina heterodentata* Duncan, 1977 from skin, fins and gills of tadpoles of the African clawed toad *Xenopus laevis laevis* (Daudin,1802). 5 and 6 - from a quarry north of Bloemfontein; 7 and 8 - from the Zoo Lake of Bloemfontein

ca before the advent of the cichlids. According to Tinsley (1981) the parasite fauna of *Xenopus* is morphologically and taxonomically distinct from their nearest relatives. In our opinion this is true concerning *T. xenopodos,* but not for *T. heterodentata,* which we believe to be a relatively recent association. All known cases of trichodinid associations with tadpoles so far reported (Chen 1963, Lom 1961, Arthur and Lom 1984, Kazubski 1988) are trichodinids previously described from fish. The African clawed toad *X. l. laevis* has been distributed throughout the world due to its use, until recently, in human pregnancy tests as well as its popularity as laboratory animals. The wide transcontinental distribution of *T. heterodentata* can in our opinion not be linked to the translocation of *Xenopus* as it is always the adults rather than the larvae that are exported. Our information indicates that *T. heterodentata* can not survive on the skin of adult *Xenopus* and is restricted to the larvae. The world wide trade in cichlids is responsible for regular movements of live fish, mostly fingerlings and fry, which are ideal hosts for trichodinids. It remains our opinion that the origin of *T. heterodentata* is from cichlid fish in Africa, from where it was translocated via the exportations of cichlids for the purpose of aquaculture and the lucrative ornamental fish industry.

REFERENCES

Alabaladejo J.D., Arthur J.R. (1989) Some trichodinids (Protozoa: Ciliophora: Peritrichida) from freshwater fishes imported into the Philippines. Asian Fish. Sci. 3: 1-25.

Arthur J.R., Lom J. (1984) Some trichodinid ciliates (Protozoa: Peritrichida) from Cuban fishes, with a description of *T. cubanensis* n. sp. from the skin of *Cichlasoma tetracantha.* Trans. Am. microsc. Soc. 103: 172-184.

Basson L., Van As J.G., Paperna I. (1983) Trichodinid ectoparasites of cichlid and cyprinid fishes in South Africa and Israel. Syst. Parasitol. 5: 245-257.

Basson L., Van As J.G. (in press) Trichodinid ectoparasites (Ciliophora: Peritrichida) of wild and cultured freshwater fishes in Taiwan, with notes on their origin. Syst. Parasitol.

Bondad-Reantaso M.G., Arthur J.R. (1989) Trichodinids (Protozoa: Ciliophora: Peritrichida) of nile tilapia (*Oreochromis niloticus*) in the Philippines. Asian Fish. Sci. 3: 27-44.

Chen C-L. (1963) Studies on the ectoparasitic trichodinids from freshwater fish, tadpole and crustacean in China. Acta Hydrobiol. Sin. 3: 99-111.

Diller W.F. (1928) Binary fission and endomixis in the *Trichodina* from tadpoles (Protozoa, Ciliata). J. Morphol. 46: 521-561.

Duncan B.L. (1977) Urceolariid ciliates, including three new species, from cultured Philippine fishes. Trans. Am. microsc. Soc. 96: 76-81.

Fantham H.B. (1924) Some parasitic Protozoa found in South Africa. VII. S. Afr. J. Sci. 21: 435-444.

Kattar, M.R. (1975) Sob *Trichodina steini* Claparède & Lachmann (Protozoa, Urcoelariidae) encontrada em girino de *Bufo ictericus* do Brasil. Rev. Brasil. Biol. 35: 253-258.

Kazubski S.L. (1988) Morphological variation in a ciliate, *Trichodina reticulata* Hirschmann et Partsch, 1955 (Peritrichida), in tadpoles from small ponds. Acta Protozool. 27: 259-269.

Kruger J., Basson L., Van As J.G. (1991) Redescription of *Trichodina xenopodos* Fantham, 1924 (Ciliophora: Peritrichida), a urinary bladder parasite of *Xenopus laevis laevis* Daudin, 1802, with notes on transmission. Syst. Parasitol. 19: 43-50.

Lom J. (1958) A contribution to the systematics and morphology of endoparasitic trichodinids from amphibians, with a proposal of uniform specific characteristics. J. Protozool. 5: 251-263.

Lom J. (1961) Ectoparasitic trichodinids from freshwater fish in Czechoslovakia. Acta Soc. Zool. Bohemoslov. 25: 215-228.

Pai K.T. (1950) The fibrillar system of *Trichodina pediculus* Ehrb. and *Trichodina bulbosa* Davis. Sinensia 1: 99-111.

Sandon H. (1965) A new species of *Trichodina* from South Africa. Acta Protozool. 3: 39-65.

Thurston J.P. (1970) Studies on some Protozoa and helminth parasites of *Xenopus*, the African clawed toad. Rev. Zool. Bot. Afr. 82: 349-369.

Tinsley R.C. (1981) The evidence from parasite relationships for the evolutionary status of *Xenopus* (Anura Pipidae). Monit. Zool. Ital. (N.S.) Suppl. 15: 367-385.

Tinsley R.C., Whitear M. (1980) The surface fauna of *Xenopus* skin. Proc. Roy. Soc. Edin. 79B: 127-129.

Van As J.G., Basson L. (1986) Trichodinids (Ciliophora: Peritrichida) ectoparasites of cultured cichlids from Taiwan. Bull. Inst. Zool. Acad. Sinica, 25: 135-139.

Van As J.G., Basson L. (1989) A further contribution to the taxonomy of trichodinid ciliophorans (Ciliophora: Peritrichida) and a review of the taxonomic status of some fish ectoparasites. Syst. Parasitol. 14: 157-179.

Van As J. G., Basson L. (1992) Trichodinid ectoparasites (Ciliophora: Peritrichida) of freshwater fishes of the Zambesi River System, with a reappraisal of host specificity. Syst. Parasitol. 22: 81-109.

Received on 21st May, 1993; accepted 21st June, 1993

ACTA
PROTOZOOLOGICA

Acta Protozoologica (1993) 32: 261 - 268

Ciliated Protozoa (Ciliophora) from Arctic Sea Ice

Sabine AGATHA[1,2], Michael SPINDLER[3,4] and Norbert WILBERT[5]

[1] c/o Dr. J.C. Riedel-Lorjé, Hamburg; [2] Institut für Hydrobiologie und Fischereiwissenschaften, Hamburg; [3] Alfred Wegener Institute for Polar und Marine Research, Bremerhaven; [4] present address: Institute for Polar Ecology, Kiel; [5] Zoological Institute, Bonn, Germany

Summary. The morphology and infraciliature of seven ciliate species from a sea ice floe west of Spitzbergen (Arctic Ocean) are described. Four of these ciliates are new to science: *Spiroprorodon intermedius* sp. n., *Euplotes longicirratus* sp. n., *Euplotes sigmolateralis* sp.n., and *Pleuronema arctica* sp. n. The three other species belong to the genera *Euplotes*, *Chlamydonella* and *Zosterodasys*. The diagnoses are based on protargol-stained specimens. Two species, *Euplotes sigmolateralis* and *Euplotes* sp. colonize both Arctic and Antarctic sea ice. On the level of substrate structure, sea ice can be compared with an interstitial turned upside down, but the karyorelictids typically found in interstitials are absent. The ciliate coenosis of the sea ice containing mainly "crawling" species also differs from the plankton community in the water column beneath the ice.

Key words. Arctic, sea ice, ciliates.

INTRODUCTION

During the formation of ice in sea water, freshwater crystals are formed and the excluded brine is concentrated in channels and pockets. Therefore, sea ice possesses an internal brine system and is not as compact as freshwater ice. This brine channel system serves as a habitat for a variety of organisms in both ice covered oceans (Bunt 1963, Spindler 1990). In Arctic ice floes the organisms are concentrated in the lowermost 20-30 cm of the ice; this region is densely populated by a species-rich community of unicellular algae, bacteria, fungi, protozoans, nematodes, polychaetes, turbellarians, copepods and amphipods (Carey 1985, Grainger and Hsiao 1990, Gulliksen and Lonne 1989, Melnikov 1989). Among the protozoans, ciliates constitute a major faunistic element (Gradinger et al. in press).

Although the Arctic sea ice biocoenosis was first described 150 years ago by Ehrenberg (1841), almost all subsequent studies have concentrated on the algae and bacteria. Within this study the attempt was to remedy this deficiency, with an account of ciliates found in an ice floe in the Arctic Ocean.

MATERIALS AND METHODS

During the "Polarstern"-expedition (ARK V/1) a SIPRE auger was used to take ice cores from a floe drifting in the East Greenland Current over a period of 20 days (5. - 24. May 1988). During this time the ice floe drifted between 80°12' N and 80°52' N, and 0°20' W and 5°24' E. For further details (e.g. physical parameters of the ice, meteorological and oceanographical data) see Spindler (1989). The organisms were extracted from the ice by thawing it according to the method of

Address for correspondence: S. Agatha, c/o Dr. J.C. Riedel-Lorjé, Rainvilleterrasse 9, 22765 Hamburg, Germany.

Spindler and Dieckmann (1986). The ciliates found in the samples were fixed with Bouin's fluid and subsequently stained with Protargol (Wilbert 1975), drawn by camera lucida, and evaluated biometrically. Unfortunately, the opportunity was not available to make live observations. Therefore, information on the prey of the ciliates only was obtained by examining food vacuole contents using light microscopy.

RESULTS

Prorodontidae Kent, 1881
Genus *Spiroprorodon* Fenchel & Lee, 1972
Spiroprorodon intermedius sp. n. (Fig. 1, Table 1)

Morphology and infraciliature: Body ovoid to spherical, cytostome apical, cytopharynx composed of about 36 nematodesmata. Four kineties encircle the cytostome in a clockwise direction. Spiral somatic kineties 1, 2 and 3 run only about three-quarters of the way around the cytostome. Six to ten kineties extend from the dorsal pole to the cytostome. Spiral somatic kinety 4 is truncated both aborally and in its spiral course. Another kinety named kinetofragmon (Corliss and Snyder 1986) forms an arc to the right of spiral somatic kinety 4. Eight short kineties with a single kinetosome in front of each are enclosed by spiral somatic kinety 1. Cilia about 11 µm long. Macronucleus situated centrally, possessing a notch and many nucleoli; micronucleus adjacent.

Species comparison: Representatives of the genus *Spiroprorodon* inhabit exclusively the polar sea ice. In *S. glacialis* (Fenchel and Lee 1972) five spiral somatic kineties each pass halfway around the cytostome. *Spiroprorodon garrisoni* (Corliss and Snyder 1986) posesses four spiral somatic kineties, which encircle the cytostome to varying degrees and a reduced fifth spiral somatic kinety (kinetofragmon). Unfortunately, neither of these species descriptions includes a biometric characterization. Furthermore, Corliss and Snyder (1986) observed considerable morphological variation in *S. garrisoni*, but, again, provided no detailed information.

Spiroprorodon intermedius is similar to *S. garrisoni* in possessing a reduced fifth somatic kinety (kinetofragmon), but is distinguished by the possession of kineties which extend from the anterior to the posterior pole and a reduced spiral somatic kinety 4. *Spiroprorodon intermedius* resembles *S. glacialis* in that the meridional kineties extend to the buccal infraciliatur. The differences between both species are the number of spiral somatic kineties and the presence of a reduced fifth spiral somatic kinety.

Trichocysts, such as are present in *S. glacialis* were not observed.

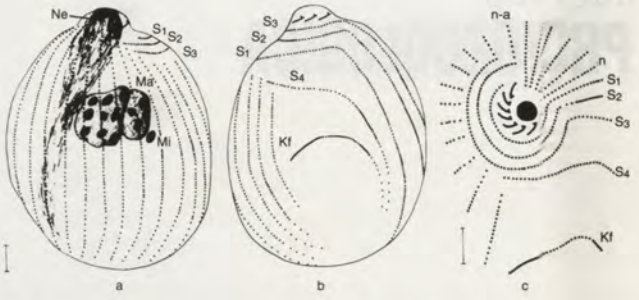

Fig. 1. *Spiroprorodon intermedius* sp. n., after protargol peparation. a, b - side view, c - apical view. a - number of polar kineties, Kf - kinetofragmon, Ma - macronucleus, Mi - micronucleus, n - number of kineties, Ne - nematodesmata, S1-4 - spiral somatic kineties 1 to 4. Bars - 10 µm

Table 1

Biometric characterization of Spiroprorodon intermedius sp. n. All data based on protargol impregnated individuals. max - naximum, min - minimum, n - number of individuals examined, S - standard deviation, $S\bar{x}$ - standard deviation of arithmetic mean, V - coefficient of variability in %, $\bar{x}$ - arithmetic mean.

Character	min	max	$\bar{x}$	S	$S\bar{x}$	V	n
Length in µm	48	129	76.53	19.11	3.75	24.97	26
Width in µm	33	97	59.61	15.87	3.11	26.62	26
No. of kineties	22	28	24.88	2.47	0.88	9.93	8
Cytopharynx length in µm	50	79	64.17	9.95	4.06	15.51	6
Macronucleus length in µm	19	32	26.04	3.85	0.99	14.79	15
Macronucleus width in µm	8	21	14.56	4.34	4.34	29.81	15

Euplotidae Ehrenberg, 1838
Genus *Euplotes* Ehrenberg, 1830
Euplotes longicirratus sp. n. (Fig. 2, Table 2)

Morphology and infraciliature: Body oval to elliptical in outline. Posterior end narrows, dorsal side deeply furrowed. Cirri I/1 and II/2 (Wallengren 1900) extraordinary long (36-56 µm). Adoral zone of membranelles extreme long, extending over 97% of body length. Macronucleus J-shaped to slightly sigmoid; micronucleus could not be discerned.

Species comparison: *E. longicirratus* possesses an unusual oblonge shape which is reminescent of *E. antarcticus* Fenchel and Lee, 1972, but differs from its congenes mainly by the elongated cirri I/1 and II/2. Furthermore, the character constellation of 7 frontoventral cirri, 2 caudal cirri and 5-7 dorsolateral kineties is unique.

Table 2

Biometric characterization of *Euplotes longicirratus* sp. n. All data based on protargol impregnated individuals. AM - adoral membranelles, AZM - adoral zone of membranelles, Bk - basal bodies (kinetosomes), Cc - caudal cirri, Dk - dorsolateral kineties, FV - frontoventral cirri, max - maximum, min - minimum, n - number of individuals examined, S - standard deviation, $S\bar{x}$ - standard deviation of arithmetic mean, Tr - transverse cirri, V - coefficient of variability in %, $\bar{x}$ - arithmetic mean.

Character	Min	Max	$\bar{x}$	S	$S\bar{x}$	V	n
Length in µm	74	110	90.62	8.46	1.8	9.34	22
Width in µm	42	67	54.34	6.89	1.54	12.68	20
Length of AZM in µm	57	91	75.08	7.84	1.75	10.44	20
No. of AM	46	64	51.33	4.07	0.89	7.93	21
No. of FV	7	7	7	0	0	0	19
No. of Tr	5	5	5	0	0	0	21
No. of Cc	2	2	2	0	0	0	20
No. of Dk	5	7	5.89	0.58	0.14	9.85	18
No. of Bk in the middle Dk	11	15	12.83	1.4	0.41	10.91	12

Table 3

Biometric characterization of *Euplotes sigmolateralis* sp. n. a - from Arctic sea ice, b - from Antarctic sea ice. All data based on protargol impregnated individuals. See Table 2 for abbreviations.

Character		min	max	$\bar{x}$	S	$S\bar{x}$	V	n
Length in µm	a	88	149	115.46	16.64	3.4	14.41	24
	b	78	98	85.71	4.97	1.0	5.8	24
Width in µm	a	59	113	72.28	12.62	2.52	17.46	25
	b	46	65	52.16	4.91	1.0	9.41	24
Length of	a	64	104	87.41	11.34	2.54	12.97	20
AZM in µm	b	57	74	63.75	3.71	0.76	5.82	24
No. of AM	a	47	67	56.76	5.68	1.24	10.01	21
	b	47	56	51.74	2.43	0.51	4.7	23
No. of FV	a	7	7	7	0	0	0	19
	b	7	7	7	0	0	0	23
No. of Tr	a	5	5	5	0	0	0	24
	b	5	5	5	0	0	0	25
No. of Cc	a	2	2	2	0	0	0	23
	b	2	2	2	0	0	0	26
No. of Dk	a	7	13	10.14	1.6	0.34	15.78	21
	b	11	11	11	0	0	0	17
No. of Bk in	a	17	23	18.56	1.8	0.6	9.7	9
the midle Dk	b	15	19	16.6	1.52	0.68	9.16	5

Fig. 2. *Euplotes longicirratus* sp. n., after protargol preparation. a - ventral surface, b - nuclear apparatus, c - dorsal surface. AZM - adoral zone of membranelles, Cc - caudal cirri, Dc - dorsal cilia, FV - frontoventral cirri, Ma - macronucleus, pM - paroral membranelles, Tr - transverse cirri. Bars - 10 µm

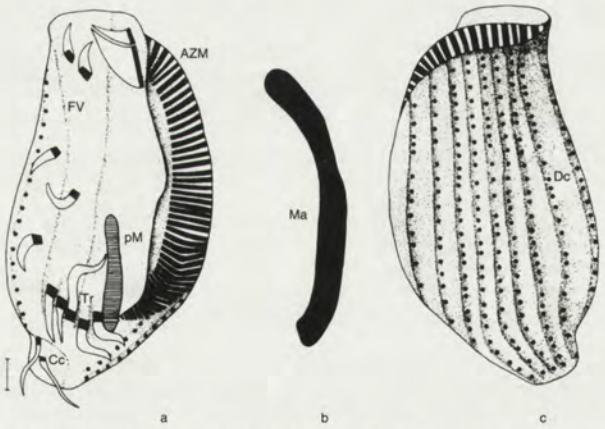

Fig. 3. *Euplotes sigmolateralis* sp. n., after protargol preparation. a - ventral surface, b - nuclear apparatus, c - dorsal surface. AZM - adoral zone of membranelles, Cc - caudal cirri, Dc - dorsal cilia, FV - frontoventral cirri, Ma - macronucleus, pM - paroral membranelles, Tr - transverse cirri. Bars - 10 µm

Euplotes sigmolateralis sp. n. (Fig. 3, Table 3)

Morphology and infraciliature: Body elongated, right side more or less sigmoid, caudal end set off by an abrupt constriction. Peristomial lip usually projects beyond the anterior part of the adoral zone of membranelles. Cirri I/1 and II/2 (Walengren 1900) rectangular in outline, cirrus II/2 particularly massive. At present we cannot decide whether the special shape of cirrus II/2 is derived from the fusion of two cirri, because the necessary morphogenetic stages are not available. Cilia 2-3 µm long and spaced 3 µm apart. Macronucleus bent slightly towards the right; micronucleus could not be discerned. Pennate diatoms are ingested.

Species comparison: Distinguishing characteristics include the massive cirrus II/2, with its rectangular outline, and the shape of the nucleus; neither of these features is present in any *Euplotes* species so far described.

E. sigmolateralis was also found in the sea ice of the Antarctic Weddell Sea. The form living there is slightly smaller than the Arctic form.

Euplotes sp. (Fig. 4, Table 4)

Morphology and infraciliature: Body oval in outline. Cirral equipment comprises 10 frontoventral and 4

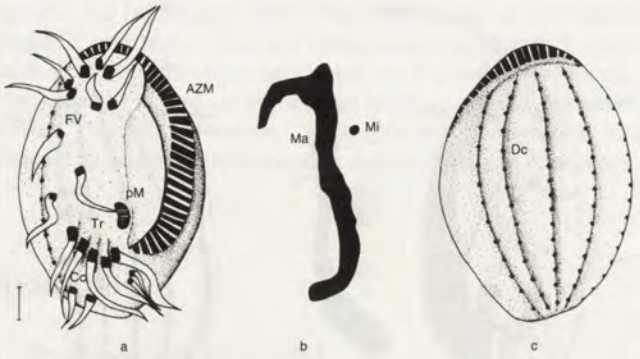

Fig. 4. *Euplotes* sp., after protargol preparation. a - ventral surface, b - nuclear apparatus, c - dorsal surface. AZM - adoral zone of membranelles, Cc - caudal cirri, Dc - dorsal cilia, FV - frontoventral cirri, Ma - macronucleus, Mi - micronucleus, pM - paroral membranelles, Tr - transverse cirri. Bars - 10 µm

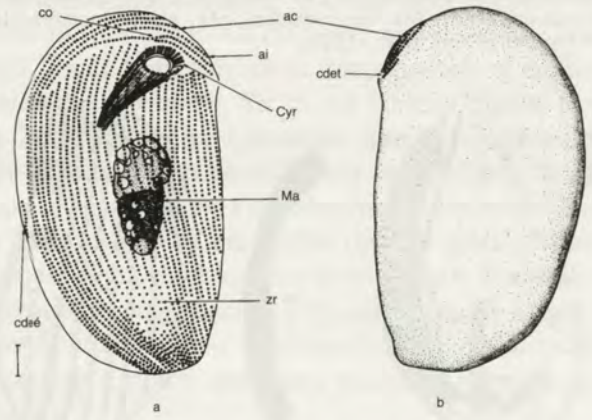

Fig. 5. *Chlamydonella* sp., after protargol preparation. a - ventral surface, b - dorsal surface. ac - arcs préoraux externes en continuité avec les dernières cinéties droites, ai - arc préoraux interne isolé, cdeé - tronçon équatorial de la cinétie droite externe discontinue, cdet - tronçon terminal dorsal, co - oral infraciliature, Cyr - cyrtos, Ma - macronucleus, zr - zone de la raréfaction cinétosomienne. Bars - 10 µm

caudal cirri (the two on the right being sturdier than the two on the left), 5 transverse cirri and 7 dorsolateral kineties with 15 dorsal cilia in the middle kinety. The 68- to 70-µm-long adoral zone of membranelles contains 46-60 membranelles. Macronucleus C-shaped with adjacent micronucleus.

Species comparison: Thompson (1972) found a *Euplotes* species with 10 frontoventral and 4 caudal cirri in fresh water rock pools of the Antarctic Peninsula. Unfortunately, the description is incomplete (e.g. a figure of the nuclear apparatus is lacking). Valbonesi and Luporini (1990 a,b) described *Euplotes focardii* and *E. euryhalinus*, two new *Euplotes*-species of cirrotype 10 (Gates 1978) from the Antarctic Ross Sea. The first species was detected in the marine interstitial,

Table 4

Biometric characterization of *Euplotes* sp.. a - from Arctic sea ice, b - from Antarctic sea ice. All data based on protargol impregnated individuals. See Table 2 for abbreviations

Character		min	max	$\bar{x}$	S	$S\bar{x}$	V	n
Length in µm	a	91	92	91.5	0.74	0.53	0.81	2
	b	66	83	73.37	6.38	1.65	8.7	14
Width in µm	a	54	63	58.5	6.72	4.73	11.49	2
	b	33	54	47.08	5.17	1.43	10.98	14
Length of	a	68	70	69	1.47	1.05	2.13	2
AZM in µm	b	46	62	53.9	3.52	0.99	6.53	14
No. of AM	a	46	60	53	9.9	7	18.68	2
	b	42	61	49.75	5.07	1.46	10.19	12
No. of FV	a	10	10	10	0	0	0	2
	b	10	10	10	0	0	0	10
No. of Tr	a	5	5	5	0	0	0	2
	b	5	5	5	0	0	0	11
No. of Cc	a	4	4	4	0	0	0	2
	b	4	4	4	0	0	0	11
No. of Dk	a	7	7	7	0	0	0	2
	b	7	7	7	0	0	0	10
No. of Bk in	a	15	15	15	0	0	0	1
the middle Dk	b	8	10	8.7	0.95	0.36	10.92	7

Table 5

Biometric characterization of *Chlamydonella* sp.. All data based on protargol impregnated individuals. See Table 2 for abbreviations

Character	min	max	$\bar{x}$	S	$S\bar{x}$	V	n
Length in µm	83	141	107.3	21.53	9.66	20.07	5
Width in µm	50	87	66.98	15.91	7.96	23.75	4
No. of kineties	21	36	29.25	6.24	3.12	21.33	4
No. of nemato -desmata	20	28	24	5.66	4	23.58	2
Macronucleus length in µm	36	36	36	0	0	0	1
Macronucleus width in µm	17	17	17	0	0	0	1

whilst the latter occured in shallow pools along the shore line. Our *Euplotes* sp. also belongs to cirrotype 10 and bears 4 caudal cirri. Size and number of adoral membranelles corresponds with *E. focardii*. However, *Euplotes* sp., *E. focardii* and *E. euryhalinus* differ in the number of dorsolateral kineties and in the number of dorsal cilia of the middle kinety. In addition, the caudal cirri are all of the same shape in *E. focardii* and *E. euryhalinus*. The macronuclei-shapes are also also distinct. Whereas the latter have horseshoe-shaped ones, the macronucleus of *Euplotes* sp. is C-shaped. The staining of the silverline system has to clarify, whether *Euplotes* sp. also possesses a 'double' argyrome of the sub-type "eurystomus" like *E. focardii* and *E. euryhalinus*.

Euplotes sp. also inhabits the Antarctic sea ice of the Weddell Sea, the form living there being somewhat smaller than the Arctic form (Table 4).

Lynchellidae Jankowski, 1968
Genus *Chlamydonella* Deroux, 1970
Chlamydonella sp. (Fig. 5, Table 5)

Morphology and infraciliature: Body oval in outline, flattened ventrally and arched dorsally. Anterior to the Y-shaped oral infraciliature are 4 kineties (arcs préoraux externes en continuité avec les dernières cinéties droites; arc préoraux interne isolé; Deroux 1970). Outermost right kinety consists of an equatorial part (tronçon équatorial de la cinétie droite externe discontinue), and a dorsal part (tronçon terminal dorsal). Five to six kineties loosely ciliated at their posterior ends (zone de la raréfaction cinétosomienne). Apart from the three long preoral kineties and the dorsal part of the outermost right kinety, the dorsal surface is unciliated. Heteromerous macronucleus situated centrally containing many nucleoli; micronucleus could not be discerned. Cyrtos slightly curved. Like many other species of this genus *Chlamydonella* sp. ingests pennate diatoms.

Species comparison: The infraciliature and the heteromerous macronucleus are typical of the genus *Chlamydonella*. *Chlamydonella* sp. resembles *C. pseudochilodon* (Deroux 1970) in body shape and in the form of the macronucleus. However, the body size and the number of kineties exceed the values of all species known to us.

Orthodonellidae Jankowski, 1968
Genus *Zosterodasys* Deroux, 1978
Zosterodasys sp. (Fig. 6).

Morphology and infraciliature: Body elongated, cylindrical, 133 x 32 µm. Infraciliature (about 40-50 kineties) interrupted below the cyrtos or cytopharyngeal basket by a synhymenium. Anterior continuation of the right kineties passes around the cyrtos; no preoral kineties to the left of the buccal opening. At the posterior pole the kineties also fuse without a suture. Synhymenium passes diagonally, consisting of a dense array of single kinetosomes, accompanied by a shallow groove. Macronucleus round except for a posterior notch, 19 µm in diameter, containing many oval nucleoli, located in a nuclear sac at the beginning of the last third of the body. No micronucleus could be discerned. Cyrtos at the beginning of the second third of the body consists of 11 nematodesmata.

Species comparison: The genus *Zosterodasys* is the only genus in the order Synhymeniida, the members of which possess a synhymenium, which is, according to Jankowski's definition (1968), composed of kinetosomes closely packed together.

The synhymenium has become separated from the somatic ciliature in which it originated, and extends on both sides of the cytostome. In this representative of the genus the synhymenium has a distinctly more diagonal orientation than in *Z. agamalievi* Deroux, 1978 and *Z. derouxi* Sola, 1990, so that the anterior section of the right kineties describes an angle of only 90 around the cyrtos. The synhymenium in both *Z. agamalievi* (Deroux 1978) and *Z. derouxi* (Sola et al. 1990) is composed of dikinetids, whereas in *Zosterodasys* sp. it appears to be formed by single kinetosomes standing very close together. With respect to body size, *Zosterodasys* sp. occupies a position midway between the larger *Z. derouxi* and the smaller *Z. agamalievi*. *Zosterodasys* sp. differs from the two other species of the genus both in the shape of the macronucleus and in the number of kineties and nematodesmata. This ciliate has not been described as a new species because only a single specimen was available.

The kinetosome-free field to the right of the buccal opening may be an artifact.

Pleuronematidae Kent, 1881
Genus *Pleuronema* Dujardin, 1836
Pleuronema arctica sp. n. (Fig. 7, Table 6)

Morphology and infraciliature: Egg-shaped ciliate with a long peristome. Bipolar kineties come together in a preoral and a postoral suture. Cilia 6-21 µm long. Three to four preoral kineties, postoral kineties are lacking. Membranelle 1 (alpha membranoid; Small 1967) with apical thickening. Membranelle 2 (beta membranoid) comprises of two parts. First part bounds the peristome field on the left and is of the "coronatum" type. The second part is V-shaped. Buccal surface striped radially by 63-72 argentophilic folds resembling the oral stripes of *Schizocalyptra* Dragesco, 1968; no discernible subdivision into a "rib-field I" and a "rib-field II" (Dragesco 1968). Macronucleus egg-shaped, located centrally, containing some oval nucleoli; micronucleus adjacent. Trichocysts present.

Species comparison: On the basis of the shape of membranelle 2 *P. arctica* can be assigned to the large group of *Pleuronema* species of the "coronatum" type. The biometric values, however, correspond with no species known to us. It is bigger than the known marine *Pleuronema* species. The number of kineties corre-

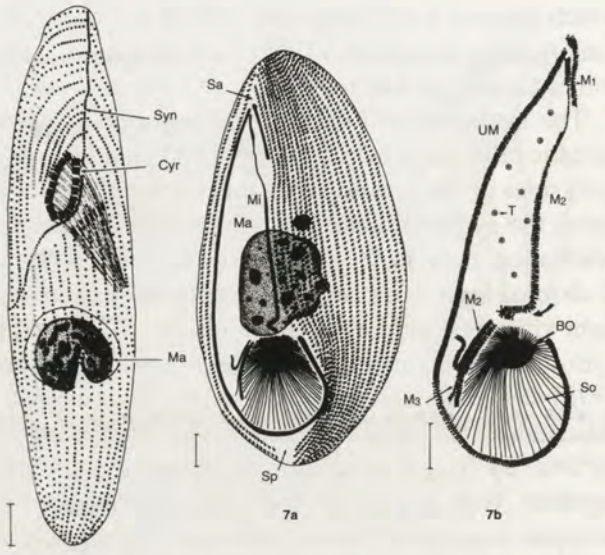

Fig. 6. *Zosterodasys* sp., after protargol preparation. Cyr - cyrtos, Ma - macronucleus, Syn - synhymenium. Bar - 10 µm
Fig. 7. *Pleuronema arctica* sp. n., after protargol preparation. a - ventral view, b - buccal infraciliature. BO - buccal opening, M1, M2, M3 - membranelle 1, 2, 3, Ma - macronucleus, Mi- micronucleus, Sa - preoral suture, Sp - postoral suture, So - oral stripes, T - trichocysts, UM - undulating membrane. Bars - 10 µm

Table 6

Biometric characterization of Pleuronema arctica sp. n. All data based on protargol impregnated individuals. See Table 2 for abbreviations

Character	min	max	$\bar{x}$	S	$S\bar{x}$	V	n
Length in µm	131	242	173	27.2	7.9	15.72	12
Width in µm	48	116	70	19.74	5.46	28.2	13
No. of kineties	39	61	48.5	6.63	2.35	13.67	8
No. of preoral kineties	3	4	3.3	0.52	0.21	15.76	6
Peristome length in µm	109	152	127	13.55	4.5	10.67	9
Peristome width in µm	32	51	37.8	6.7	2.5	17.73	7
Apex/peristome distance in µm	8	21	16	4.5	1.9	28.13	6
Macronucleus length in µm	29	47	41	5.7	2.0	13.9	8
Macronucleus width in µm	18	41	24	7.9	2.73	32.92	8

sponds with that of species found by Thompson (1972) at the Antarctic Peninsula and with *P. glaciale* from Antarctic sea ice (Corliss and Snyder 1986), while it differs in the number of preoral kineties of both species and from *P. glaciale* in the form of the membranelles 1 and 3.

The samples from the Arctic sea ice also contained representatives of the genera *Diophrys*, *Loxophyllum*, *Peritromus* and *Placus*. Although the genus of these specimens could be determined, further identification was impossible because the protargol staining technique produced insufficient results.

Apart from the species described above we found *Didinium* sp., *Strobilidium minimum*, *Uronychia transfuga* and *Histiobalantium natans*.

DISCUSSION

In contrast to investigations of ciliates from Antarctic sea ice (Agatha et al. 1991, Corliss and Snyder 1986, Fenchel and Lee 1972), there are no recent publications about this group from the sea ice of the Arctic Ocean. Nansen (1906) published an account of protozoa of an Arctic ice floe. Included therein are camera lucida drawings and free hand sketches of several types of ciliates with a possible assignment to the genera *Lacrymaria*, *Chilodonella* and *Stylonychia*. Later, Usachev (1949) published an account of sea ice organisms from the Kara Sea with *Euplotes caudata*, *E. truncata*, *Proboscidium armatum* and *Cephalotrichium tonsuratum*. In this study we found 15 species, including both previously known forms and four ciliates that have been identified as new species.

The autotrophic components of the sea ice biocoenosis are either enclosed as the water freezes or are washed into the capillaries within the ice by wave action (Ackley 1982, Ackley et al. 1987, Garrison et al. 1983). Ciliates presumably enter the sea ice in a similar way.

Euplotes sigmolateralis and *Euplotes* sp. are found in Arctic sea ice as well as in Antarctic sea ice, and therefore, we expect further correlations in the species spectra since the environmental conditions to which the bottom communities on the underside of the ice are exposed differ only slightly in Arctic and Antarctic sea ice. Colonizable hard substrate and food are available in sufficient quantities, and the temperature of the bottom zone is relatively constant at -1,8 to -3°C. The salinity of the enclosed brine at these temperatures is 32-53‰ (Bartsch 1989).

We assume that the sea ice ciliates are euryhaline, like the ice algae (Bartsch 1989). The polar sea ice dwelling species are adapted physiologically to this particular habitat in that their tolerance ranges are shifted to lower temperatures (Coppellotti 1990, Hempel 1987, Lee and Fenchel 1972, Spindler et al. 1990) and higher salinities. Apart from the genera *Spiroprorodon* (Fenchel and Lee 1972) and *Cytharoides* (Tuffrau 1974, Agatha et al. 1991), they comprise morphotypes commonly found at temperate latitudes.

This pilot investigation, although based on relatively small samples and only fixed material, has given us some insight into an intact animal community. It is a characteristic of intact communities that the genus:species ratio approaches 1:1; that is, most genera are represented by a single species only (Elton 1946). The Arctic ciliate coenosis is no exception. Only the genus *Euplotes* is represented by three species. However, conclusions about character species and differential species in this ciliate coenosis would be premature at this stage.

The ciliate coenosis of sea ice is clearly distinct from the underlying plankton community (Hada 1970). For example, sea ice is inhabitated mainly by benthic types such as the Euplotidae, which can live only where there is a substrate to which they can attach.

On the level of substrate structure, Fenchel and Lee (1972), Corliss and Snyder (1986), Hempel (1987) and Spindler and Dieckmann (1991) compare the sea ice with an interstitial turned upside down. Hartwig (1974) lists 207 ciliate species found in the interstitial of the German North Sea coast. 25% of the species belong to the Karyorelictida, the character form of the interstitial which are incapable of forming cysts (Corliss and Hartwig 1977). These distinctive, nematomorphic ciliates are absent from polar sea ice. However, about half of the ciliate genera represented in the polar sea ice are also found in the marine interstitial - for example, *Uronychia*, *Euplotes*, *Histiobalantium*, *Didinium*, *Strobilidium*, *Holosticha* and *Peritromus* (Hartwig 1974).

So far, our knowledge of the Arctic ciliate coenosis is limited to the data from these first, rather small random samples. The spectrum of species encountered in a sample is influenced by a number of factors, including the structure and age of the ice, the season and the geographical site of the sample, and the patchiness of ciliate distribution. At present the number of ciliate species that have been found in sea ice is considerably smaller than the number of known interstitial ciliates. The harsh conditions (e.g. cold temperatures and high salinities) in sea ice could be responsible for a comparatively low abundance of species, in accordance with the Second Basic Principle of biocoenosis from Thienemann. However, because of sufficient food quantities in the channel system we would expect further investigations to reveal additional sea ice dwelling ciliate species which are adapted to these environmental conditions.

Acknowledgements. We would like to thank R. Gradinger for critically reading the manuscript and K. Beyer and R. Steinmetz for assistance in the field. This is contribution No. 463 of the Alfred Wegener Institute for Polar and Marine Research.

REFERENCES

Ackley S.F. (1982) Ice scavening and nucleation: Two mechanisms for incorporation of algae into newly forming sea ice. Eos 63: 54.
Ackley S.F., Dieckmann G., Shen H. (1987) Algal and foram incorporation into new sea ice. Eos 68: 1736.
Agatha S., Wilbert N., Spindler M., Elbrächter M. (1991) Euplotide ciliates in sea ice of the Weddell Sea (Antarctica). Acta Protozool. 29: 221-228.
Bartsch A. (1989) Die Eisalgenflora des Weddellmeeres (Antarktis): Artenzusammensetzung und Biomasse sowie Ökophysiologie ausgewählter Arten. Ber. Polarf. 63: 1-110.
Bunt J.S. (1963) Diatoms of Antarctic sea-ice as agents of primary production. Nature (London) 199: 1255-1257.
Carey A.G. Jr. (1985) Marine ice fauna: Arctic. In: Sea ice biota, (Ed. R.A. Horner), CRC Press, Inc., Boca Raton, Florida 173-190.
Coppellotti O. (1990) Description of *Uronema marinum* (Ciliophora, Scuticociliatida) from the Antarctica and observations on the nuclear events in conjugation. Polar Biol. 10: 365-371.
Corliss J.O., Hartwig E. (1977) The "primitive" interstitial ciliates: Their ecology, nuclear uniquenesses, and postulated place in the evolution and systematics of the phylum Ciliophora. In: The meiofauna species in time and space, (Eds. W. Sterrer, P. Ax), Workshop Symposium, Bermuda Biological Station, 65-88.
Corliss J.O., Snyder R.A. (1986) A preliminary description of several new ciliates from the Antarctica, including *Cohnilembus grassei* n. sp.. Protistologica 22: 39-46.
Deroux G. (1970) La série "Chlamydonellienne" chez les Chlamydodontidae (Holotriches, Cyrtophorina Fauré-Fremiet). Protistologica 6: 155-182.
Deroux G. (1978) The hypostome ciliate order Synhymeniida: From *Chilodontopsis* of Blochmann to *Nassulopsis* of Fauré-Fremiet. Trans. Amer. Microsc. Soc. 97: 458-469.
Dragesco J. (1968) Les genres *Pleuronema* Dujardin, *Schizocalyptra* nov. gen. et *Histiobalantium* Stokes (Ciliés Holotriches Hymenostomes). Protistologica 4: 85-106.
Dragesco J., Dragesco-Kernéis A. (1986) Ciliés libres de l'Afrique intertropicale. Faune Tropicale 36: Paris (Edition de l'Oston).
Ehrenberg C.G. (1841) Ein Nachtrag zu dem Vortrage über Verbreitung und Einfluß des mikroskopischen Lebens in Süd- und Nord-Amerika. Monatsber. Dtsch. Akad. Wiss. Berlin 1841: 202-207.
Elton C. (1946) Competition and structure of ecological communities. J. Anim. Ecol. 15: 54-68.
Fenchel T., Lee C.C. (1972) Studies on ciliates associated with the sea ice from Antarctica. I. The nature of the fauna. Arch. Protistenk. 114: 231-236.
Garrison D.L., Ackley S.F., Buck K.R. (1983) A physical mechanism for establishing algal populations in frazil ice. Nature 306: 363-365.
Gates M.A. (1978) Morphometric variations in the hypotriche ciliate genus *Euplotes*. J. Protozool. 25: 338-350.
Gradinger R., Spindler M., Henschel D. (in press) Development of Arctic sea ice organisms under graded snow cover. Polar Res..
Grainger E.H., Hsiao S.I.C. (1990) Trophic relationships of the sea ice meiofauna in Frobisher Bay, Arctic Canada. Polar Biol. 10: 283-292.
Gulliksen B., Lonne O.J. (1989) Distribution, abundance, and ecological importance of marine sympagic fauna in the Arctic. Rapp. P.-v. Reun. Cons. int. Explor. Mer. 199: 133-138.
Hada Y. (1970) The protozoan plankton of the Antarctic and Subantarctic Seas. JARE Sci. Rep., Ser. E 31: 1-51.
Hartwig E. (1974) Verzeichnis der im Bereich der deutschen Meeresküste angetroffenen interstitiellen Ciliaten. Mitt. Hamburg. Zool. Mus. Inst. 71: 7-21.
Hempel G. (1987) Die Polarmeere - ein biologischer Vergleich. Polarforschung 57: 173-189.
Jankowski A.W. (1968) Taxonomy of the suborder Nassulina Jank., 1967 (Ciliophora, Ambihymenida). Zool. Zh. 47: 990-1001.
Lee C.C., Fenchel T. (1972) Studies on ciliates associated with sea ice from Antarctica, II. Temperature responses and tolerances in ciliates from Antarctic, temperate and tropical zones. Arch. Protistenk. 114: 237-244.

Melnikov I.A. (1989) Ecosystem of the Arctic sea ice. Akad. Nauk. SSSR, Shirshov Institut of Oceanology, Moscow.

Nansen F. (1906) Protozoa on the ice-floes of the North Polar Sea. Sci. Res. Norw. N. Polar Exped. 5(16): 1-22.

Small E.B. (1967) The Scuticociliatida, a new order of the class Ciliatea (Phylum Protozoa, Subphylum Ciliophora). Trans. Amer. Microsc. Soc. 86: 345-370.

Sola A., Guinea A., Fernandez-Galiano D., Longas J.F., Corliss J.O. (1990) Description of two species of Nassophorean ("Hypostome") ciliates, *Nassulopsis elegans* (Ehrenberg, 1833) and *Zosterodasys derouxi* n. sp., with comments on their systematic and phylogenetic affinities. Europ. J. Protistol. 26: 15-24.

Spindler M. (ed.) (1989) Die Expedition ARKTIS V/1a, 1b und 2 mit FS "Polarstern" 1988. Ber. Polarforsch. 59: 1-197.

Spindler M. (1990) A comparison of Arctic and Antarctic sea ice and the effects of different properties on sea ice biota. In: Geologic history of the polar oceans: Arctic versus Antarctic (Eds. U. Bleil, J. Thiede), Kluwer Academic Publishers 173-186.

Spindler M., Dieckmann G.S. (1986) Distribution and abundance of the planktic foraminifer, *Neogloboquadrina pachyderma* in sea ice of the Weddell Sea (Antarctica). Polar Biol. 5: 185-191.

Spindler M., Dieckmann G.S., Lange M.A. (1990) Seasonal and geographic variations in sea ice community structure of the Weddell Sea, Antarctica. In: Antarctic Ecosystems. Ecological change and conservation (Eds. K.R. Kerry, G. Hempel), Springer-Verlag Berlin, Heidelberg 129-135.

Spindler M., Dieckmann G.S. (1991) Meereis als Lebensraum. Spektrum der Wissenschaft 2: 48-57.

Thompson J. C. Jr. (1972) Ciliated Protozoa of the Antarctic Peninsula. In: Antarctic terrestrial biology. Antarctic research series 20, American geophysical union, (G.A. Llano) 261-288.

Tuffrau M. (1974) Un nouvel Euplotidae: *Cytharoides balechi* n. g., sp. n., cilié hypotriche de l'Antarctique. Protistologica 10: 311-317.

Usachev P.I. (1949) The microflora of polar ice. Tr. Inst. Okeanol. Akad. Nauk SSR 3: 216-259.

Valbonesi A., Luporini P. (1990) A new marine species of *Euplotes* (Ciliophora, Hypotrichida) from Antarctica. Bull. Br. Mus. nat. Hist. (Zool.) 56: 57-61.

Valbonesi A., Luporini P. (1990) Description of two new species of *Euplotes* and *Euplotes rariseta* from Antarctica. Polar Biol. 11: 47-53.

Wallengren H. (1900) Vergleichende Morphologie der hypotrichen Infusorien. Bih. Svensk. Vetensk. Akad. Handl. 26: 1-30.

Wilbert N. (1975) Eine verbesserte Technik der Protargolimprägnation für Ciliaten. Mikrokosmos 6: 171-179.

Received on 10th March, 1993; accepted 17th June, 1993

ACTA
PROTOZOOLOGICA

Acta Protozoologica (1993) 32: 269 - 270

Eimeria melanuri sp. n. (Coccidia, Eimeriidae), an Intestinal Parasite of *Eliomys melanurus* Wagner, 1840 (Rodentia, Gliridae) from Syria

Vassil G. GOLEMANSKY and Akram I. DARWISH

Institute of Zoology, Sofia, Bulgaria

Summary. A new coccidian parasite *Eimeria melanuri* sp.n. was found in *Eliomys melanurus* Wagner, 1840 from West Syria. The oocysts of the new taxon are spheric or subspheric, 21.5 ± 0.16 x 19.4 ± 0.11 µm. Sporulation time at 25°C is 72-96 h.

Key words. *Eimeria melanuri* sp. n., *E. myoxi, Eliomys melanurus,* oocyst morphometry, sporulation time.

INTRODUCTION

The information about coccidian parasites of rodents of *Eliomys* genus is very scanty. Up to now, the only known coccidium is *Eimeria myoxi*, described by Galli-Valerio (1940) in *Eliomys quercinus* from Switzerland. According to this author the ovoid oocysts of *E. myoxi* measure 18 x 15 µm, aspherical sporont is about 12 µm in diameter.

Pellérdy (1965, 1974) notes that he also observed oocysts of *Eimeria myoxi* from *Eliomys quercinus*, but they had larger sizes, i. e. 20 to 27 by 19 to 25 µm. According to Pellérdy (1974) the smooth wall of the observed oocysts bears an indistinct micropyle. Sporulation takes 4-7 days and the sporocysts are 7.5 x 6 µm in size. The cited author did not observe an oocyst or sporocysts residuum and concluded, that they are probably absent.

Address for correspondence: V. G. Golemansky, Institute of Zoology, blvd. Zar Osvoboditel No 1, 1000 Sofia, Bulgaria

MATERIALS AND METHODS

The subject of this investigation is one adult specimen of *Eliomys melanurus* Wagner, 1840, collected in 1990 in Damascus. After dissection of the animal part of its small intestine was preserved in a 2.5% solution of $K_2Cr_2O_7$. Microscopical examination was done after the Fülleborn flotation method. For estimating the sporulation time of the oocysts the content of the small intestine was incubated in a thermostat at 25 ± 1°C. The variation of the oocyst size is calculated by the equations:

$$x_i = \frac{\Sigma x}{n}, \quad C.V. = \frac{S.D. \times 100}{x} \text{ and } S.D. = \sqrt{\frac{(x - x_i)}{n}},$$

where: n is the number of oocysts measured; x - the size of oocysts; x_1 - arithmetical mean size; S.D. - standard deviation; C.V. - coefficient of variation and S.E. - standard error. The other abbreviations used in the text and in the tables are: L - length of the oocysts; W - width of the oocysts; M - mean and Lim. - limits of the variation.

RESULTS

In the examined *Eliomys melanurus* from Syria two species of *Eimeria* were found: *Eimeria myoxi* Galli-Valerio, 1940 and an unknown species, considered by us

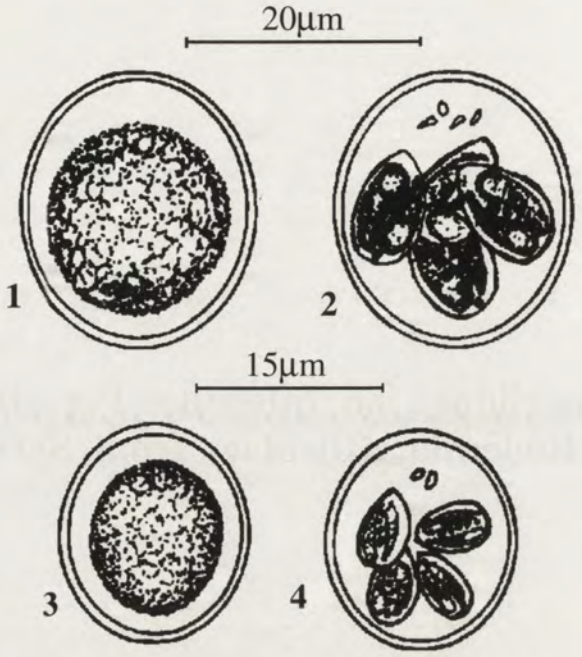

Figs. 1, 2. *Eimeria melanuri* sp. n.: 1 - unsporulated oocyst; 2 - sporulated oocyst
Figs. 3, 4. *Eimeria myoxi* Galli-Valerio, 1940: 3 - unsporulated oocyst; 4 - sporulated oocyst

as a new taxon. The description of the oocysts of the new species and comparison with those of *E. myoxi* are given below.

Eimeria melanuri sp. n. (Figs. 1, 2)

Syn. *Eimeria myoxi* Galli-Valerio, 1940, pro parte Pellérdy, 1914, 609-610.

Oocysts' morphometry: The oocysts are subspheric, rarely spheric, colourless, with a double oocysts wall. The oocyst wall is smooth, without micropyle, about 1.2-1.5 µm thick. Oocyst residuum is absent, but in the sporulated oocysts 1-4 polar granules are visible. The oocyst sizes and their variations are presented in Table 1.

Table 1

E. melanuri sp. n.: sizes of the oocysts and their variations

	$x_1 \pm$ S.E.	L/W	S.D.	C.V	Lim.	n
L:	21.5 ± 0.16	1.0-1.2	1.1	5.12	18-24	50
W:	19.4 ± 0.11	M = 1.1	0.8	4.13	17.5-21.2	50

Table 2

E. myoxi: sizes of the oocyst and their variations, according to our measurements

	$x_1 \pm$ S.E.	L/W	S.D.	C.V.	Lim.	n
L:	18.1 ± 0.2	1.0-1.2	1.0	5.52	16.2-20.0	26
W:	16.4 ± 0.2	M = 1.1	1.22	7.42	13.0-19.0	26

The sporocysts are ovoid, without Stieda body. L: 10-12 µm; W: 6.2-8 µm (M = 11.2 x 7.5 µm). The sporocyst residuum is formed by some granules, dispersed among the sporozoites.

The sporulation time at 25°C varies within 72-96 h.

Localization of oocysts: small intestine.

Locality: Damascus, West Syria.

DISCUSSION

Eimeria melanuri sp. n. was found in the intestinal content of *Eliomys melanurus* in a mixed population with *Eimeria myoxi* Galli-Valerio, 1940. The oocysts of *E. myoxi* are also spheric of subspheric, colourless, with a smooth oocyst wall, but their dimensions are smaller than those of *E. melanuri* sp. n. (Figs. 3, 4). Our measurements, based on 26 oocysts of *E. myoxi* isolated from E. melanururs are presented at Table 2. They are very close to oocyst dimensions given by Galli-Valerio (1940).

The dimensions of the oocysts, observed by Pellérdy (1974) in *E. quercinus* from Hungary and considered by him as *E. myoxi* are quite bigger (20-27 x 19-25 µm) and closer to the oocysts of *E. melanuri* sp. n. Another morphological difference between the two observed coccidian species is the number of the polar granules. In the sporulated oocysts of *E. myoxi* there are 1-2 granules, while in those of *E. melanuri* sp. n. these number is 2-4, being disposed in one pole. The number of the polar granules is not discussed by Galli-Valerio (1940) and Pellérdy (1965, 1974).

In conclusion, we consider that *Eliomys melanurus* and *E. quercinus* are hosts of two different intestinal coccidia: *Eimeria myoxi* Galli-Valerio, 1940 and *E. melanuri* sp. n. described in the present paper.

Acknowledgement. We express our thanks to professor T. Peshev from the University of Sofia for the identification of *Eliomys melanurus*.

REFERENCES

Galli-Valerio B. (1940) Notes de parasitologie et de technique parasitologique. Schweizer Arch. Tierheilk. 82: 279-285, 352-358, 387-392.
Pellérdy L. (1965) Coccidia and Coccidiosis. Kiadó, Budapest.
Pellérdy L. (1974) Coccidia and Coccidiosis. 2nd ed. Kiadó, Budapest.

Received on 10th January, 1992; accepted on 7th May, 1993

ACTA
PROTOZOOLOGICA

Acta Protozoologica (1993) 32: 271 - 272

Book review

Mehlhorn, Heinz & Ruthmann, August (1992) Allgemeine Protozoologie

Gustav Fischer Verlag, Jena - Stuttgart. 335 pp. 181 Figs. 17 x 24 cm, paperback, price 89.- DM, ISBN 3-334-60390-3.

The most recent textbook on general protozoology in German is written by two scientists from the Ruhr-University Bochum, a parasitologist (H. M.) and a cell biologist (A. R.). Faced with the tremendous genetic, molecular, morphological and ecological diversity of more than 50 different phyla of unicellular eukaryotes it certainly was a great venture to write a textbook on general protozoology. Presumably following the traditional approach of teaching protozoology, the book is organized in two main sections, one dealing with the free-living protozoa and the other with parasites. One may argue that it is at large for practical reasons to maintain this somewhat artificial division. No doubt both groups offer their own highlights for particular areas of research, but it makes little or no sense to deal twice with the few general topics all protozoa have in common like mitosis, meiosis, cytokinesis, and sexuality, once for the free-living protozoa and again for the parasitic protozoa. This is prone to redundancy, inconsistent terminology and wastes space. But let's see first what we have got.

The contents of the book are subdivided in three main parts. The first part gives a systematic surview of the protozoa (42 pp.), based largely on the Levine et al. classification published in 1980. The second part (136 pp.) deals with the free-living protozoa under the following subheadings: functional morphology, reproduction, nutrition, motility, and protozoa in ecosystems. The third part (111 pp.) covers the parasitic protozoa but also includes mutualistic flagellates from cockroaches and termitea. Here the three major topics are again functional morphology, reproduction, and nutrition, supplemented with shorter comments on the mechanisms of transmission, cryopreservation, in vitro cultivation techniques, pathogenic effects of these protozoa on their hosts, diagnosis, isolation techniques, immunology and chemotherapy.

In a textbook on general protozoology the main purpose of a survey on protozoan systematics is to give a rough orientation where the organisms dealt with in the later chapters are placed. Though the authors can easily argue that there is no more recent generally accepted system of protozoan classification than the Levine et al. classification, 13 years later, they should have eliminated the most serious misconceptions ofthis scheme. It is a real disaster still to see the Zoomastigophora and Phytomastigophora listed as classes of a phylum Sarcomastigophora. Since this textbook is written primarily for students, such conceptional misunderstandings, I fear, will be perpetuated for another generation. Comparatively little harm is done to the ciliates for which the authors use the Honigberg et al. classification from 1964. The notes on the Microsporea, Haplosporea, Paramyxea, Myxozoa and Actinospora (p. 54-57) are by far too brief. Without even sketchy illustrations of their life cycles a student studying protozoa for the first time could not get the slightest idea of these organisms. Moreover, I have the impression that the phototrophic fllagellates are underrepresented in this book. Is this another conflict of concepts, e.g., protozoa versus protists? Current ideas on the evolution of the unicellular eukaryotes by serial endosymbiosis, hardly touched in this book, deserved a broader treatment in a modern textbook on general protozoology.

The chapters on cell biology of the free-living protozoa are written in a very clear and smooth style, logically leading from one problem to the next. One clearly recognizes the author's interest and competence in such topics as functional morphology and chromosome research. The chapter "Stoffwechsel" deals with the various strategies of food capture observed in free-living protozoa and deacriptive features of osmoregulation, hardly touching any biochemistry. The chapter on motility of free-living protozoa is very concise. It gives an

up-to-date description of all major modes of locomotion and intracellular transport, this time helpfully down to molecular aspects. In the chapter entitled "Protozoa in Ecosystems" it would have been appropriate to include some remarks on the phenomenon, seen in many protistan phyla, how free-living represenatives gradually shift over to a parasitic life style. Such comments would have led logically to the next part.

The third part of the book is devoted to parasitic protozoa with the endosymbiotic hypermastigine flagellates included. Its two main chapters on morphology and reproduction are lavishly illustrated, in particular the one on morphology, where EM micrographs from the author's laboratory take more than half the space, while the text comes in bits and pieces. The text on reproduction contains several vague statements. The layout of p. 212 - 219 is not very satisfying. The legends to figures 170, 172, 173 have been mixed up completely. Fig. 170 shows the life cycle of Trichonyrnpha and not Barbulanympha, Fig. 172 shows Notila, not Trichonympha, Fig. 173 shows Barbulanympha and not Notila. Thus, if one is interested in these beautiful flagellates, it is better to refer to the original papers by Cleveland, none of which are mentioned in this book (see e.g., Cleveland's review paper in J. Protozool. 3, 161-180, 1956). On the other hand, the reader is informed about the latest speculations on genetic recombination in Trypanosoma, on a third genome found in Plasmodium, and on AIDS -associated opportunistic pathogens. So, this chapter is likewise quite contemporary.

The coverage of the literature is somewhat inconsistent. While the chapter on systematics and the five subchapters on free-living protozoa have their own literature, the literature referring to the parasitic protozoa comes only with the subchapters on immunology and chemotherapy, these then containing several references which refer to other topics. The book closes with a list of 24 recent textbooks on protozoology and parasitology and a list of 27 monographs.

Furthermore, there is a very short appendix with four recipes for preparing media for free-living protozoa, followed by a taxonomic index and a separate subject index. Besides some older but still valuable books from Dogiel, Doflein-Reichenow, Grasse, and Kudo another more recent horn of plenty, the Handbook of Protoctista, edited by Margulis et al. and published by Jones and Barlett, Boston in 1985, is not mentioned.

What else do I miss? Current ideas on protist evolution based on comparative morphology and RNA sequences should have been discussed. Side lines of biochemical pathways so important for the understanding of the mode of action of chemotherapy, as well as the various strategies of vaccine production, might have been described in a more detailed way, since these are topics which might attract students to the field of protozoology.

My first impression of the book - two authors, two styles of writing, two styles of illustrations, two grades of confidence (due to an unequal distribution of errors) has not changed much after closer inspection. I still wonder why two authors working in the same building have not presented a more homogeneous book? It is perhaps of secondary importance, but I somehow feel sorry for the Letra-Setfinished parasitic protozoa in close neighbourhood with the beautiful drawings of the free-living protozoa, taken from Grell's Protozoology. By the way, the ciliate Saprodinium dentatum on the cover is printed upside down. One might argue that ciliates swim in all directions, but the same figure on p. 65 shows how little mistakes are perpetuated from patriarchs.

I know it is easy to criticize, and very difficult to do better. I apologize if I have been too direct with my comments. Perhaps my expectations have been too high. Should I say anything else? Yes - the book is printed in high quality.

Christian F. Bardele, Tubingen, Germany

Acknowledgement

The editors wish to acknowledge the help of the following colleagues who have served as reviewers for one or more manuscripts submitted for publication in our journal.

Christian F. Bardele
S. Jost Casper
Isabelle Desportes-Livage
Michael J. Doughty
Anne Fleury
Tom Fenchel
Wilhelm Foissner
Krystyna Golińska
Andrzej Grębecki
Elio Hildebrand
Lothar Krienitz
Andrzej Kubalski
Armand M. Kuris
Michael Levandowsky
Jerzy J. Lipa
Jiri Lom
Pierangelo Luporini
Hans Machemer
Jean-Pierre Mignot
Jytte R. Nilsson
Wilfried Schönborn
Michael Sleigh
Victor Smetacek
Pill-Soon Song
Jiri Vavra
Patricia L. Walne
Norbert Wilbert

Author Index: Acta Protozoologica 32 (1-4) 1993

Subject Index: Acta Protozoologica 32 (1-4) 1993

ACTA PROTOZOOLOGICA

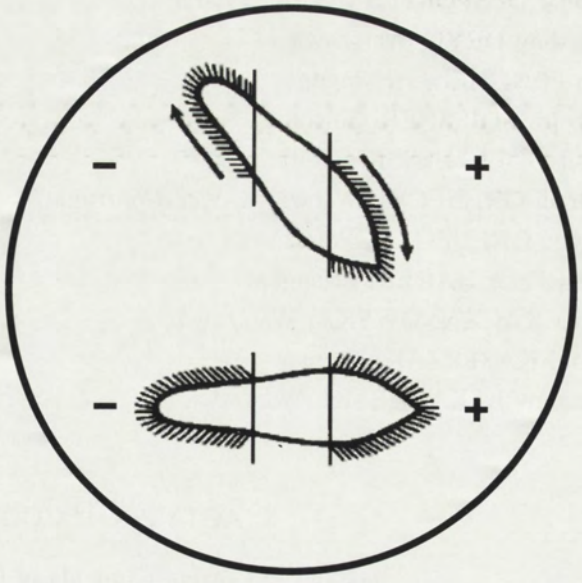

NENCKI INSTITUTE OF EXPERIMENTAL BIOLOGY
WARSAW, POLAND
1993
VOLUME 32
ISSN 0065-1583

Polish Academy of Sciences
Nencki Institute of Experimental Biology

ACTA PROTOZOOLOGICA

International Journal on Protistology

ACTA PROTOZOOLOGICA appears quarterly.

Indexed in Current Contents in CABS and in Protozoological Abstracts.

Front cover: The ciliary reversal on cathodal side of *Paramecium*. S. Dryl 1963, Acta Protozool. 1,193-199

Contents of Volume 32 (1-4) 1993

Number 1

Number 2

Number 3

Number 4

Erratum to Vol.32, No. 3, July 1993 Issue of Acta Protozoologica

Editors regrets authors M.S. Rautanian, I. I. Skoblo, N. A. Lebedeva and D. V. Ossipov for numerous mistakes in their contribution "Genetics of Symbiotic Interactions between *Paramecium bursaria* and the Intranuclear Bacterium *Holospora acuminata*, Natural Genatic Variability by Infectivity and Susceptibility". The final proof was unfortunately not avaiable in time.

Page 167, left column, line 29 *is:*... to form the SB.
should be:...to form the symbiotic system (SS).

Page 168, left column, line 18 *is:* SB *should be:* SS

Page 169, Table 3 *(corrected see next page)*

Page 170, left column, line 26, *is* ... where the infection process in syngen 1 clones is blocked in the most cases ...!!
should be: ...was that stage which was blocked in most other unsusceptable cases in syngen 1.

Page 170 left column, line 31 *is:* (marked as "+" in Table 3)
should be: ±

Page 170, right column, line 1 *is:*... come away...
should be: ... exit...

Page 170, right column, line 13 *instead of:*...(Ba1-4/E2-10, Bal-1/AS65-8 et al.),...
should be:...(Va1-4/E2-10, Va1-1/AS65-8),...

Page 170, right column, line 20 *is:*... BM-3/E2-10, BM-3/MS-9, Ba1-3/AK-1,...
should be: VM-3/E2-10, VM-3/MS-9, Va1-3/AK-1,...

Page 170, right column, line 27 *is* Fig. 3
should be: Fig 3b

Page 170, right column, line 35 *is:* ...penetrates..
should be:... penetrate...

Page 171, right column, line 6, the word ...leave...
should be ommited

Page 172, left column, line 14, words ...Symbiont reproduction, when...
should be ommited

Page 172, right column, line 4. *is:* (3) The stage of differentiation of infectious forms.
should be: (3) Breach of differentiation of infectious forms.

Page 173, right column, line 22 *is:* (in press)
should be: 29: 61-71.

Table 3

Ability of *Holospora acuminata* to pass particular stages during the infection process

Paramecium bursaria		*Holospora acuminata* isolates						
		From clones of syngen 1				From clones of syngen 2		
		E2-10	AS65-8	NP-54	MS-9	DS1-22	KM10-7	AK-1
		infection stages						
syngenes	clones	1 2 3 4	1 2 3 4	1 2 3 4	1 2 3 4	1 2 3 4	1 2 3 4	1 2 3 4
1	AS62-14	+ + + +	+ + + +	+ + + +	+ + + +	+ + + +	+ + + +	+ + + +
	NP-18	+ + + +	+ + + +	+ + + +	+ + + +	−	−	−
	GG-26	+ + + +	+ + + +	+ + + +	+ + + +	−	−	−
	GoB-4	+ + + +	+ + + +	+ + + +	+ + + +	−	−	−
	AS62-9	+ + + +	+ + + +	+ + + +	± −	−	+ −	−
	AS63-4	+ + + +	+ + + +	+ + + +	−	−	−	−
	GB-10	+ + + +	−	+ + + +	+ −	−	−	−
	MS87-1	+ + + +	+ + − −	−	−	−	−	−
	MS87-6	+ + + +	+ −	−	−	−	−	−
	MS-7	−	+ + + +	−	−	−	−	−
	NP-28	−	+ + + +	−	−	+ −	−	−
	MS1-18	−	−	−	+ + + +	−	−	−
	ET87-2	−	−	−	−	−	−	−
	NP-2	−	−	−	−	−	−	−
	NP-17	−	−	−	−	−	−	−
	88T32-3	−	−	−	−	−	−	−
	88T32-8	−	−	−	−	−	−	−
2	ES9-1	−	−	+ −	−	+ + + +	+ + + +	+ + + +
	KJ-1	± −	+ −	+ −	± −	+ + + +	+ + + +	+ + + +
	BM6-4	+ −	+ −	+ −	+ $-^{1}$	+ + + +	+ + + +	+ + + +
	Va1-1	+ −	+ $-^{1}$	+ $-^{1}$	+ $-^{1}$	+ + + +	+ + + +	+ + + +
	Va1-4	+ $-^{1}$	+ $-^{1}$	+ + −	+ −	+ + + +	+ + + +	+ + + +
	Va1-5	+ $-^{1}$	+ $-^{1}$	+ $-^{1}$	+ $-^{1}$	+ + + +	+ + + +	+ + + +
	SO4-10	+ + −	+ −	+ + −	−	+ + + +	+ + + +	+ + + +
	KJ-22	+ + −	+ −	+ + −	+ + −	+ + + +	+ + + +	+ + + +
	KM10-7-31	−	−	−	−	+ + + +	+ + + +	−
	KM10-3	−	−	−	± −	+ + + +	+ + + +	± −
	DS1-19	+ −	+ −	+ + −	+ −	+ + + +	+ + + +	± −
	VM-14	−	+ $-^{1}$	+ + −	−	+ + + +	+ + + +	−
	VM-3	+ $-^{2}$	+ −	+ + −	+ + $-^{2}$	+ + + +	+ + + +	± −
	VM-1	+ −	+ −	+ + −	+ $-^{1}$	+ + + +	+ + + +	+ + −
	Va1-3	+ −	+ $-^{1}$	+ + $-^{1}$	+ $-^{1}$	+ + + +	+ + + +	+ + $-^{2}$
3	BP-5	+ −	+ −	± −	± −	± −	+ + −	± −
	BP-28	−	+ −	−	−	± −	+ −	−
	BP-39	± −	± −	−	−	± −	+ + −	−
	D12-2	−	−	−	−	−	−	−
	D12-9	−	−	−	−	−	−	−
	D12-12	−	−	−	−	−	−	−
	D9-24	−	−	−	−	−	−	−

Stages:
1 - penetration of *Holospora acuminata* into the micronucleus.
2 - division of euinfective forms of *Holospora acuminata* - chain formation.
3 - division of vegetative forms of *Holospora acuminata*.
4 - maturation of infectious forms of *Holospora acuminata*.

Abbreviations:
+ Existence of SB at the respective stage.
− Absence of SB at the respective stage.
$-^{1}$ Rapid lysis of *Holospora acuminata*.
$-^{2}$ Delayed lysis of *Holospora acuminata*.
± Small amount of SB penetrate the micronuclei of low number (less than 5%) of *P. bursaria* cells.

INSTRUCTIONS FOR AUTHORS

ACTA PROTOZOOLOGICA publishes original papers embodying the results of experimental or theoretical research in all fields of protistology, with the exception of faunistic notices of local character and purely clinical reports. Short (rapid) communications are acceptable as are long review articles. The papers should be as concise as possible, be written in English, French or German, although English is preferred to keep printing costs lower. Submission of a manuscript to ACTA PROTOZOOLOGICA implies that it has not been submitted for publication elsewhere and that it contains unpublished, new information. There are no page charges. Authors should submit papers to:

Miss Małgorzata Woronowicz
Managing Editor of ACTA PROTOZOOLOGICA
Nencki Institute of Experimental Biology,
ul. Pasteura 3
02-093 Warszawa, Poland
Fax: (48) 225342

Organization of Manuscripts

Submissions

Please enclose three copies of the text, one set of original line drawings (without lettering!) and three sets of copies with lettering, four sets of photographs (one without lettering). In the case of photographs arranged in plate form, please submit one set of original photographs unmounted and without lettering, and three sets of plates with lettering.

ACTA PROTOZOOLOGICA prefers to use the author's word-processor disk copy (3.5"and 5.25" format IBM or IBM compatible, and MacIntosh 6 or 7 system on 3.5" 1.44 MB disk only) of manuscripts instead of rekeying articles. If available, please send a copy of the disk with your manuscript. Disks will be returned with galley proof of accepted article at the same time. Please observe the following instructions:

1. Label the disk with your name: the word processor/computer used, e.g. IBM; the printer used, e.g. Laserwriter; the name of the program, e.g. Wordperfect 5.l; and any special characters used, and how you obtained them (i.e. dedicated key pressed or printer control codes used directly).
2. Send the manuscript as a single file: do not split it into smaller files.
3. Give the file a name which is no longer than 8 characters.
4. Create and /or edit your manuscript, using the document mode (or equivalent) in the word-processor program.
5. If necessary, use only italic, bold, underline, subscript and superscript. Multiple font, style or ruler changes, or graphics inserted the text, reduce the usefulness of the disc.
6. Do not right-justify and use a hyphen at the end of the line.
7. Avoid the use of footnotes.
8. Distinguish the numerals 0 and 1 from the letters O and l.

Text (three copies)

The text must be typewritten, doublespaced, with numbered pages. The manuscript should be organized into Summary, Introduction, Material and Methods, Results, Discussion, Acknowledgments, References, Tables and Figure Legends. The Title Page should include the full title of the article, first name(s) in full and surname(s) of author(s), the address(es) where the work was carried out, page heading of up to 40 characters, and up to 6 Key Words. The present address for correspondence, telephone, FAX, and E-mail numbers should also be given.

The Titles, Summary and Key Words of the manuscripts submitted in French and German should be translated into English according to the demands of Current Contents. Each table must be on a separate page. Figure legends must be in a single series at the end of the manuscript. References must be listed alphabetically, abbreviated according to the World List of Scientific Periodicals, 4th ed. (1963). Nomenclature of genera and species names must agree with the International Code of Zoological Nomenclature, third edition, London (1985) or International Code of Botanical Nomenclature, adopted by XIV International Botanical Congress, Berlin, 1987. SI units are preferred.

Examples for bibliographic arrangement of references:

Journals:

Häder D-P., Reinecke E. (1991) Phototactic and polarotactic responses of the photosynthetic flagellate, *Euglena gracilis. Acta Protozool.* **30:** 13-18

Books:

Wichterman R. (1986) The Biology of Paramecium. 2 ed. Plenum Press, New York

Articles from books:

Allen R. D. (1988) Cytology. In: Paramecium, (Ed. H.-D. Görtz). Springer-Verlag, Berlin, 4-40

Zeuthen E., Rasmussen L. (1972) Synchronized cell division in protozoa. In: Research in Protozoology, (Ed. T.T. Chen). Pergamon Press, Oxford, **4:** 9-145

Illustrations

All line drawings and photographs should be labelled with the first author's name written on the back. Figures should be numbered in the text as arabic numerals (e.g. Fig. 1). Illustrations must fit within either one column (86 x 231 mm) or the full width and length of the page (177 x 231 mm). Figures and legends should fit on the same page. Lettering will be inserted by the printers and should be indicated on a tracing-paper overlay or duplicate copy.

Line drawings (three copies + one copy without lettering)

Line drawings should preferably be drawn about twice as large as the desired final size, and be suitable for reproduction in the form of well-defined line drawings and should have a white background. Avoid fine stippling or shading. Computer printouts of laser printer quality may be accepted, however *.TIF, *.PCX, *.BMP graphic formats on disk are preferred.

Photographs (three copies + one copy without lettering)

Photographs at final size should be sharp, gloss finished, bromide prints. Photographs grouped as plates (in size not exceeding 177 x 231 mm including legend) must be trimmed at right angles accurately with edges touching and mounted on firm board. The engraver will then cut a fine line of separation between figures. Magnification should be indicated. There is a page charge for colour illustration.

Proof sheets and offprints

Authors will receive one set of page proofs for correction and are asked to return these to the Editor within 48-hours. Fifty reprints will be furnished free of charge. Orders for additional reprints must be submitted with the proofs.

Indexed in Current Contents in CABS and in Protozoological Abstracts.

ACTA
PROTOZOOLOGICA

1993 OCTOBER
VOLUME 32 NUMBER 4